UNITED STATES AIR FORCE

SUMMER RESEARCH PROGRAM -- 1996

HIGH SCHOOL APPRENTICESHIP PROGRAM FINAL REPORTS

VOLUME 13

PHILLIPS LABORATORY

RESEARCH & DEVELOPMENT LABORATORIES

5800 Uplander Way

Culver City, CA 90230-6608

Program Director, RDL
Gary Moore

Program Manager, AFOSR
Major Linda Steel-Goodwin

Program Manager, RDL
Scott Licoscos

Program Administrator, RDL
Johnetta Thompson

Program Administrator
Rebecca Kelly

Submitted to:

AIR FORCE OFFICE OF SCIENTIFIC RESEARCH

Bolling Air Force Base

Washington, D.C.

December 1996

REPORT DOCUMENTATION PAGE

AFRL-SR-BL-TR-00-

0745

1. AGENCY USE ONLY *(Leave blank)*	2. REPORT DATE	3. REPORT TYPE AND DATES COVERED
	December, 1996	

4. TITLE AND SUBTITLE
1996 Summer Research Program (SRP), High School Apprenticeship Program (HSAP), Final Reports, Volume 13, Phillips Laboratory

5. FUNDING NUMBERS
F49620-93-C-0063

6. AUTHOR(S)
Gary Moore

7. PERFORMING ORGANIZATION NAME(S) AND ADDRESS(ES)
Research & Development Laboratories (RDL)
5800 Uplander Way
Culver City, CA 90230-6608

8. PERFORMING ORGANIZATION REPORT NUMBER

9. SPONSORING/MONITORING AGENCY NAME(S) AND ADDRESS(ES)
Air Force Office of Scientific Research (AFOSR)
801 N. Randolph St.
Arlington, VA 22203-1977

10. SPONSORING/MONITORING AGENCY REPORT NUMBER

11. SUPPLEMENTARY NOTES

12a. DISTRIBUTION AVAILABILITY STATEMENT
Approved for Public Release

12b. DISTRIBUTION CODE

13. ABSTRACT *(Maximum 200 words)*

The United States Air Force Summer Research Program (USAF-SRP) is designed to introduce university, college, and technical institute faculty members, graduate students, and high school students to Air Force research. This is accomplished by the faculty members (Summer Faculty Research Program, (SFRP)), graduate students (Graduate Student Research Program (GSRP)), and high school students (High School Apprenticeship Program (HSAP)) being selected on a nationally advertised competitive basis during the summer intersession period to perform research at Air Force Research Laboratory (AFRL) Technical Directorates, Air Force Air Logistics Centers (ALC), and other AF Laboratories. This volume consists of a program overview, program management statistics, and the final technical reports from the HSAP participants at the Phillips Laboratory.

14. SUBJECT TERMS
Air Force Research, Air Force, Engineering, Laboratories, Reports, Summer, Universities, Faculty, Graduate Student, High School Student

15. NUMBER OF PAGES

16. PRICE CODE

17. SECURITY CLASSIFICATION OF REPORT	18. SECURITY CLASSIFICATION OF THIS PAGE	19. SECURITY CLASSIFICATION OF ABSTRACT	20. LIMITATION OF ABSTRACT
Unclassified	Unclassified	Unclassified	UL

Standard Form 298 (Rev. 2-89) (EG)
Prescribed by ANSI Std. 239.18
Designed using Perform Pro, WHS/DIOR, Oct 94

GENERAL INSTRUCTIONS FOR COMPLETING SF 298

The Report Documentation Page (RDP) is used in announcing and cataloging reports. It is important that this information be consistent with the rest of the report, particularly the cover and title page. Instructions for filling in each block of the form follow. It is important to ***stay within the lines*** to meet ***optical scanning requirements.***

Block 1. Agency Use Only *(Leave blank)*.

Block 2. Report Date. Full publication date including day, month, and year, if available (e.g. 1 Jan 88). Must cite at least the year.

Block 3. Type of Report and Dates Covered. State whether report is interim, final, etc. If applicable, enter inclusive report dates (e.g. 10 Jun 87 - 30 Jun 88).

Block 4. Title and Subtitle. A title is taken from the part of the report that provides the most meaningful and complete information. When a report is prepared in more than one volume, repeat the primary title, add volume number, and include subtitle for the specific volume. On classified documents enter the title classification in parentheses.

Block 5. Funding Numbers. To include contract and grant numbers; may include program element number(s), project number(s), task number(s), and work unit number(s). Use the following labels:

C - Contract	**PR** - Project
G - Grant	**TA** - Task
PE - Program Element	**WU** - Work Unit Accession No.

Block 6. Author(s). Name(s) of person(s) responsible for writing the report, performing the research, or credited with the content of the report. If editor or compiler, this should follow the name(s).

Block 7. Performing Organization Name(s) and Address(es). Self-explanatory.

Block 8. Performing Organization Report Number. Enter the unique alphanumeric report number(s) assigned by the organization performing the report.

Block 9. Sponsoring/Monitoring Agency Name(s) and Address(es). Self-explanatory.

Block 10. Sponsoring/Monitoring Agency Report Number. *(If known)*

Block 11. Supplementary Notes. Enter information not included elsewhere such as: Prepared in cooperation with....; Trans. of....; To be published in.... When a report is revised, include a statement whether the new report supersedes or supplements the older report.

Block 12a. Distribution/Availability Statement. Denotes public availability or limitations. Cite any availability to the public. Enter additional limitations or special markings in all capitals (e.g. NOFORN, REL, ITAR).

DOD -	See DoDD 5230.24, "Distribution Statements on Technical Documents."
DOE -	See authorities.
NASA -	See Handbook NHB 2200.2.
NTIS -	Leave blank.

Block 12b. Distribution Code.

DOD -	Leave blank.
DOE -	Enter DOE distribution categories from the Standard Distribution for Unclassified Scientific and Technical Reports.
	Leave blank.
NASA -	Leave blank.
NTIS -	

Block 13. Abstract. Include a brief *(Maximum 200 words)* factual summary of the most significant information contained in the report.

Block 14. Subject Terms. Keywords or phrases identifying major subjects in the report.

Block 15. Number of Pages. Enter the total number of pages.

Block 16. Price Code. Enter appropriate price code *(NTIS only)*.

Blocks 17. - 19. Security Classifications. Self- explanatory. Enter U.S. Security Classification in accordance with U.S. Security Regulations (i.e., UNCLASSIFIED). If form contains classified information, stamp classification on the top and bottom of the page.

Block 20. Limitation of Abstract. This block must be completed to assign a limitation to the abstract. Enter either UL (unlimited) or SAR (same as report). An entry in this block is necessary if the abstract is to be limited. If blank, the abstract is assumed to be unlimited.

PREFACE

Reports in this volume are numbered consecutively beginning with number 1. Each report is paginated with the report number followed by consecutive page numbers, e.g., 1-1, 1-2, 1-3; 2-1, 2-2, 2-3.

This document is one of a set of 16 volumes describing the 1996 AFOSR Summer Research Program. The following volumes comprise the set:

VOLUME	TITLE
1	Program Management Report
	Summer Faculty Research Program (SFRP) Reports
2A & 2B	Armstrong Laboratory
3A & 3B	Phillips Laboratory
4	Rome Laboratory
5A, 5B & 5C	Wright Laboratory
6	Arnold Engineering Development Center, Wilford Hall Medical Center and Air Logistics Centers
	Graduate Student Research Program (GSRP) Reports
7A & 7B	Armstrong Laboratory
8	Phillips Laboratory
9	Rome Laboratory
10A & 10B	Wright Laboratory
11	Arnold Engineering Development Center, United States Air Force Academy, Wilford Hall Medical Center and Wright Patterson Medical Center
	High School Apprenticeship Program (HSAP) Reports
12A & 12B	Armstrong Laboratory
13	Phillips Laboratory
14	Rome Laboratory
15A&15B	Wright Laboratory
16	Arnold Engineering Development Center

SRP Final Report Table of Contents

SRP Final Report Table of Contents

SRP Final Report Table of Contents

SRP Final Report Table of Contents

SRP Final Report Table of Contents

SRP Final Report Table of Contents

SRP Final Report Table of Contents

SRP Final Report Table of Contents

SRP Final Report Table of Contents

SRP Final Report Table of Contents

SRP Final Report Table of Contents

INTRODUCTION

The Summer Research Program (SRP), sponsored by the Air Force Office of Scientific Research (AFOSR), offers paid opportunities for university faculty, graduate students, and high school students to conduct research in U.S. Air Force research laboratories nationwide during the summer.

Introduced by AFOSR in 1978, this innovative program is based on the concept of teaming academic researchers with Air Force scientists in the same disciplines using laboratory facilities and equipment not often available at associates' institutions.

The Summer Faculty Research Program (SFRP) is open annually to approximately 150 faculty members with at least two years of teaching and/or research experience in accredited U.S. colleges, universities, or technical institutions. SFRP associates must be either U.S. citizens or permanent residents.

The Graduate Student Research Program (GSRP) is open annually to approximately 100 graduate students holding a bachelor's or a master's degree; GSRP associates must be U.S. citizens enrolled full time at an accredited institution.

The High School Apprentice Program (HSAP) annually selects about 125 high school students located within a twenty mile commuting distance of participating Air Force laboratories.

AFOSR also offers its research associates an opportunity, under the Summer Research Extension Program (SREP), to continue their AFOSR-sponsored research at their home institutions through the award of research grants. In 1994 the maximum amount of each grant was increased from $20,000 to $25,000, and the number of AFOSR-sponsored grants decreased from 75 to 60. A separate annual report is compiled on the SREP.

The numbers of projected summer research participants in each of the three categories and SREP "grants" are usually increased through direct sponsorship by participating laboratories.

AFOSR's SRP has well served its objectives of building critical links between Air Force research laboratories and the academic community, opening avenues of communications and forging new research relationships between Air Force and academic technical experts in areas of national interest, and strengthening the nation's efforts to sustain careers in science and engineering. The success of the SRP can be gauged from its growth from inception (see Table 1) and from the favorable responses the 1996 participants expressed in end-of-tour SRP evaluations (Appendix B).

AFOSR contracts for administration of the SRP by civilian contractors. The contract was first awarded to Research & Development Laboratories (RDL) in September 1990. After

completion of the 1990 contract, RDL (in 1993) won the recompetition for the basic year and four 1-year options.

2. PARTICIPATION IN THE SUMMER RESEARCH PROGRAM

The SRP began with faculty associates in 1979; graduate students were added in 1982 and high school students in 1986. The following table shows the number of associates in the program each year.

YEAR	SRP Participation, by Year			TOTAL
	SFRP	GSRP	HSAP	
1979	70			70
1980	87			87
1981	87			87
1982	91	17		108
1983	101	53		154
1984	152	84		236
1985	154	92		246
1986	158	100	42	300
1987	159	101	73	333
1988	153	107	101	361
1989	168	102	103	373
1990	165	121	132	418
1991	170	142	132	444
1992	185	121	159	464
1993	187	117	136	440
1994	192	117	133	442
1995	190	115	137	442
1996	188	109	138	435

Beginning in 1993, due to budget cuts, some of the laboratories weren't able to afford to fund as many associates as in previous years. Since then, the number of funded positions has remained fairly constant at a slightly lower level.

3. RECRUITING AND SELECTION

The SRP is conducted on a nationally advertised and competitive-selection basis. The advertising for faculty and graduate students consisted primarily of the mailing of 8,000 52-page SRP brochures to chairpersons of departments relevant to AFOSR research and to administrators of grants in accredited universities, colleges, and technical institutions. Historically Black Colleges and Universities (HBCUs) and Minority Institutions (MIs) were included. Brochures also went to all participating USAF laboratories, the previous year's participants, and numerous individual requesters (over 1000 annually).

RDL placed advertisements in the following publications: *Black Issues in Higher Education, Winds of Change,* and *IEEE Spectrum.* Because no participants list either *Physics Today* or *Chemical & Engineering News* as being their source of learning about the program for the past several years, advertisements in these magazines were dropped, and the funds were used to cover increases in brochure printing costs.

High school applicants can participate only in laboratories located no more than 20 miles from their residence. Tailored brochures on the HSAP were sent to the head counselors of 180 high schools in the vicinity of participating laboratories, with instructions for publicizing the program in their schools. High school students selected to serve at Wright Laboratory's Armament Directorate (Eglin Air Force Base, Florida) serve eleven weeks as opposed to the eight weeks normally worked by high school students at all other participating laboratories.

Each SFRP or GSRP applicant is given a first, second, and third choice of laboratory. High school students who have more than one laboratory or directorate near their homes are also given first, second, and third choices.

Laboratories make their selections and prioritize their nominees. AFOSR then determines the number to be funded at each laboratory and approves laboratories' selections.

Subsequently, laboratories use their own funds to sponsor additional candidates. Some selectees do not accept the appointment, so alternate candidates are chosen. This multi-step selection procedure results in some candidates being notified of their acceptance after scheduled deadlines. The total applicants and participants for 1996 are shown in this table.

1996 Applicants and Participants			
PARTICIPANT CATEGORY	TOTAL APPLICANTS	SELECTEES	DECLINING SELECTEES
SFRP	572	188	39
(HBCU/MI)	(119)	(27)	(5)
GSRP	235	109	7
(HBCU/MI)	(18)	(7)	(1)
HSAP	474	138	8
TOTAL	1281	435	54

4. SITE VISITS

During June and July of 1996, representatives of both AFOSR/NI and RDL visited each participating laboratory to provide briefings, answer questions, and resolve problems for both laboratory personnel and participants. The objective was to ensure that the SRP would be as constructive as possible for all participants. Both SRP participants and RDL representatives found these visits beneficial. At many of the laboratories, this was the only opportunity for all participants to meet at one time to share their experiences and exchange ideas.

5. HISTORICALLY BLACK COLLEGES AND UNIVERSITIES AND MINORITY INSTITUTIONS (HBCU/MIs)

Before 1993, an RDL program representative visited from seven to ten different HBCU/Mis annually to promote interest in the SRP among the faculty and graduate students. These efforts were marginally effective, yielding a doubling of HBCI/MI applicants. In an effort to achieve AFOSR's goal of 10% of all applicants and selectees being HBCU/MI qualified, the RDL team decided to try other avenues of approach to increase the number of qualified applicants. Through the combined efforts of the AFOSR Program Office at Bolling AFB and RDL, two very active minority groups were found, HACU (Hispanic American Colleges and Universities) and AISES (American Indian Science and Engineering Society). RDL is in communication with representatives of each of these organizations on a monthly basis to keep up with the their activities and special events. Both organizations have widely-distributed magazines/quarterlies in which RDL placed ads.

Since 1994 the number of both SFRP and GSRP HBCU/MI applicants and participants has increased ten-fold, from about two dozen SFRP applicants and a half dozen selectees to over 100 applicants and two dozen selectees, and a half-dozen GSRP applicants and two or three selectees to 18 applicants and 7 or 8 selectees. Since 1993, the SFRP had a two-fold applicant

increase and a two-fold selectee increase. Since 1993, the GSRP had a three-fold applicant increase and a three to four-fold increase in selectees.

In addition to RDL's special recruiting efforts, AFOSR attempts each year to obtain additional funding or use leftover funding from cancellations the past year to fund HBCU/MI associates. This year, 5 HBCU/MI SFRPs declined after they were selected (and there was no one qualified to replace them with). The following table records HBCU/MI participation in this program.

SRP HBCU/MI Participation, By Year				
YEAR	**SFRP**		**GSRP**	
	Applicants	**Participants**	**Applicants**	**Participants**
1985	76	23	15	11
1986	70	18	20	10
1987	82	32	32	10
1988	53	17	23	14
1989	39	15	13	4
1990	43	14	17	3
1991	42	13	8	5
1992	70	13	9	5
1993	60	13	6	2
1994	90	16	11	6
1995	90	21	20	8
1996	119	27	18	7

6. SRP FUNDING SOURCES

Funding sources for the 1996 SRP were the AFOSR-provided slots for the basic contract and laboratory funds. Funding sources by category for the 1996 SRP selected participants are shown here.

1996 SRP FUNDING CATEGORY	SFRP	GSRP	HSAP
AFOSR Basic Allocation Funds	141	85	123
USAF Laboratory Funds	37	19	15
HBCU/MI By AFOSR (Using Procured Addn'l Funds)	10	5	0
TOTAL	188	109	138

SFRP - 150 were selected, but nine canceled too late to be replaced.
GSRP - 90 were selected, but five canceled too late to be replaced (10 allocations for the ALCs were withheld by AFOSR.)
HSAP - 125 were selected, but two canceled too late to be replaced.

7. COMPENSATION FOR PARTICIPANTS

Compensation for SRP participants, per five-day work week, is shown in this table.

1996 SRP Associate Compensation

PARTICIPANT CATEGORY	1991	1992	1993	1994	1995	1996
Faculty Members	$690	$718	$740	$740	$740	$770
Graduate Student (Master's Degree)	$425	$442	$455	$455	$455	$470
Graduate Student (Bachelor's Degree)	$365	$380	$391	$391	$391	$400
High School Student (First Year)	$200	$200	$200	$200	$200	$200
High School Student (Subsequent Years)	$240	$240	$240	$240	$240	$240

The program also offered associates whose homes were more than 50 miles from the laboratory an expense allowance (seven days per week) of $50/day for faculty and $40/day for graduate students. Transportation to the laboratory at the beginning of their tour and back to their home destinations at the end was also reimbursed for these participants. Of the combined SFRP and

GSRP associates, 65 % (194 out of 297) claimed travel reimbursements at an average round-trip cost of $780.

Faculty members were encouraged to visit their laboratories before their summer tour began. All costs of these orientation visits were reimbursed. Forty-five percent (85 out of 188) of faculty associates took orientation trips at an average cost of $444. By contrast, in 1993, 58 % of SFRP associates took orientation visits at an average cost of $685; that was the highest percentage of associates opting to take an orientation trip since RDL has administered the SRP, and the highest average cost of an orientation trip. These 1993 numbers are included to show the fluctuation which can occur in these numbers for planning purposes.

Program participants submitted biweekly vouchers countersigned by their laboratory research focal point, and RDL issued paychecks so as to arrive in associates' hands two weeks later.

In 1996, RDL implemented direct deposit as a payment option for SFRP and GSRP associates. There were some growing pains. Of the 128 associates who opted for direct deposit, 17 did not check to ensure that their financial institutions could support direct deposit (and they couldn't), and eight associates never did provide RDL with their banks' ABA number (direct deposit bank routing number), so only 103 associates actually participated in the direct deposit program. The remaining associates received their stipend and expense payments via checks sent in the US mail.

HSAP program participants were considered actual RDL employees, and their respective state and federal income tax and Social Security were withheld from their paychecks. By the nature of their independent research, SFRP and GSRP program participants were considered to be consultants or independent contractors. As such, SFRP and GSRP associates were responsible for their own income taxes, Social Security, and insurance.

8. CONTENTS OF THE 1996 REPORT

The complete set of reports for the 1996 SRP includes this program management report (Volume 1) augmented by fifteen volumes of final research reports by the 1996 associates, as indicated below:

1996 SRP Final Report Volume Assignments

LABORATORY	SFRP	GSRP	HSAP
Armstrong	2	7	12
Phillips	3	8	13
Rome	4	9	14
Wright	5A, 5B	10	15
AEDC, ALCs, WHMC	6	11	16

APPENDIX A -- PROGRAM STATISTICAL SUMMARY

A. Colleges/Universities Represented

Selected SFRP associates represented 169 different colleges, universities, and institutions, GSRP associates represented 95 different colleges, universities, and institutions.

B. States Represented

SFRP -Applicants came from 47 states plus Washington D.C. and Puerto Rico. Selectees represent 44 states plus Puerto Rico.

GSRP - Applicants came from 44 states and Puerto Rico. Selectees represent 32 states.

HSAP - Applicants came from thirteen states. Selectees represent nine states.

Total Number of Participants	
SFRP	188
GSRP	109
HSAP	138
TOTAL	435

Degrees Represented			
	SFRP	GSRP	TOTAL
Doctoral	184	1	185
Master's	4	48	52
Bachelor's	0	60	60
TOTAL	188	109	297

SFRP Academic Titles	
Assistant Professor	79
Associate Professor	59
Professor	42
Instructor	3
Chairman	0
Visiting Professor	1
Visiting Assoc. Prof.	0
Research Associate	4
TOTAL	188

Source of Learning About the SRP		
Category	Applicants	Selectees
Applied/participated in prior years	28%	34%
Colleague familiar with SRP	19%	16%
Brochure mailed to institution	23%	17%
Contact with Air Force laboratory	17%	23%
IEEE Spectrum	2%	1%
BIIHE	1%	1%
Other source	10%	8%
TOTAL	100%	100%

APPENDIX B – SRP EVALUATION RESPONSES

1. OVERVIEW

Evaluations were completed and returned to RDL by four groups at the completion of the SRP. The number of respondents in each group is shown below.

Table B-1. Total SRP Evaluations Received

Evaluation Group	Responses
SFRP & GSRPs	275
HSAPs	113
USAF Laboratory Focal Points	84
USAF Laboratory HSAP Mentors	6

All groups indicate unanimous enthusiasm for the SRP experience.

The summarized recommendations for program improvement from both associates and laboratory personnel are listed below:

A. Better preparation on the labs' part prior to associates' arrival (i.e., office space, computer assets, clearly defined scope of work).

B. Faculty Associates suggest higher stipends for SFRP associates.

C. Both HSAP Air Force laboratory mentors and associates would like the summer tour extended from the current 8 weeks to either 10 or 11 weeks; the groups state it takes 4-6 weeks just to get high school students up-to-speed on what's going on at laboratory. (Note: this same argument was used to raise the faculty and graduate student participation time a few years ago.)

2. 1996 USAF LABORATORY FOCAL POINT (LFP) EVALUATION RESPONSES

The summarized results listed below are from the 84 LFP evaluations received.

1. LFP evaluations received and associate preferences:

Table B-2. Air Force LFP Evaluation Responses (By Type)

		How Many Associates Would You Prefer To Get ? (% Response)											
		SFRP				GSRP (w/Univ Professor)				GSRP (w/o Univ Professor)			
Lab	Evals Recv'd	0	1	2	3+	0	1	2	3+	0	1	2	3+
AEDC	0	-	-	-	-	-	-	-	-	-	-	-	-
WHMC	0	-	-	-	-	-	-	-	-	-	-	-	-
AL	7	28	28	28	14	54	14	28	0	86	0	14	0
FJSRL	1	0	100	0	0	100	0	0	0	0	100	0	0
PL	25	40	40	16	4	88	12	0	0	84	12	4	0
RL	5	60	40	0	0	80	10	0	0	100	0	0	0
WL	46	30	43	20	6	78	17	4	0	93	4	2	0
Total	84	32%	50%	13%	5%	80%	11%	6%	0%	73%	23%	4%	0%

LFP Evaluation Summary. The summarized responses, by laboratory, are listed on the following page. LFPs were asked to rate the following questions on a scale from 1 (below average) to 5 (above average).

2. LFPs involved in SRP associate application evaluation process:
   a. Time available for evaluation of applications:
   b. Adequacy of applications for selection process:
3. Value of orientation trips:
4. Length of research tour:
5. a. Benefits of associate's work to laboratory:
   b. Benefits of associate's work to Air Force:
6. a. Enhancement of research qualifications for LFP and staff:
   b. Enhancement of research qualifications for SFRP associate:
   c. Enhancement of research qualifications for GSRP associate:
7. a. Enhancement of knowledge for LFP and staff:
   b. Enhancement of knowledge for SFRP associate:
   c. Enhancement of knowledge for GSRP associate:
8. Value of Air Force and university links:
9. Potential for future collaboration:
10. a. Your working relationship with SFRP:
    b. Your working relationship with GSRP:
11. Expenditure of your time worthwhile:

(Continued on next page)

12. Quality of program literature for associate:
13. a. Quality of RDL's communications with you:
    b. Quality of RDL's communications with associates:
14. Overall assessment of SRP:

Table B-3. Laboratory Focal Point Reponses to above questions

	AEDC	*AL*	*FJSRL*	*PL*	*RL*	*WHMC*	*WL*
# Evals Recv'd	0	7	1	14	5	0	46
Question #							
2	-	86 %	0 %	88 %	80 %	-	85 %
2a	-	4.3	n/a	3.8	4.0	-	3.6
2b	-	4.0	n/a	3.9	4.5	-	4.1
3	-	4.5	n/a	4.3	4.3	-	3.7
4	-	4.1	4.0	4.1	4.2	-	3.9
5a	-	4.3	5.0	4.3	4.6	-	4.4
5b	-	4.5	n/a	4.2	4.6	-	4.3
6a	-	4.5	5.0	4.0	4.4	-	4.3
6b	-	4.3	n/a	4.1	5.0	-	4.4
6c	-	3.7	5.0	3.5	5.0	-	4.3
7a	-	4.7	5.0	4.0	4.4	-	4.3
7b	-	4.3	n/a	4.2	5.0	-	4.4
7c	-	4.0	5.0	3.9	5.0	-	4.3
8	-	4.6	4.0	4.5	4.6	-	4.3
9	-	4.9	5.0	4.4	4.8	-	4.2
10a	-	5.0	n/a	4.6	4.6	-	4.6
10b	-	4.7	5.0	3.9	5.0	-	4.4
11	-	4.6	5.0	4.4	4.8	-	4.4
12	-	4.0	4.0	4.0	4.2	-	3.8
13a	-	3.2	4.0	3.5	3.8	-	3.4
13b	-	3.4	4.0	3.6	4.5	-	3.6
14	-	4.4	5.0	4.4	4.8	-	4.4

3. 1996 SFRP & GSRP EVALUATION RESPONSES

The summarized results listed below are from the 257 SFRP/GSRP evaluations received.

Associates were asked to rate the following questions on a scale from 1 (below average) to 5 (above average) - by Air Force base results and over-all results of the 1996 evaluations are listed after the questions.

1. The match between the laboratories research and your field:
2. Your working relationship with your LFP:
3. Enhancement of your academic qualifications:
4. Enhancement of your research qualifications:
5. Lab readiness for you: LFP, task, plan:
6. Lab readiness for you: equipment, supplies, facilities:
7. Lab resources:
8. Lab research and administrative support:
9. Adequacy of brochure and associate handbook:
10. RDL communications with you:
11. Overall payment procedures:
12. Overall assessment of the SRP:
13. a. Would you apply again?
    b. Will you continue this or related research?
14. Was length of your tour satisfactory?
15. Percentage of associates who experienced difficulties in finding housing:
16. Where did you stay during your SRP tour?
    a. At Home:
    b. With Friend:
    c. On Local Economy:
    d. Base Quarters:
17. Value of orientation visit:
    a. Essential:
    b. Convenient:
    c. Not Worth Cost:
    d. Not Used:

SFRP and GSRP associate's responses are listed in tabular format on the following page.

Table B-4. 1996 SFRP & GSRP Associate Responses to SRP Evaluation

	Arnold	Brooks	Edwards	Eglin	Griffis	Hanscom	Kelly	Kirtland	Lackland	Robins	Tyndall	WPAFB	average
# res	6	48	6	14	31	19	3	32	1	2	10	85	257
1	4.8	4.4	4.6	4.7	4.4	4.9	4.6	4.6	5.0	5.0	4.0	4.7	4.6
2	5.0	4.6	4.1	4.9	4.7	4.7	5.0	4.7	5.0	5.0	4.6	4.8	4.7
3	4.5	4.4	4.0	4.6	4.3	4.2	4.3	4.4	5.0	5.0	4.5	4.3	4.4
4	4.3	4.5	3.8	4.6	4.4	4.4	4.3	4.6	5.0	4.0	4.4	4.5	4.5
5	4.5	4.3	3.3	4.8	4.4	4.5	4.3	4.2	5.0	5.0	3.9	4.4	4.4
6	4.3	4.3	3.7	4.7	4.4	4.5	4.0	3.8	5.0	5.0	3.8	4.2	4.2
7	4.5	4.4	4.2	4.8	4.5	4.3	4.3	4.1	5.0	5.0	4.3	4.3	4.4
8	4.5	4.6	3.0	4.9	4.4	4.3	4.3	4.5	5.0	5.0	4.7	4.5	4.5
9	4.7	4.5	4.7	4.5	4.3	4.5	4.7	4.3	5.0	5.0	4.1	4.5	4.5
10	4.2	4.4	4.7	4.4	4.1	4.1	4.0	4.2	5.0	4.5	3.6	4.4	4.3
11	3.8	4.1	4.5	4.0	3.9	4.1	4.0	4.0	3.0	4.0	3.7	4.0	4.0
12	5.7	4.7	4.3	4.9	4.5	4.9	4.7	4.6	5.0	4.5	4.6	4.5	4.6
Numbers below are percentages													
13a	83	90	83	93	87	75	100	81	100	100	100	86	87
13b	100	89	83	100	94	98	100	94	100	100	100	94	93
14	83	96	100	90	87	80	100	92	100	100	70	84	88
15	17	6	0	33	20	76	33	25	0	100	20	8	39
16a	-	26	17	9	38	23	33	4	-	-	-	30	
16b	100	33	-	40	-	8	-	-	-	-	36	2	
16c	-	41	83	40	62	69	67	96	100	100	64	68	
16d	-	-	-	-	-	-	-	-	-	-	-	0	
17a	-	33	100	17	50	14	67	39	-	50	40	31	35
17b	-	21	-	17	10	14	-	24	-	50	20	16	16
17c	-	-	-	-	10	7	-	-	-	-	-	2	3
17d	100	46	-	66	30	69	33	37	100	-	40	51	46

4. 1996 USAF LABORATORY HSAP MENTOR EVALUATION RESPONSES

Not enough evaluations received (5 total) from Mentors to do useful summary.

5. 1996 HSAP EVALUATION RESPONSES

The summarized results listed below are from the 113 HSAP evaluations received.

HSAP apprentices were asked to rate the following questions on a scale from 1 (below average) to 5 (above average)

1. Your influence on selection of topic/type of work.
2. Working relationship with mentor, other lab scientists.
3. Enhancement of your academic qualifications.
4. Technically challenging work.
5. Lab readiness for you: mentor, task, work plan, equipment.
6. Influence on your career.
7. Increased interest in math/science.
8. Lab research & administrative support.
9. Adequacy of RDL's Apprentice Handbook and administrative materials.
10. Responsiveness of RDL communications.
11. Overall payment procedures.
12. Overall assessment of SRP value to you.
13. Would you apply again next year? Yes (92 %)
14. Will you pursue future studies related to this research? Yes (68 %)
15. Was Tour length satisfactory? Yes (82 %)

	Arnold	Brooks	Edwards	Eglin	Griffiss	Hanscom	Kirtland	Tyndall	WPAFB	Totals
# resp	5	19	7	15	13	2	7	5	40	113
1	2.8	3.3	3.4	3.5	3.4	4.0	3.2	3.6	3.6	3.4
2	4.4	4.6	4.5	4.8	4.6	4.0	4.4	4.0	4.6	4.6
3	4.0	4.2	4.1	4.3	4.5	5.0	4.3	4.6	4.4	4.4
4	3.6	3.9	4.0	4.5	4.2	5.0	4.6	3.8	4.3	4.2
5	4.4	4.1	3.7	4.5	4.1	3.0	3.9	3.6	3.9	4.0
6	3.2	3.6	3.6	4.1	3.8	5.0	3.3	3.8	3.6	3.7
7	2.8	4.1	4.0	3.9	3.9	5.0	3.6	4.0	4.0	3.9
8	3.8	4.1	4.0	4.3	4.0	4.0	4.3	3.8	4.3	4.2
9	4.4	3.6	4.1	4.1	3.5	4.0	3.9	4.0	3.7	3.8
10	4.0	3.8	4.1	3.7	4.1	4.0	3.9	2.4	3.8	3.8
11	4.2	4.2	3.7	3.9	3.8	3.0	3.7	2.6	3.7	3.8
12	4.0	4.5	4.9	4.6	4.6	5.0	4.6	4.2	4.3	4.5
Numbers below are percentages										
13	60%	95%	100%	100%	85%	100%	100%	100%	90%	92%
14	20%	80%	71%	80%	54%	100%	71%	80%	65%	68%
15	100%	70%	71%	100%	100%	50%	86%	60%	80%	82%

SYNTHESIS OF A HIGH-ENERGY BINDER

Michael L. Berry

Highland High School
39055 25th St. West
Palmdale, CA 93551

Final Report for:
High School Apprentice Program
Phillips Laboratory

Sponsored by:
Air Force Office of Scientific Research
Bolling Air Force Base, DC

and

Phillips Laboratory

August 1996

SYNTHESIS OF A HIGH-ENERGY BINDER

Michael L. Berry
Highland High School

Abstract

Certain ingredients are necessary in order to create an effective propellant. Different methods of preparing solid propellants have been attempted over the years. However, with the high cost of sending material into space, it has become imperative that we develop a cheaper means of making a more cost efficient rocket fuel. What is needed is a propellant ingredient that will create a high-energy propellant at less cost.

The processes and results of experiments attempting to produce a more effective and energetic additive for the liquid oxidizer hydroxylammonium nitrate (HAN) are presented.

SYNTHESIS OF A HIGH-ENERGY BINDER

Michael L. Berry

Introduction

Tests throughout the 1980s demonstrated the energetic potential of the solution propellant hydroxylammonium nitrate (HAN). In the 1990s, there has been renewed interest in HAN because it's environmentally safe. Other chlorated oxidizers, such as ammonium perchlorate (AP), have acidic byproducts, such as hydrocloric acid (HCl), and can cause acid rain and other damaging effects to the environment. However, HAN is a unique liquid monopropellant in that the cation is a reducing agent, while the anion is an oxidizer. All modern propellants use an elastomeric matrix which imparts rubber-like elasticity to the propellant grain. The matrix, or binder, also serves as fuel for the oxidizer, producing the necessary exhaust gases for propulsion.[1] Since HAN is a liquid salt, it is easily broken down by other substances, as well as ionizing in water. Therefore, it is difficult to develop a binder compatible with HAN. Currently, the most effective binder being used is poly vinyl alcohol (PVA). However, over time this mixture may eventually become defective by "creeping", or losing its shape. If this happens, the strain-augmented burning will cause the fuel not to burn at a constant rate. Also this causes the propellant to peel off the sides of the rocket case and debond, which yields more surface area, allowing for a possible explosion. This occurrence necessitates the development of a binder with a greater potential energy (although the hydroxyl groups included in PVA do possess some) and one that is compatible with HAN for many years. Also, it is desirable that the additive can be manipulated in such a way that other molecular groups (nitro-, nitrato-, cyano, and azido) may be added to the straight chain polymer in order to create a more powerful substance. Ultimately, the goal is to attain additional performance with high-energy binders and an increased specific impulse, or I_{sp}.

Specific impulse is a relative term with numerous definitions. It is a rate used to compare and contrast the efficiencies of rockets and to determine which performance is optimal. The specific impulse of a rocket is equal to the thrust (the force exerted by the propellants) divided by the propellant flow rate.

$$I_{sp} = v_e/g_o = 1/g_o\sqrt{(2(h_c-h_e))}$$

$$= 1/g_o\sqrt{(((2\gamma(1-(p_e/p_c)^{\gamma-1/\gamma})R) + (\gamma-1))(Tc/M))}$$

γ = Cp(heat capacity at constant pressure) + Cv(heat capacity at constant volume)

R = gas constant, Tc = chamber temperature

M = mean molar mass of exhaust gas

p_e, p_c = pressure in nozzle and chamber

h_n, h_c = enthalpy in nozzle and chamber

v_n = propellant gas velocity

g_o = acceleration due to gravity at sea level

From a chemist's standpoint, there are limitations as to what can be done to improve the specific impulse. There, are however, a couple of conditions that are available for alteration, the chamber temperature, or Tc, being one of them. Ideally, one would want a high exothermicity (high negative heat formation per gram) of the combustion products, low exothermicity for the propellant components before combustion, low molecular weight exhaust gases, and high density reactants. Accomplishing these will achieve a greater heat release during the combustion reaction, which will cause a higher chamber temperature and a higher performance.

The molecular weight of a propellant ingredient is another aspect of specific impulse that is able to be modified. To obtain a lower average molecular weight of the exhaust gases, combustion is often controlled so that some of the hydrogen is left unburned. While this method will not realize the maximum heat of combustion, the light H_2 molecules and the larger number of gas molecules in the exhaust will yield a higher specific impulse than there would be possible otherwise.

This synthesis will eventually lead to a linear polymer-like material that can be manipulated to place different functional groups and versatile enough to be used with other oxidizers besides HAN, as well as form a copolymer-like structure so it could be used as a plasticizer.

Methodology

Began experiment by refluxing 63.02 g (685 mmol) of Bicyclo [2,2,1] hepta [2,5] diene (Norbornadiene) and 202 mL of 96% formic acid (HCO_2H) at 120-125°C to produce 104.9 g (576 mmol) of a yellowish diformate at an 84% yield.

A thin layer chromatograph (TLC) was conducted to see whether or not the reaction was complete. To do so, a small glass plate coated on one side with a thin layer of silicon was used. The starting material was spotted on the bottom left using a capillary, and the reaction material was spotted on the bottom right. This plate was then placed, with the spots facing down, in a solvent chamber containing a small amount of a 20% ethyl acetate, 80% hexane solution. This percentage ratio was chosen because, for our purposes, it will carry the molecules far enough up the plate., while under other circumstances this ratio may need to be different. The molecules will be carried up the plate at a different rate depending on their polarities and a spot may be visualized using either UV rays, iodine gas, or a special reagent spray (phosphomolybolic acid, 15 g, and ceric ammonium sulfate, 2.5 g, dissolved in a mixture of water, 985 mL, and concentrated sulfuric acid). If the two spots are at an equal height, there is still starting material left in the compound and the reaction is not yet complete.

Step 1

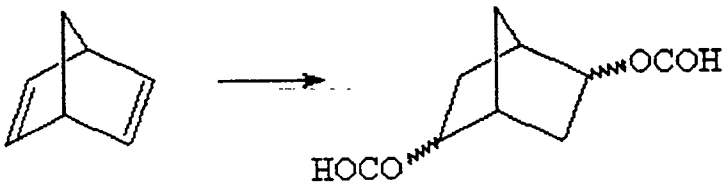

63.02 g, 685 mmol 104.91 g, 576 mmol

Compound was then distilled to remove excess formic acid at 26-30°C and 14-16 torr. When this process was completed, the remaining diformate was distilled from the dark residue in a separate flask at 125-132°C and 10-15 torr. Oxidation was conducted according to established procedures[2]. A Jones Reagent consisting of 52.40 g CrO_3 and 46 mL Sulfuric acid was diluted to 200 mL and added to a mixture of chilled diformate (25.1 g, 138 mmol, 84% yield) and reagent grade acetone (400 mL). This blend was set in an ice bath due to the exothermicity of the reaction and left to stir mechanically overnight. The reaction yielded a clear solution which was decanted from a thick green sludge of inorganic chromate salt. The remaining sludge was rinsed with acetone which was then extracted with dry potassium carbonate. The K_2CO_3 was filtered out and the filterate concentrated with rotary vaporization. The excess water was removed by azeotroping the mixture with benzene. The resulting product was again subjected to rotary vaporization to remove excess solvent and the dried mixture was washed with acetone to dissolve the product while excluding the thin, brown layer of impurities. The acetone was removed and the compound was sublimed at 80°C and 1 torr to furnish a solid white crystal (6.71 g, 54.1 mmol, 40% yield).

Step 2

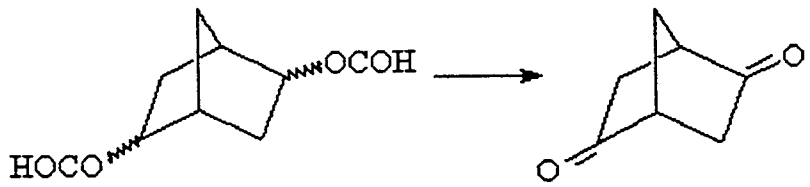

25.1 g, 138 mmol 6.71 g, 54.1 mmol

After the crystal was collected, a infrared spectroscopy(IR) test was performed using KBr pellets. This test investigates the changes in the vibrational motions of the atoms in its molecules. The energy associated with each vibrational transition depends on the masses of the atoms that are bonded together and on the strength of the bond. The IR is a source of information about the types of bonds the compound contains and is most useful in identifying the presence of specific functional groups, such as hydroxyl and carbonyl groups[3]. Using the results

from this series of tests, it was determined that the compound was indeed a ketone but contained small traces of some impurities.

Conclusion

IR RESULTS

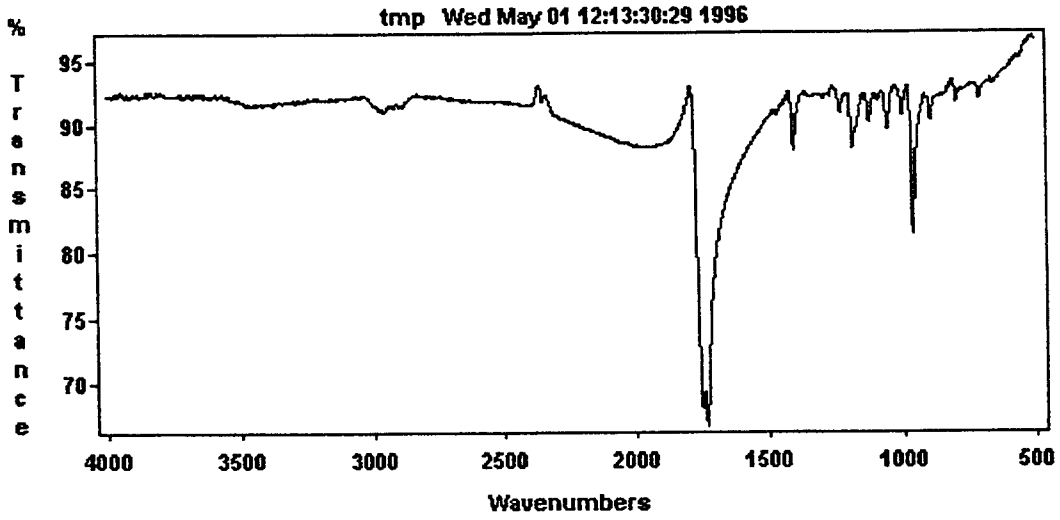

The picture above represents what a reading of the sample of the dione should look like. It was created by the students at USC. Notice that there is only one dip in the 1705-1725 range, which is exactly where a ketone group should appear. Also, there are few other dips in the graph, indicating a lack of impurities. Another important part of the graph worthy of noting is the fingerprint region, located on the far right. This region is immensely useful in making a positive identification of a compound. If two species show the same bands with similar intensities in this region, as well as similarities in the rest of the graph, that is considered to be proof that they are the same.

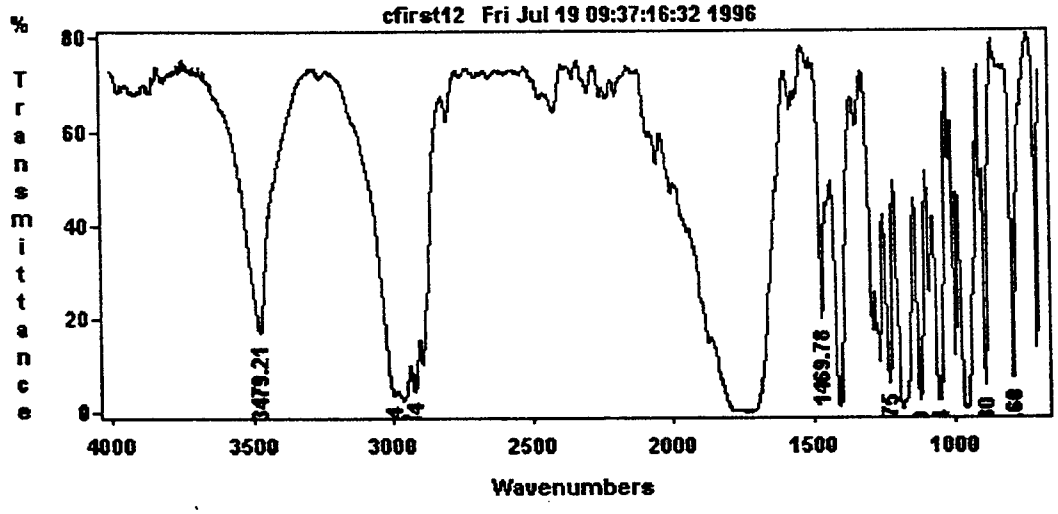

Pictured above is a graph of the original dione sample produced preliminarily. The dips on the left side of the graph represent a small amount of water contaminating the sample. This can be corrected by simply dehydrating the crystal.

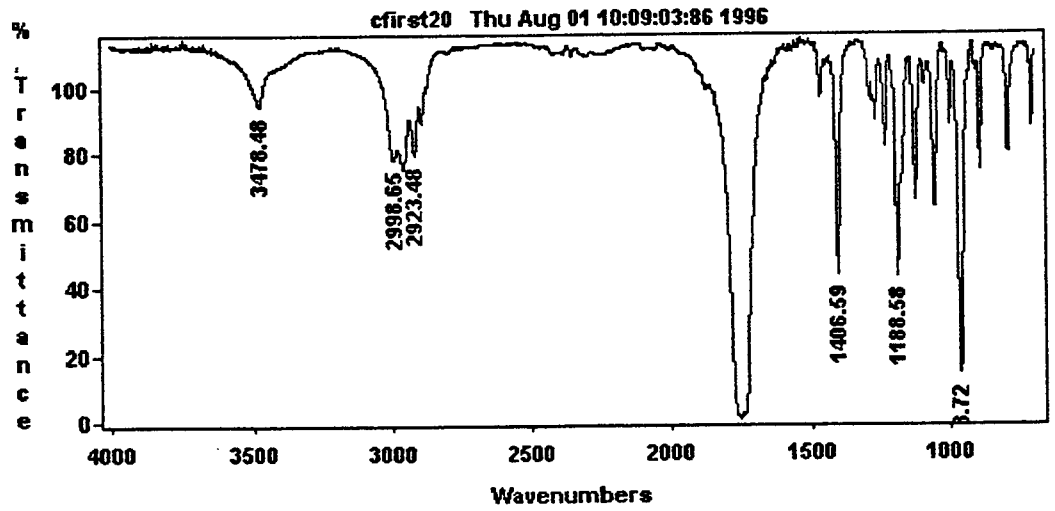

This third and final graph was taken after dehydrating the sample to remove excess water. Notice the dips on the left have significantly decreased, while the ketone remains.

The research described in this paper was only part of the overall synthesis, which was too lengthy too have been completed in eight weeks. The processes previously illustrated will be continued further until the binder is successfully completed.

References

1. Oberth, Adolf E. *Principles of Solid Propellant Development*, Laurel, Maryland **1987** p. 2-1.

2. Kleinfelter, D.C. and Schleyer, P.v.R. *Organic Syntheses*, Collect. Vol. V, ed. H.E. Baumgarten, Wiley, New York, **1973**, p 852.

3. Ege, Seyhan N. *Organic Chemistry*, Lexington, Massachusetts **1989** p. 355.

USING A SCANNER AND COMPUTER TO UPDATE A TECHNICAL INSTRUCTION MANUAL

Emily R. Blundell

Rosamond High School
2925 Rosamond Blvd.
Rosamond, CA 93560

Final Report for:
High School Apprentice Program
Phillips Laboratory

Sponsored by:
Air Force Office of Scientific Research
Bolling Air Force Base, DC

and

Phillips Laboratory

August 1996

USING A SCANNER AND COMPUTER TO UPDATE A TECHNICAL INSTRUCTION MANUAL

Emily R. Blundell
Rosamond High School

Abstract

When using the computer to update the technical instruction manual, many different applications were used (the computer applications that were used were from Windows 95). Using an OP Scanner, the pages were scanned into the computer. Occasionally, the scanner would not allow some pages to be scanned. Then pages that could not be scanned needed to be typed into the computer using a word processing program, such as Microsoft Word. The book included graphs and pictures that needed to be put in the computer also. In doing this the picture or graph was scanned in and then was transferred to an application that could read the pictures, such as Picture Publisher or Image Writer. Once everything is scanned and corrected then it can printed out and put into a binder.

USING A SCANNER AND COMPUTER TO UPDATE A TECHNICAL INSTRUCTION MANUAL

Emily R. Blundell
Rosamond High School

The technical instruction manual is a book on project instructions for uses of piping, valves, compounds, etc. The instruction manual hadn't been updated in a few years. So many of the instructions, use of compounds, symbols, standards, and specifications were old and needed to be updated with the new specifications, standards, symbols, use of compounds, and instructions. Scanning the pages was the best way to put the manual into the computer. Now and then the scanner wouldn't scan so the only other way was to re-type it into the computer.

The method of using a scanner and computer when updating the manual is quite straightforward (the applications used were part of the Windows 95). With the scanner, the OP Scanner application must be open on the computer. Paper is placed in the scanner and then the auto button is clicked on. The paper is scanned in, then it is auto zoned and finally OCR reads the scanned in paper (occasionally the OCR doesn't recognize words or even the entire paper). Now the paper is given a file name. Once this is done, the OP Scanner application is closed and Microsoft Word, or the word processing program, is opened. The file is then reviewed and necessary corrections are made. This is done for every page of the Technical Instruction Manual until finished. Finally, when corrections have been done to all the files make then they are printed out and combined, in order, into a binder and is labeled "Technical Instructions".

The method above was used and was efficacious. To be assured that the new instruction manual is technically correct then an Engineer might be brought in to read it over.

I conclude that the process of updating a technical instruction manual is quite simple.

USING A SCANNER AND COMPUTER TO UPDATE A TECHNICAL INSTRUCTION MANUAL

Emily R. Blundell
Rosamond High School

References

1.) Windows 95

(a) Microsoft Word
(b) OP Scanner (includes OCR)
(c) Picture Publisher
(d) Image Writer

THE SYNTHESIS OF 3-OXAQUADRICYCLANE

Lillian A. Capell

Quartz Hill High School

6040 West Avenue L

Quartz Hill, Ca 93536

Final Report for:

High School Apprentice Program

Phillips Laboratory

Sponsored by:

Air force Office of Scientific Research

Bolling Air Force Base, DC

and

Phillips Laboratory

August 1996

The Synthesis of 3-Oxaquadricyclane

Lillian A. Capell
Quartz Hill High School

Abstract

During the summer of 1996 at Phillips Laboratory, Edwards Air Force Base, the synthesis of 3-oxaquadricyclane was studied. 3-oxaquadricyclane is synthesized from the photolytic conversion of 7-oxanorbornadiene, which was synthesized via the Diels-Alder Reaction. 3-oxaquadricyclane is a strained ring hydrocarbon which is of interest because it can be used as a rocket fuel additive. 3-oxaquadricyclane is also being researched because it decomposes to form an oxepin as an intermediate which has optical absorption. Since 3-oxaquadricyclane has to be made in the laboratory many techniques were used including distilling and deoxygenating fluids as well as the preparation of sodium amalgam.

THE SYNTHESIS OF 3-OXAQUADRICYCLANE

Lillian A. Capell
Quartz Hill High School

Introduction

Since World War II, rocket propulsion has matured from an elementary science to an engineering art. Today, industry can produce sophisticated liquid-propellant rocket engines capable of delivering payloads to low or geosynchronous earth orbit or to the planets and beyond. The engine makes this possible by converting the propellants into high-temperature gas through combustion, which releases the chemical energy of the propellant.

The most preferable propellant combination is that of liquid oxygen and liquid hydrogen. This combination has an energy per unit mass content above almost any other combination; however, both oxygen and hydrogen are cryogenic (temperature near absolute zero) when stored as liquids. Therefore, special containers are needed for storage on a spacecraft. While the available energy makes the combination attractive, the expense and weight associated with handling becomes a drawback in certain applications.

One alternative is to replace the liquid hydrogen with a fuel that is cheaper and easier to store. At first, this might seem to be an easy task, and one might consider replacing both cryogens with chemicals that release nearly the same energy. This has been tried, but the current environmental standards demand that "friendly" alternatives be found. To meet these somewhat conflicting requirements, science old and new must come together in innovative ways.

For centuries, people have known that hydrocarbon-based liquids make excellent fuels. For example, crude oil has been used since nearly the dawn of human existence to light homes with oil lamps and torches. On a more modern note, kerosene was used to power the launch vehicles that sent men to the moon. Additionally, kerosene is fuel that can be easily stored and is relatively inexpensive. The problem with kerosene, as with practically all other hydrocarbon-based fuels, is that the available energy from combustion is significantly below that of hydrogen.

Lately, researchers have been exploring methods to increase the amount of energy that can be obtained from hydrocarbon-based fuels during the combustion process. This is not to say that the focus is one of extracting energy where none exists, but rather that of finding ways to increase the efficiency of combustion. While efficiency increases are important, the reduced energy content of the hydrocarbons must still be addressed. To this end, researchers have found that certain compounds can be added to kerosene to yield greater performance and still retain the benefits of a readily storable fuel. In the summer of 1995, a compound called quadricyclane was tested in a liquid-propellant engine that was originally designed

specifically for kerosene. For those tests, quadricyclane, in concentrations between 25 and 75 percent, was mixed with kerosene and evaluated. Data from those tests is still being reviewed, but researchers indicate that the engine performance was enhanced by the addition of quadricyclane. However, the preliminary findings did validate the approach of additives, which led to expanded research.

Based on the apparent success of quadricyclane, the synthesis of 3-oxaquadricyclane (fig. 1) was studied during the summer of 1996. 3-oxaquadricyclane is a strained ring hydrocarbon that also can be used as a rocket propellant additive to enhance engine performance. Also, this form is of interest because it decomposes to form an oxepin (fig. 2) as an intermediate, which has optical absorption. This paper addresses the production of 3-oxaquadricyclane.

Synthesis

The synthesis of 3-oxaquadricyclane involves the photolytic conversion of 7-oxanorbornadiene (the IUPAC name of 7-oxanorbornadiene is bicyclo[2.2.1]-7-oxa-hepta-3-5 2,5-diene) synthesized via the Diels-Alder Reaction. The synthesis of 7-oxanorbornadiene is a complex process of distilling and deoxygenating fluids as well as preparing sodium amalgam.

The Diels-Alder Reaction, as it pertains to this study, is an addition reaction in which carbon-1 and carbon-4 of the conjugated diene reaction become attached to a second doubly-bonded carbon dieneophile to form a six member ring. Furan, the diene, is combined with trans-1,2- Bis(phenylsulfonyl)ethylene to complete the Diels-Alder Reaction (fig. 3).

The 7-oxanorbornadiene preparation started with the distillation of furan. Furan is a colorless liquid that combines with trans-1,2-Bis(phenylsulfonyl)ethylene in a dichloromethane solvent to complete the Diels-Alder reaction. After the completing the synthesis the yield was calculated to be 94.5%. The product of the reaction is bicyclo[2.2.1]7-oxa-5,6-Bis(phenylsulfonyl)-2-heptene. Bicyclo[2.2.1]7-oxa-5,6-Bis(phenylsulfonyl)-2-heptene is then added to a solution containing a methanol solvent, sodium dihydrogenphosphate as a buffer, and sodium amalgam (Na/Hg) to strip bicyclo[2.2.1]7-oxa-5,6-Bis(phenylsulfonyl)-2-heptene of the two phenylsulfonyl group and the result is 7-oxanorbornadiene (see below reaction).

$$C_{18}O_5H_{16}S_2 + Na/Hg \xrightarrow[NaH_2PO_4]{MeOH} C_6OH_6$$

Methodology

Oxygen reacts with the products in the various reactions; therefore, to ensure that no unwanted reactions involving oxygen would take place, the dichloromethane and the 2,2,4-trimethylpentane solvents

were deoxygenated. In order to deoxygenate the dichloromethane a freeze/pump/thaw method was used. A flask of dichloromethane was placed into a bath of liquid nitrogen. After the dichloromethane froze it was pumped under vacuum until the pressure gauge read under two microns. The dichloromethane was then taken out of the bath of nitrogen to thaw. While thawing, the solvent outgassed the oxygen. The process was completed three times.

In order to prepare sodium amalgam at 2% concentration, an initial amount of 10 gram of solid sodium was heated to 97.8 °C, its melting point. Thirty-three cubic centimeters of liquid mercury was then slowly added dropwise onto the molten sodium. After stirring, the amalgam was permitted to solidify. Sodium and mercury amalgams must be used immediately before oxidation in air occurs and removes the metallic sodium. This process also was completed three times.

Most hydrocarbons do not have optical absorption that is why the oxepin in this reaction was so unique in this aspect, because it does have optical absorption. Optical absorption is a technique used to follow the rapid change from starting material to intermediates to product. Since the intermediate step does not last, optical absorption uses a pulsed light source and a detector that can detect the presence of the intermediate, making the intermediate's mechanisms computable and leading to better understanding which can lead to process control.

The photolytic conversion of 7-oxanorbornadiene to 3-oxaquadricyclane involves the breaking up of carbon bonds by means of light, the broken carbons then bond to each other. Through that process 3-oxaquadricyclane is formed (fig. 4). First the 7-oxanorbornadiene is dissolved in a solvent of deoxygenated 2,2,4-trimethylpentane. The solution is then placed into a jacket of UV light, where the bonds are then broken and reattached. The 2,2,4-trimethylpentane is evaporated out and the product is distilled, leaving pure 3-oxaquadricyclane. The progress is monitored by taking aliquots from the solutions and analyzing them through a gas chromatograph . This process will be completed after participation ends.

Techniques

Throughout the synthesis process there were miscellaneous techniques used in addition to the ones indicated above, they included determining a melting point, reading nucleic magnetic resonance (NMR) and gas chromatographs, and using such apparatus as a rotoevaporator.

Conclusion

This research is the beginning step to try and produce a more cost efficient and easier stored fuel. Although the synthesis of 7-oxanorbornadiene was completed, the photolytic conversion of the 7-oxanorbornadiene to 3-oxaquadricyclane has not yet begun. The techniques listed above were essential to the completion of the synthesis of 7-oxanorbornadiene.

Figure 1

3-oxaquadricyclane

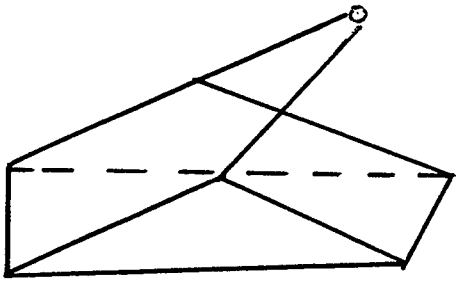

Figure 2

oxepin

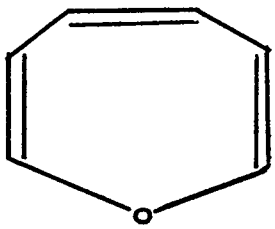

Figure 3

The Diels-Alder Reaction

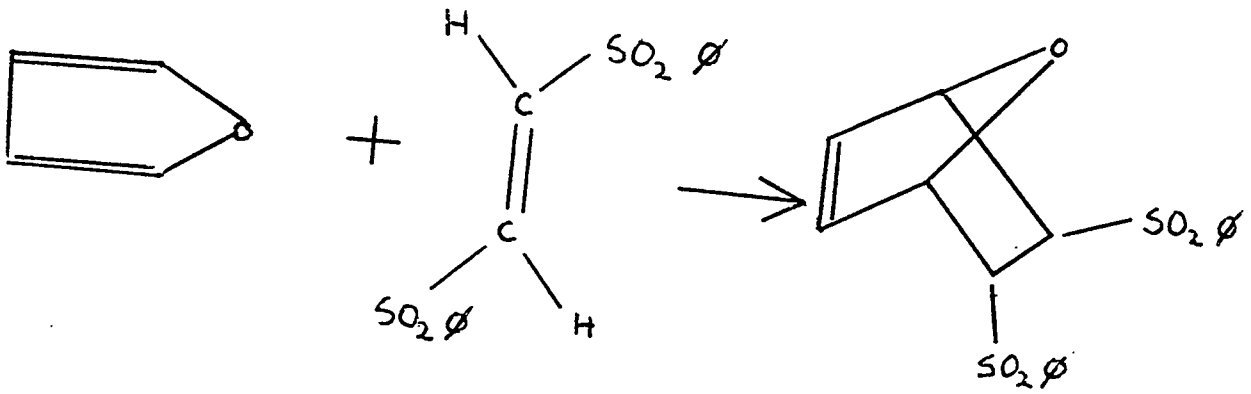

Figure 4

Photolytic Converison of 3-oxaquadricyclane

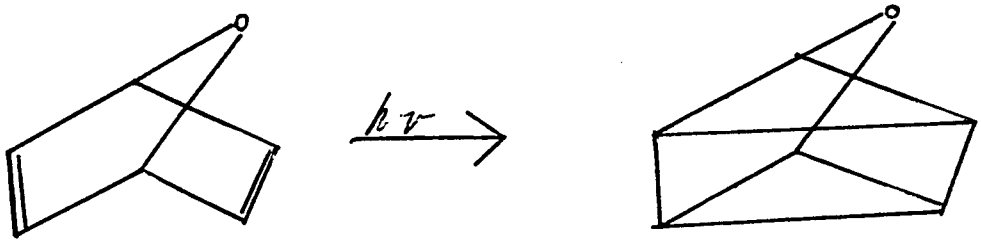

Acknowledgments

I would like to thank Angelo Alfano Ph.D. who gave me the knowledge and the skills that made this summer apprenticeship program for me a success and an enjoyable experience. I would also like to thank Angelo for the advice that he has given me succeed. Also I would like to express my appreciation to Doug Talley Ph.D. and Jay Levine for a new sense of guidance and direction. And to Pete Strakey who made me measure all of those orifice plates, thank you. A great thanks to Mike Griggs who made me literate of the mechanical world and who made me laugh. To Scott Bellamy for whom I owe thanks for teaching me rocketry in three days, for making me smile, and also for making me realize that I can do anything that I want to do if I apply myself. And to Dick Chapleau who has helped me in many ways with this program and who has broadened my understanding of computers. As well as Julie Carlisle who took the time teach me what I needed to know. And a final thanks goes to my parents who have supported me and who have stood by me my entire life.

Bibliography

1. R. Morrison and R. Boyd, *Organic Chemistry* ., 876, (1973).
2. W. Notes, J r. and P. Leighton, *The photo chemistry of gases.*, 12-40, (1966).
3. Huzel and Huang, *Design of Liquid-Propellant Rocket Engines.*, 50, (1992)

THE PRODUCTION OF CARBON COMPOSITE GRID STRUCTURES UTILIZING AN AUTOMATED PROCESS

Rebecca Cohen

Sandia Preparatory School
532 Osuna Rd, NE
Albuquerque, NM 87113

Final Report For:
High School Apprentice Program
Phillips Laboratory

Sponsored by:
Air Force Office of Scientific Research
Bolling Air Force Base, DC

and

Phillips Laboratory

July 1996

Abstract

As carbon composites strive for new growth and acceptance within the scientific community, new problems arise and need to be solved. One of these problems is the lack of ease in large scale manufacturing carbon composite structures with underlying support grids. The grid is necessary as it lends increased strength with minimal addition to the original weight. In order to find a process that could be shared with industry and used in further government enterprises, extensive research was done during the production of the first gridded, carbon composite shroud.

THE PRODUCTION OF CARBON COMPOSITE GRID STRUCTURES UTILIZING AN AUTOMATED PROCESS

Rebecca Cohen

Introduction

The usage of carbon composites in both technological and commercial applications has increased dramatically in recent years. The benefits of composites are twofold; they combine strength with diminished weight. Adding a gridded support system to the inside of a structure will increase the strength without dramatically changing the weight. A reinforcement grid will also reduce a structure's tendency to buckle without trapping heat or water as aluminum honeycomb does. Although there has been limited use of carbon composites within government aircraft, it has not yet been popularized due to the lack of an automated process. In order to compete with other industrial materials, the mass manufacture of large, composite grid products needs to be made available and inexpensive. A rocket scheduled to be launched early next year will incorporate the first carbon composite grid shroud wound using an automated process.

The obstacles to creating such a process are numerous. Although filament winders have long been used to "wrap" composite structures, never before have they been applied to creating a structure with an underlying support grid. In the past, panels demonstrating that such a grid was possible, were made by hand. Fibers were wound tightly into rubber grooves. Special sheets of rubber were made for this by pouring the liquid compound over metal ribs mirroring the pattern the fibers would be in. These "sheets" of rubber were three or four inches thick. This was acceptable when making a flat panel, but finished products were notably warped when the same technique was applied to circular or conic geometries.

Procedure

Because the rubber was an exceptional material for the grooves themselves, it was determined that rubber grooves would be set into a base material flush with the surface. The base material would stop warpage while simultaneously producing a "mold" weighing less than the bulky sheets of rubber. Fiber could be wound first into the grooves and then enclosing them. The original base material chosen was particle board. It was selected due to its performance under high temperature and pressure conditions i.e., it did not crack or collapse and could be used more than once. Unfortunately, it is a fairly heavy material and difficult to machine.

Although two test shrouds were wound successfully upon a base of particle board, the inconvenience in creating the cavities for the rubber insets was so great, a new base material was sought for the full length shroud. Balsa foam was tried as a replacement, but collapsed when tested under the pressure applied during the autoclave's full cure cycle. Advertised by one company, was a special tooling foam. Made specifically for composites, it was designed to withstand significant temperatures while being easy to machine. The first sample sent developed micro cracks when run through the cure cycle and nearly fell apart when an attempt was made to mill grooves into the surface. A different sample said to have the ability to perform under higher temperatures was then sent and tested and found to be satisfactory. Again, as the directive was to make an automated process as simple as possible, it was a pleasant surprise this foam machined so well.

While the base material was being chosen, someone else worked to calculate the ideal rib pattern to be machined into it. Load scenarios were developed using instrumentation data collected from previous rocket flights in order to determine the optimum placement of the support system. (**Figure 1-1**). Most of the load felt by a rocket shroud runs in the axial direction and occurs primarily during launch. The first load case is a simulation of the shroud as it pushes through the atmosphere. To gain the apogee, the trajectory of the rocket is angled causing low pressure to form over the upper surface and high pressure to give it lift from beneath. The second load case is generated mostly during launch. The forward thrust of the rocket causes resistance that pushes from the nose cone to the base of the rocket. This stress is added to by the rocket's own weight pushing down and back towards the earth. Because of these scenarios, it was important to have as much support in the axial direction as possible. Load cases were the main determining factor in the design of the node.

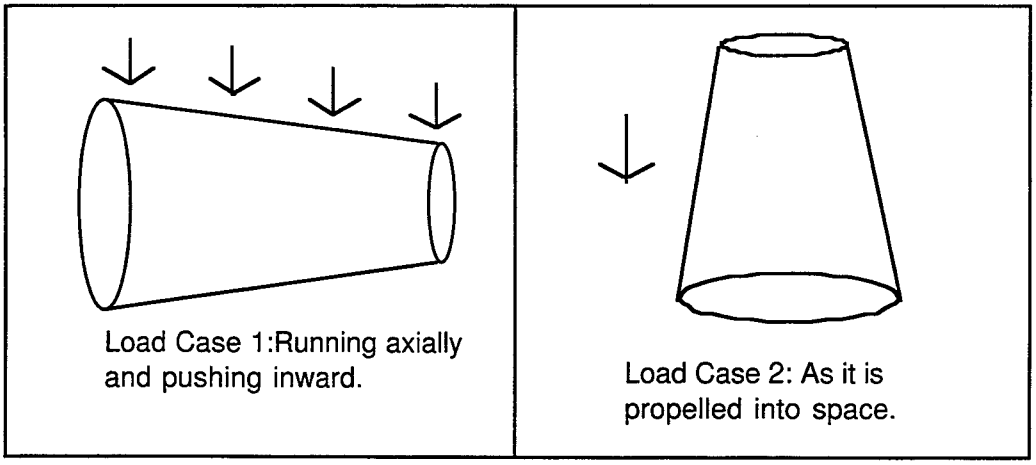

Figure 1-1: Load cases

Everywhere the fibers cross is known as a node. The nodes must be spaced evenly apart in order to properly support the outer casing. Their placement therefore is determined by the length and circumference of the shroud. Since the shroud is conic, the rubber insets were designed for the largest end and the arms and legs could then be cut shorter as the circumference diminished.

The final node design was a rib running axially with two ribs running at opposing angles circumferentially. Because the node is where so many fibers cross, there is the dilemma of fiber pileup which distorts the outer skin and adds uncertainty to the behavior of the resulting product. In anticipation of this particular problem, a nodal offset was selected. Instead of having a place where all three ribs intermingled, the ribs were slightly offset so that no more than two ribs would cross at a time in any given area. That is still twice the amount of fiber within each juncture, so a height was selected for the ribs (which translates into a particular depth for the rubber inset) that was then modified at the nodes. The depth of the rubber in that area was increased (**Figure 1-2**). This alteration, combined with the offset, left enough pileup to encourage merging with the skin but dismissed the original problem. The draft of the full node can be found in Appendix A.

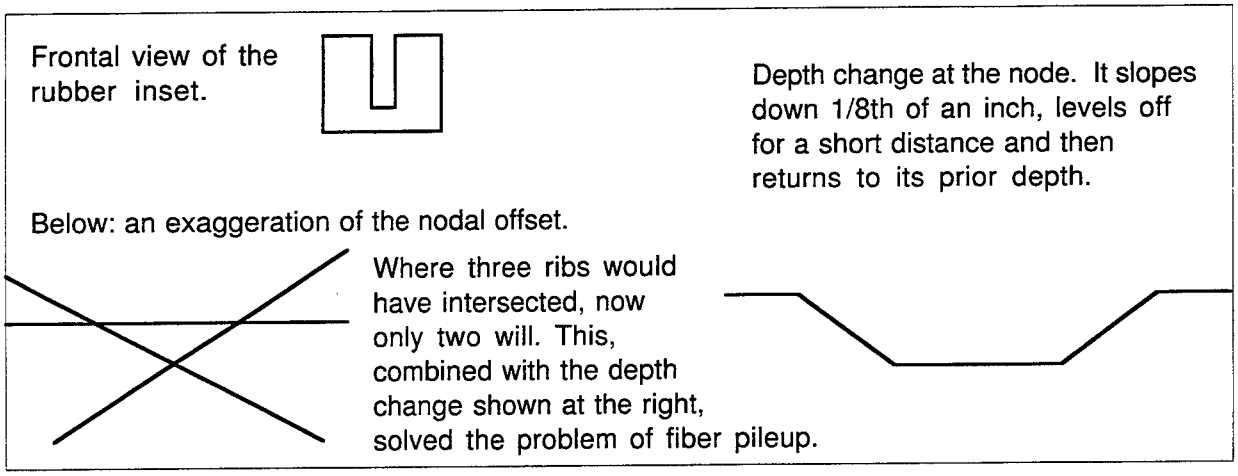

Figure 1-2: Nodal design

In conjunction with rib design, is the design for the skin. When assembling flat plates, laminates provide an easier route to making a skin. Laminates are separate sheets of carbon fiber laid one atop another. The fibers in each sheet run in the same direction. When creating a skin, multiple layers are needed and laid up at different angles so their fibers run in multiple directions. The best pattern for laying up a laminate is symmetrical so that no particular angle would be less fortified than the others, causing the skin to warp.

The behavior of laminates is easy to predict and understand because each layer is distinct

from the other. The shroud's skin, being done with the use of a winder, deviates slightly from the normal conception of a laminate and therefore, the behavior becomes harder to predict. Instead of the evident layers found in laminates, the program for the skin will be repeated several times, allowing the fibers to cross and blurring the boundaries between separate ply. (See **Figure 1-8**) Because of this unpredictability, the shroud is being designed for three times the projected loads and will be heavily tested.

Simultaneously being developed is an apparatus with the capabilities of simulating LEO (Low Earth Orbit) for testing purposes. A sample of the material to be tested is placed within a vacuum chamber. From one angle it is assailed by electrons from an electron gun. From another, UV radiation and protons. Also found in LEO are atomic Oxygen and Nitrogen. Since atmospheric oxygen and nitrogen is diatomic, they need to be split apart and then accelerated down the chamber and into the sample before they can reassociate. Electrons are used to force them apart, creating charged particles. Lining the chamber are plates with the same charge which repel the particles toward the far end, where they are again deflected and sent into the sample. Lastly, a laser is added and used to cut minute pieces of glass and then propel them into the sample in a simulation of the micro debris that exists up in space. The glass debris is so small - and it is the smallest debris in LEO that does so much damage over a period of time - the results are looked at under a scanning electron microscope.

A carbon composite structure was tested using this last method separately (**Figure 1-3**). As can be seen from the photograph taken, the structural damage . The damage done by one impact is minimal but the debris population in LEO is enough to cause concern about the durability of materials.

Photograph of impact crater formed by a microflyer. A laser beam creates the microflyer when it passes through a thin sheet of glass or metal, propelling it into the sample. The laser is a less expensive aid in the simulation of debris found in LEO (Low Earth Orbit) than the gas guns previously used.

Figure 1-3

Because a rocket is not in space for a long period of time, the structural integrity of the

shroud is not in doubt. The laser testing of materials is far more relevant for satellites or other flight hardware that will be exposed within low earth orbit for longer periods of time.

Results

Theory and experimentation culminate in the target process. It begins with a steel mandrel specially designed in the shape of a large octagon descending into a smaller octagon (**Figure 1-4**).

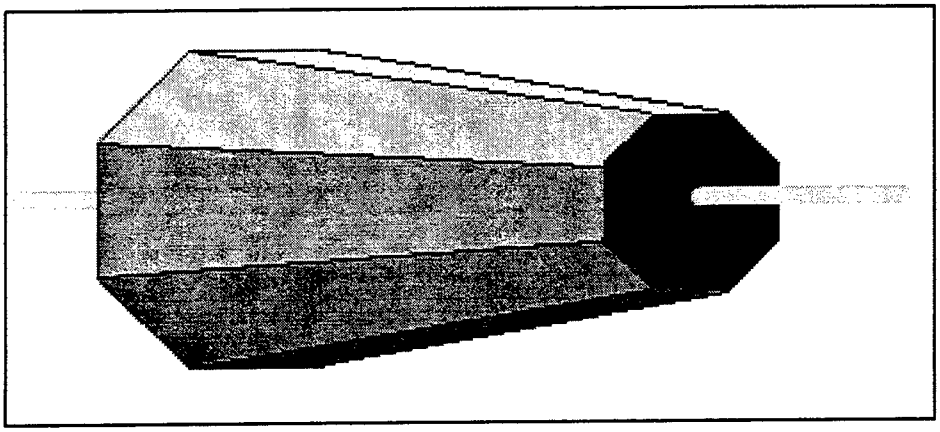

Figure 1-4: The steel mandrel and its shaft

The mandrel attaches to a shaft that fits into the filament winder. The tooling foam is in eight separate pieces that are bolted into place on the mandrel. The boards are shaped to mesh together and form the conic geometry required. The rubber insets can then be placed within the base material (**Figure 1-5**).

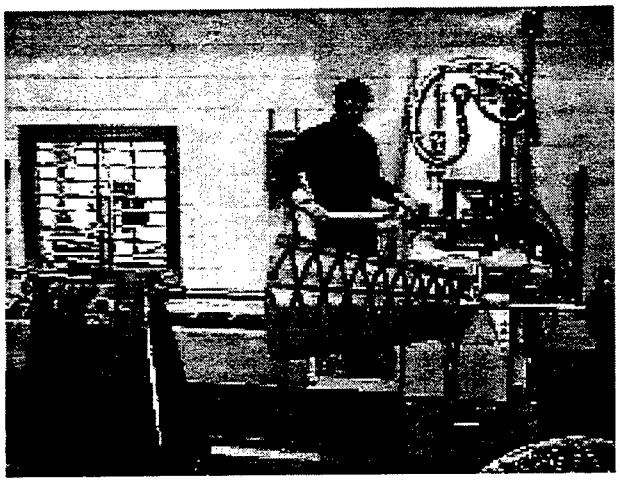

Particle board is mounted upon the steel mandrel. Set within its surface, rubber grooves are visible running axially and at opposing angles. The nodal offset is too small to be seen.

Figure 1-5

The programs have been written and tested for both the ribs and the skin. The fibers to

be wound are loaded onto a set of tensioners which keep the fiber taut during the winding. They are then threaded through a series of rollers to the head of the winder itself (The head can be seen in **Figure 1-7**). The winder can move within five axes allowing versatility in programming as well as production. The head moves within four directional planes and the turning of the mandrel creates the fifth possible axis (the winder in its entirety can be seen in **Figure 1-6**).

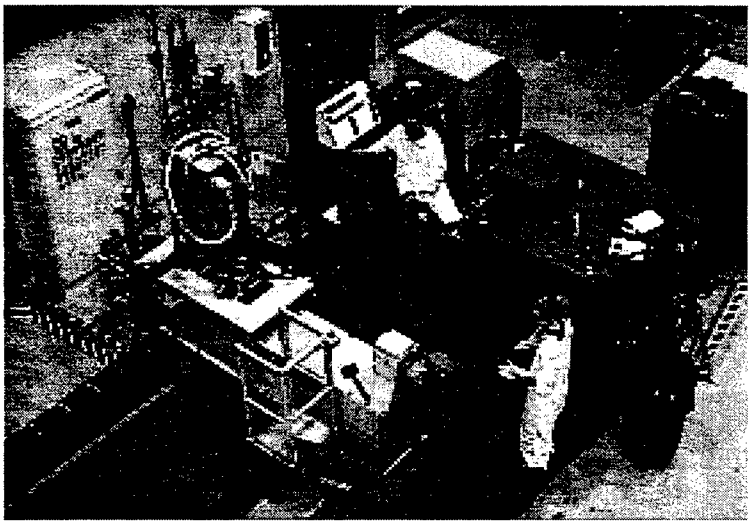

A bird's eye view of the winder shows Dr. Steven Huybrechts strategically placed between the tensioners and the controls to the winder as Rebecca Cohen oversees the winding of the ribs.

Figure 1-6

Styrofoam is cut into two domes to be placed at both ends to keep the carbon fibers from straying. The winding of the fibers can then begin. The program for the ribs and loaded and executed first. The procedure is watched closely for the foremost plys to ensure the fibers are matching correctly with the rubber grooves (**Figure 1-7**).

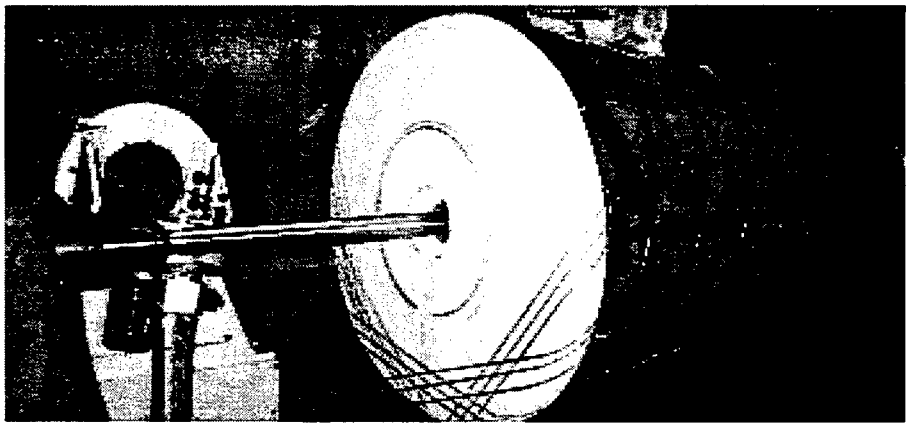

The head of the winder is slightly obscured by the mandrel's shaft, but the ribs can be seen in conjunction with the Styrofoam domes used to keep the fibers from slipping.

Figure 1-7

After the ribs, the program to wind the skin commences. The skin has a larger tendency to slide as it piles up on the ends so heat lamps are placed nearby. If needed, they will soften the resin embedded within the fibers allowing less slippage (**Figure 1-8**).

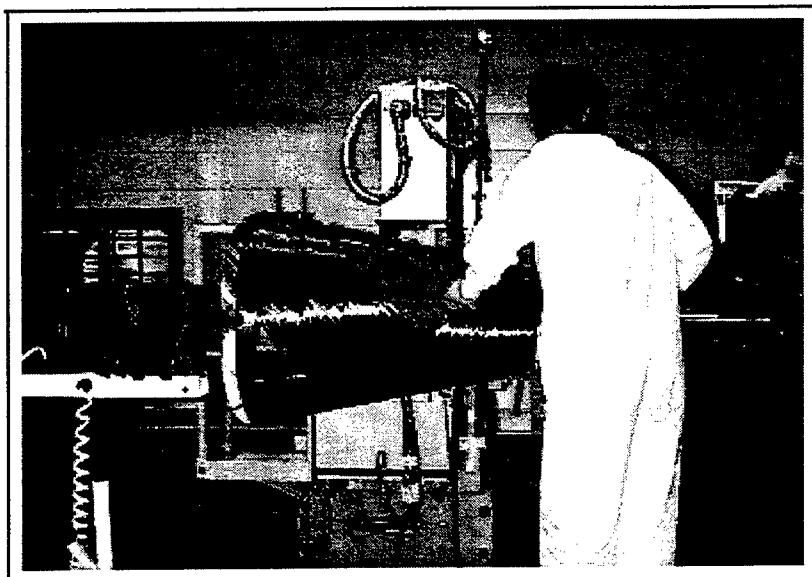

Staff Sergeant Lee Underwood stands at the mandrel as the first ply of the skin is wound. Unlike laminates, the plys wound over the shroud mesh together instead of forming separate layers. Heat lamps used to keep the carbon fiber from slipping at the ends wait off to the left.

Figure 1-8

At the completion of the skin, preparation for the autoclave begins. The shroud is wrapped in a Teflon sheet to prevent the carbon skin from sticking to the other bagging materials. A thick, cotton-like material known as bleeder ply is the next layer and is used to absorb the small amounts of resin that seep through the Teflon covering during the cure cycle. The final piece, called vacuum bagging, is a sheet of high temperature plastic (**Figure 1-9**).

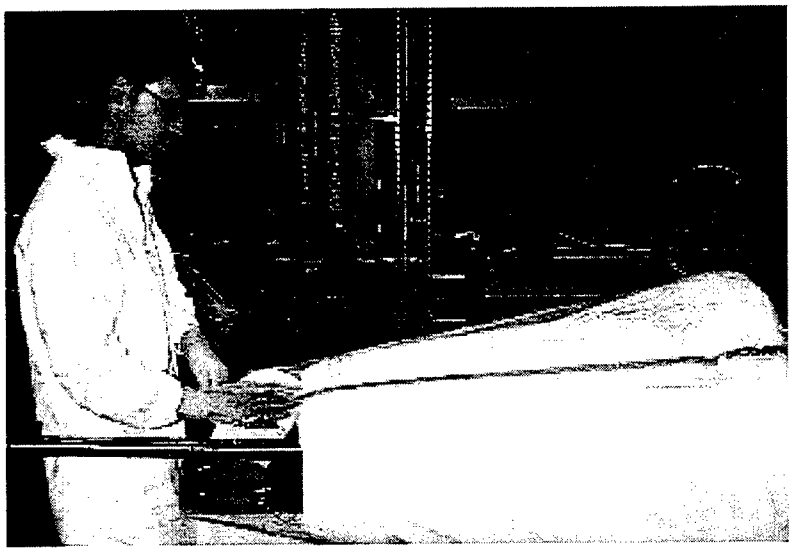

Troy Meink finishes bagging the test shroud. The bagging process consists of three different layers: the first keeps the fibers from sticking to the bagging material while the second soaks up extra resin produced during the heating. The third layer is made airtight so that a vacuum can be pulled and pressure can then be applied to the entire shroud.

Figure 1-9

In order for pressure to be applied evenly to the shroud, air is removed from the layers wrapped around it. A vacuum attachment is placed on the bleeder ply and exits through the vacuum bag where a hose from the autoclave can later be connected (the autoclave is shown in **Figure 1-10**).

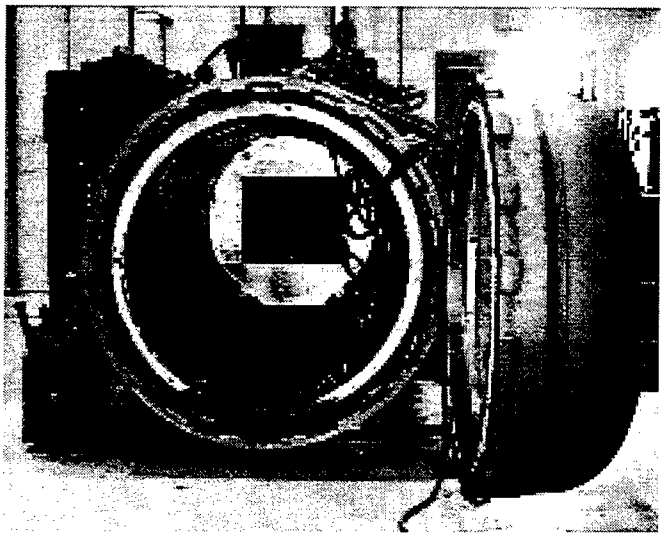

The Autoclave. A 10 x 4 ft oven, the autoclave can reach a maximum temperature of 800°F and a maximum pressure of 140 psi. It is inside here that the curing process takes place.

Vacuum attachments can be seen inside the autoclave and to the right.

Figure 1-10

The shroud - mandrel and all - is placed into the autoclave, the proper hoses are connected, and the program for the cure cycle is loaded.

During the full cycle, the shroud will undergo several different changes of temperature and pressure over varying periods of time. The resin in the fibers will liquefy and flow evenly over the ribs and skin. As it cools, the separate fibers are transformed into a solid material (**Figure 1-11**).

Figure 1-11

Conclusion

The successful production of two test shrouds indicate a bright future in the field of composites. After the final test when the rocket is launched early next year, all that remains to be done is to make the information available to others. This technology has incredible potential within further commercial applications. Already being considered is the production of other launch vehicle components, missile fins, and small aircraft. Carbon composites will be around for quite a while, as it shows continued promise and no signs of inability to compete with other materials currently in use.

Acknowledgments:

I am indebted to Dr. Steven Huybrechts, Troy Meink, and Staff Sergeant Lee Underwood for their generosity with encouragement, information, and advice.

Thanks to Charles Miglionico for sifting through the paperwork in time for May and for keeping the labs open and available to me.

Thanks also to Wayne Kellingsworth and Michael Hightower for knowledge imparted.

References:

1. S.M. Huybrechts, Analysis and behavior of grid structures, Stanford University, Stanford, California, 1995.

2. ASM International, Composites, ASM International, Metals Park, Ohio, 1987.

Appendix A:

Draft of the final node design

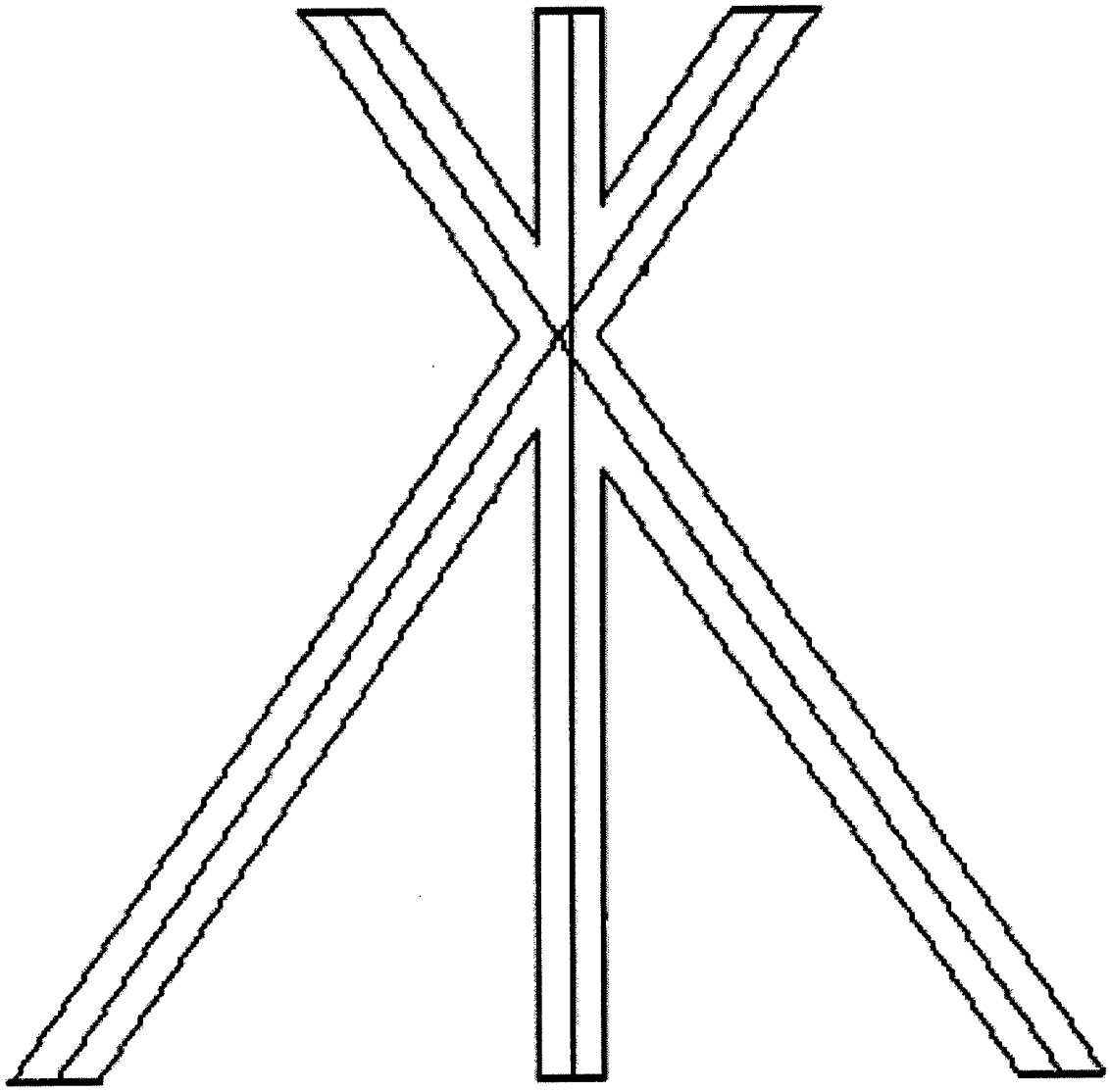

The node is in the vertical position so that the axial rib is running from top to bottom. This is a top view of the rubber inset and the middle lines denote the grooves the fiber is placed in. The legs and arms can be shortened as the circumference of the conic section changes. They are shown in place within the particle board in **Figure 1-5** . Explanation of the nodal offset and depth change can be found in **Figure 1- 2.**

Bryan S. Ericson's report was not available at the time of publication.

Jeffery A. Fisher's report was not available at the time of publication.

Greg A. Fisher's report was not available at the time of publication.

ELECTICAL AND OPTICAL CHARACTERIZATION OF STRATEGIC INFRARED DETECTORS IN BENIGN AND RADIATION ENVIRONMENTS

Erica S. Gerken

Manzano High School
12200 Lomas Blvd N E
Albuquerque, NM 87112

Final Report for:
High School Apprentice Program
Phillips Laboratory

Sponsored by:
Air Force Office of Scientific Research
Bolling Air Force Base, DC

and

Phillips Laboratory

August 1996

ELECTRICAL AND OPTICAL CHARACTERIZATION OF STRATEGIC INFRARED DETECTORS IN BENIGN AND RADIATION ENVIRONMENTS

Erica S. Gerken
Manzano High School

Abstract

The Infrared Devices Laboratory in the Space and Missiles Technology Directorate of the Air Force Phillips Laboratory, Kirtland AFB, NM is tasked with non-partisan characterization of infrared detectors and focal planes for Air Force programs. Both electrical and optical performance characteristics of the detectors are tested, the data is analyzed, and conclusions are drawn about the material. This information is then fed back to the manufacturer, forming an iterative loop of material, and therefore detector improvement. These tests are performed in both non-radiation and radiation environments, providing insight into the effective lifetime of these detectors in a natural radiation environment.

ELECTRICAL AND OPTICAL CHARACTERIZATION OF STRATEGIC INFRARED DETECTORS IN BENIGN AND RADIATION ENVIRONMENTS

Erica S. Gerken

Introduction

Complete characterization of infrared detectors involves numerous types of tests in the laboratory as well as a detailed analysis of the data measured. A complete description of the process is beyond the scope of this paper; however, I will describe three of the efforts I was involved with this summer in the Infrared Devices Laboratory (IDL). The first effort involved the design of an aluminum ionization chamber mount to be used during dosimetry measurements during radiation testing. The second effort involved collection and analysis of detector reverse bias leakage current with radiation. The third effort was the calculation of the effective optical area of lateral collection diodes on the detectors. The following paragraphs describe the effort in more detail, and document the importance of each step in the overall detector characterization effort.

Dosimetry Mounts

Strategic infrared detectors will be exposed to much natural radiation during their effective lifetimes from solar radiation, solar flares, and the van Allen belts. Before a detector design is chosen for a satellite mission, then, proper radiation testing must be performed in order to determine the degradation characteristics of the detector in a total dose environment. The IDL performs these measurements at the Cobalt-60 radiation source on Kirtland AFB. In June we performed total dose testing of two different detectors.

Proper radiation characterization naturally requires that we know how much radiation is incident on the detector in a given amount of time. The detectors are housed in stainless steel and aluminum test dewars, and much aluminum exists in the path between the detector and the radiation source. In order to determine the dose rate incident on the detector, an ionization chamber is placed on the detector mount inside the dewar and exposed to the source for a short period of time. This chamber measures the effective number of rads(Si) incident on the detector per second.

A problem existed with the design of the dewar, however. When a detector is mounted in the test dewar, an aluminum mount holds the detector in place, ensuring electrical and thermal contact. The radiation must pass through this aluminum mount before it reaches the detector. When dosimetry is performed with the ionization chamber, however, the aluminum mount does not fit over the chamber and is therefore not used. In other words, the ionization chamber receives a higher dose rate than the detectors ever would because the aluminum mount, which would attenuate the radiation, is not there.

To alleviate this problem, I designed an aluminum mount similar to those used with the detectors, but which fits over the ionization chamber. In future radiation tests, this mount will allow IDL personnel to more accurately determine the dose rate incident on the detectors. In other words, the same radiation attenuation will be present for the ionization chamber and the detector. This could significantly affect the dose rates, and lead to more realistic estimates of the detector performance in a total dose environment. The mounts have been built, and will be used in subsequent radiation tests.

Leakage Current

One of the figures-of-merit for infrared detectors is reverse bias leakage current. This is current present in the detector which is not generated by infrared energy. A low leakage current is desirable, and the measured levels of current give one insight into the material purity and hence effectiveness in a strategic space environment.

One of my tasks was to extract the leakage current values from data files from seven detectors, and to plot this current as a function of detector size. There were approximately 200 data files per detector containing leakage current data at several different reverse biases. This data will be used in a technical paper currently being written by IDL personnel, and scheduled to be presented at the Infrared Information Symposium (IRIS) in Boulder, CO on 1 Aug 96. This task took me approximately one week, and allowed IDL personnel to work on other areas of the paper, ensuring they have a camera-ready copy available to IRIS on time.

Effective Optical Area

Quantum efficiency is one of the primary figures-of-merit for infrared detectors. It is a measure of the number of electrons read out as current by the detector compared to the total number of electrons incident on the detector. One of the variables essential to calculating quantum efficiency is the area of the detector which is capturing the incident infrared energy. Several years ago, this area was assumed to be simply the junction area of the n-type and p-type material which make up these semiconductor devices. However, a material process known as lateral diffusion extends the effective collection area past the metallic junction into the material surrounding the junction. As such, in order to accurately calculate the quantum efficiency, the effective optical area, or that area beyond the edges of the metallic junction, must be calculated.

Calculating the effective optical area of square pixels is easy enough--simply increase the side of the square and multiply by the other side. Some detector designs, however, are quite complicated. Lateral collection diodes take advantage of the lateral diffusion mechanism inherent in the material. Instead of a large square metallic junction, a grid of smaller junctions is developed. The lateral diffusion mechanism then provides for complete optical fill of the non-junction areas. The effective optical area of the grid

becomes quite complicated, and special drawing programs must be utilized in order to accurately calculate the area.

I used a software program called Vellum to calculate the effective optical areas of six different lateral collection diode designs, each in a variety of test conditions. In all, I calculated approximately 100 different effective optical areas. Each of these were used to calculate quantum efficiency, and all of this data will be incorporated in the IRIS paper.

Conclusion

A variety of factors must be taken into account to properly characterize infrared detectors. I have touched on only three, but a discussion of more would be beyond the scope of this effort. Much of the work is somewhat tedious, however necessary for complete performance determination. I was involved with the characterization of only one detector from start to finish, and the process takes approximately two months. The final product, however, allows the manufacturer to design subsequent detectors to more effectively perform in a radiation environment.

James C. Ha's report was not available at the time of publication.

NEODYMIUM FIBER LASER

Doug Havlik

Albuquerque Academy
6400 Wyoming Blvd. NE
Albuquerque, NM 87109

Final Report for
High School Apprenticeship Program
Phillips Laboratory

Sponsored by:
Air force Office of Scientific Research
Bolling Air Force Base, DC

and

Phillips Laboratory

September 1996

NEODYMIUM FIBER LASER

Doug Havlik
Albuquerque Academy

Abstract

A neodymium-doped silica optical fiber laser pumped by a 817 nanometer (near-infrared or near IR) laser diode was built and successfully lased. Construction of this laser consists of two critical steps : first, aligning the diode beam so that it is coupled into the three meter fiber optic, and second, aligning the mirrors on either end of the fiber to create a laser cavity. Each of these steps has its own difficulties, including obtaining an "ideal" beam from the diode that will couple efficiently into the fiber. After building the laser, one photodetector had to be aligned for each of the two polarizations of light separated by the polarized beam splitter. This laser is an instrument for experimentation in chaotic optical systems.

NEODYMIUM FIBER LASER

Doug Havlik

Introduction

The fiber laser system is actually composed of two lasers -- a diode laser pump and a the single-mode optical fiber laser. The diode emitter produces 817 nm (monochromatic) light that must be collimated using a "collimating lens." Next the beam was contracted and rounded out to 4.4 millimeters for efficient coupling into the fiber. The fiber coupling component translates in the x-y-z direction and was adjusted until the output light was maximized. There is a mirror on the input side of the fiber that transmits light with a wavelength of 817 nm, but reflects nearly 100% at 1088 nm. The mirror on the far side of the fiber reflects 95% of 1088 nm. The mirrors create a laser cavity in which the 817 nm light is absorbed by the neodymium ions (Nd^{3+}); the exited ions relax back to the ground state via a 1088 nm transition. Emitted photons reflect back and forth between the mirrors. Soon, according to the physical laws governing stimulated emission, lasing is achieved with the emitted intensity passing through the far mirror.

Methodology

I. Laser Diode Collimation and Beam Shaping:

The laser diode used for this project was manufactured by Mitsubishi, type ML-510A. Its operating current is 53 mA with an output intensity of 15mW. The diode emits monochromatic light at 817 nm, which is just above the visible spectrum. The light from the diode diverges rapidly at its output, so a collimating lens was placed in front of the diode in order to produce a collimated beam. In theory, one needs only to place the lens directly in front of the emitting face of the diode, at a distance equal to the focal length of the lens. In practice there is some difficulty in finding the correct alignment. A one-dimensional translation stage was used to make the fine back-and-forth adjustments necessary to achieve good collimation. If the beam is truly collimated, the shape of the beam is practically the same one inch from the diode emitter as twenty or more meters away.

The working surface is an electrically grounded air-floated optical table drilled with 1/4-20 holes at the corners of a one-inch square grid. Because many optics had to be placed in the straight path of the

beam, it was important for proper alignment to begin with the diode and collimator. The diode was directed along a line of the table's holes, and the translation plate with the collimating lens was mounted directly in front (now referred to as the "far" side). The beam was collimated using the translation plate. Since the beam is infrared, an IR phosphorescing card is needed to see it. This card is charged by visible light, and then glows red where struck by the laser radiation. Once the beam was first collimated it was not directed exactly along the tapped holes of the table, so both the diode and collimating lens will had to be turned a little to straighten the beam. Unfortunately, this disrupts the collimation, so the translation plate had to be adjusted further. These two steps were repeated until the beam was properly collimated and directed along the holes.

At this point, the Gaussian characteristics of the beam must be determined. This amounts to measuring the shape of the beam and its diameter. Place a power meter probe in the path of the beam using a calibrated x-y-z translation mount—a mount that translates only up-down and left-right suffices. The probe was covered so that only a pinhole of light may pass. The power meter is calibrated to 820 nm. Find the most intense region of the beam by translating the probe in the plane perpendicular to the beam direction. Record the power reading and coordinates of the beam center. The product of that max and e^{-2} is the power at the edge of Gaussian beam. The left, right, top, and bottom-most points of the edge were found by translating to the respective directions until the power meter falls to $(power_{max})(e^{-2})$. Graphs of the beam edges, along with the heights and widths make up the Gaussian characteristics. This particular beam was about three times higher than it was wide.

Optimum mode matching for coupling into the fiber dictates that the beam be round with a diameter of 4.4 mm. Since this beam was about 2.4 mm wide by 8.0 mm tall, a 1/1.75 telescope and a 3x anamorphic prism should theoretically give a 2.4/1.75*3 = 4.11 mm wide and 8/1.75 = 4.57 mm tall beam. First, to construct a telescope, two lenses were needed. In this case, the near lens is plano-convex with a focal length of 175 mm. This means that the beam focuses to a point at 175 mm on the far side of the lens. Since a collimated beam was needed for coupling the beam into a fiber, the next lens collimated the beam at a reduced diameter. This lens is plano-concave with a focal length of -100 mm, meaning the point of focus is on the near side of the lens. This lens was placed 175-100 = 75 mm away from the first lens. For this set-up, the new beam dimensions were 4.5 mm tall by 1.6 mm wide.

The anamorphic prism placed on the far side of the telescope should now triple the beam width while leaving the height unchanged. Actual results were a height of 4.5 mm tall by 4.2 mm wide -- a very good beam for coupling into the fiber. See figure 1 which is a diagram of beam shapes.

At this point, a power meter is used to determine the beam power before and after the telescope-prism system. The relative difference after the shaping optics was .6 mW, from 14.0 to 13.4 mW. Conservation of beam power is important because the diode is weak to begin with, so all the power possible needs to get into the fiber.

II. Fiber Coupling and Fiber Lasing:

Fiber coupling begins with a good beam—correct size and shape—and aims to get the beam into the fiber such that light is detected at the far end of the fiber. First, the fiber was prepared admit the light by cleaving the ends. Methylene chloride solvent stripped the plastic cladding from around the fiber 1 to 2 centimeters from each end. Next, a diamond blade fiber cleaver nicks the exposed fiber core 3 mm from the end of the cleave. This nick fractured the fiber such that the end can be cleaved, leaving a flat, clean surface into and out of which the beam can couple and emanate.

Now, one end of the fiber was fixed in a fiber coupling component. This component, a New Focus single mode fiber coupler, allowed for ultra fine tuning through precision translation and rotation screws in order to launch the light into the fiber. Since this fiber was to be a lasing cavity, there had to be mirrors on either end. The process of coupling was as follows: the mirror was rotated so that it was perpendicular to the fiber. Next, a power meter was set up to measure the output from the fiber. Then, the vertical and horizontal translations of the fiber coupler were adjusted until power is registered and maximized. The power meter probe was shaded from stray light to get an accurate reading. This initial attempt to find the beam with the fiber was the most difficult part of the coupling process. Once accomplished, the z-translation (in-out direction) was turned and then the maximum found once again using the x- and y-translations. If this max was less than the previous max., the z-translation was turned in the opposite direction. Through this iterative process, the highest possible power was coupled into the fiber. On our laser, the most power observed at the output end was 50 μW for an efficiency of 0.37% (.05/13.6). However, most of this loss is accounted for by the absorption of the Nd^{3+} ions in the fiber along the three

meter length. Also, since the reading was taken on the far side of the output mirror, a lot of the pump beam is reflected back. As a result, the true coupling efficiency is substantially larger.

Once the light was coupled into the fiber, it was still not lasing. Assuming the fiber was long enough and the ends were cleaved properly, the only two conditions necessary for lasing were 1) enough beam coupled into the fiber and 2) proper alignment of the output mirror. Since the fiber had over the 20μW minimum, the output mirror needed adjustment. This alignment involves mostly luck, because the fiber does not lase at all until the alignment is nearly perfect, so a lot of blind adjustment is required.

Because it can be difficult to determine if the beam detected (by a phosphorescing card or power meter) is the 817 nm pump beam or the 1088 nm fiber laser beam, a low pass filter was placed directly after the output mirror. This filter absorbed the pump beam and transmitted the fiber laser beam, so no beam was detected until the fiber lased.

This fiber lased as high as 28 μW. From time to time, the fiber stopped lasing because one or more of the optics shifted out of alignment. The coupling was checked first, and then the output mirror needed to be adjusted until lasing began again. Once the fiber was lasing, the power was maximized by use of the power meter.

III. The Final Step -- Beam Splitting and Photodetectors:

At this point, the laser itself was complete, but in order to run experiments with amplitude modulation, the output power of the laser had to be measured and recorded by instrumentation such as oscilloscopes. Also, recent research into laser dynamics suggests that the different polarizations of the laser beam behave differently. For this reason, a polarizing beam splitter allows the researcher to examine the two polarizations independently.

The first step was to aim the fiber laser into a photodetector. Just as for the diode emission, the fiber laser had to be collimated because light emanating from the fiber diverges rapidly. The collimation was mounted on an x-y-z translation component. The beam was then collimated and aimed at the center of the photodetector. In this laser, once the beam was aimed correctly, the oscilloscope reading the photodetector's output was used to maximize the light entering the detector. At this point, the collimating lens was used as a focus lens to get the highest reading on the oscilloscope.

Now that the beam was aimed, the polarizing beam splitter cube was inserted between the collimating lens and the photodetector. This cube was oriented so that the transmitted beam was still oriented on the center of the photodetector. Once this was accomplished, the cube could be considered perpendicular to the beam. Fine adjustments to the x-y-z translation mount maximized the oscilloscope reading.

Light polarized in a horizontal plane is transmitted directly through the cube. On the other hand, light polarized in a vertical plane is completely reflected by the beam splitter cube. The polarized beams are subsequently focused into photodetectors for power measurements.

In Fig. 3 the total output power is plotted versus the laser diode pump current. The resulting plot clearly shows the lasing threshold current to be 43 mA. Using a polarizing beam splitter, we next measure the output power of each polarization versus the pump current, see Fig. 4. We find that the polarization intensities are not equal. The discrepancy is due to a stress induced birefringence in the coiled optical fiber.

Conclusion

A laser diode was successfully used to pump a neodymium fiber laser, which was then coupled into a photodetector, making the beam modulations available to computer-aided analysis. Seventy percent of the time spent building this laser is finding the appropriate mounting component. Another twenty percent of the time is spent attempting to align a optics only to find that the mounting component or technique will not work. Only ten percent of the work, at most, actually seems "productive", where I both had the right component and was successfully using it.

Much of time spent finding mounting components is due to lack of organization. Most components are not found on any particular shelf, but rather in a pile of partially disassembled old experiments. Other times, the right component cannot be found or is in limited supply so a more awkward, harder to align, or less effective tool or mount must be adapted. Many of these difficulties are unfortunate necessities of building unique lasers for unique needs, precluding as foreknowledge of the right components to stock.

Optical components of a laser in a lab environment are very sensitive to small changes in alignment. As a consequence, the alignment drifts from day to day, requiring constant readjusting – especially with the fiber coupler and the output mirror.

Putting the laser together from the diode to the photodetector has taught me a lot about the functions, advantages, and disadvantages of each component, and has given me patience in the search for that best component. I now better understand general optics principles, such as building a telescope, and have a grasp on some of the specific attributes of optics in the field of lasers, such a Gaussian properties. Also, this research presented me with a problem solving exercise much more comprehensive and in depth than that of any high school lab. Such experience should give me a lot of endurance for college labs.

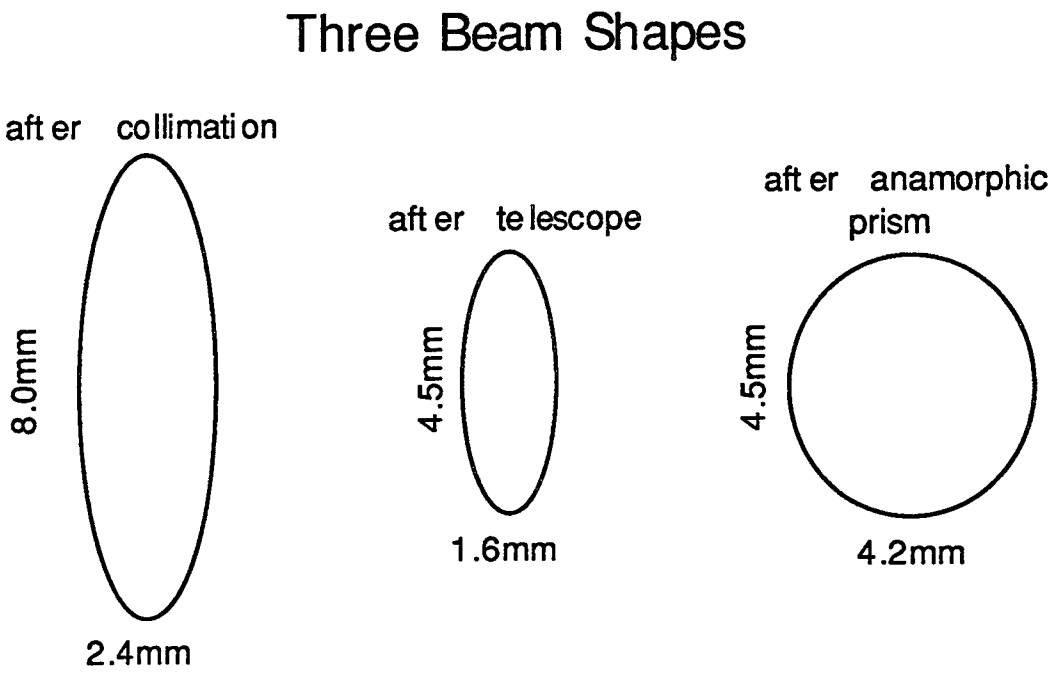

Fig. 1. This figure shows the progressive beam shaping.

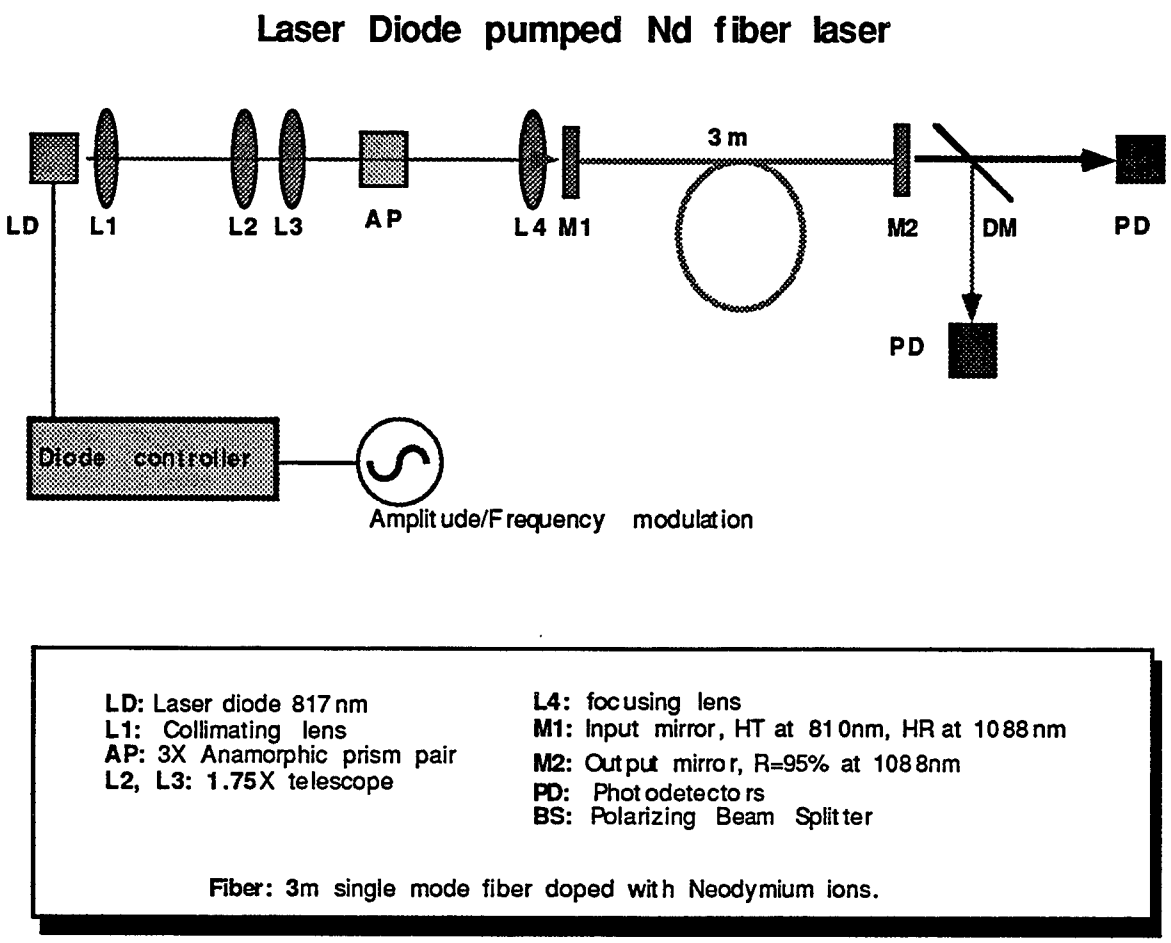

Fig. 2. The schematic of the entire fiber laser and photodetector set up.

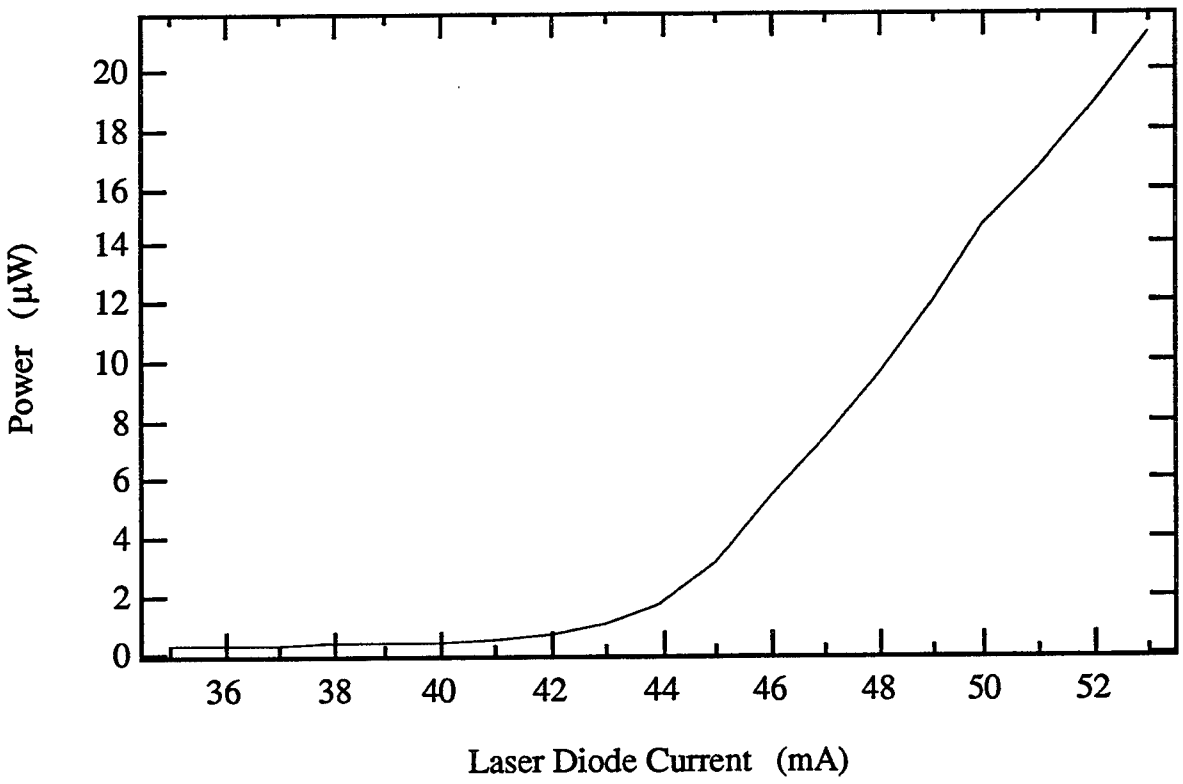

Fig. 3. Laser diode current vs. output power.

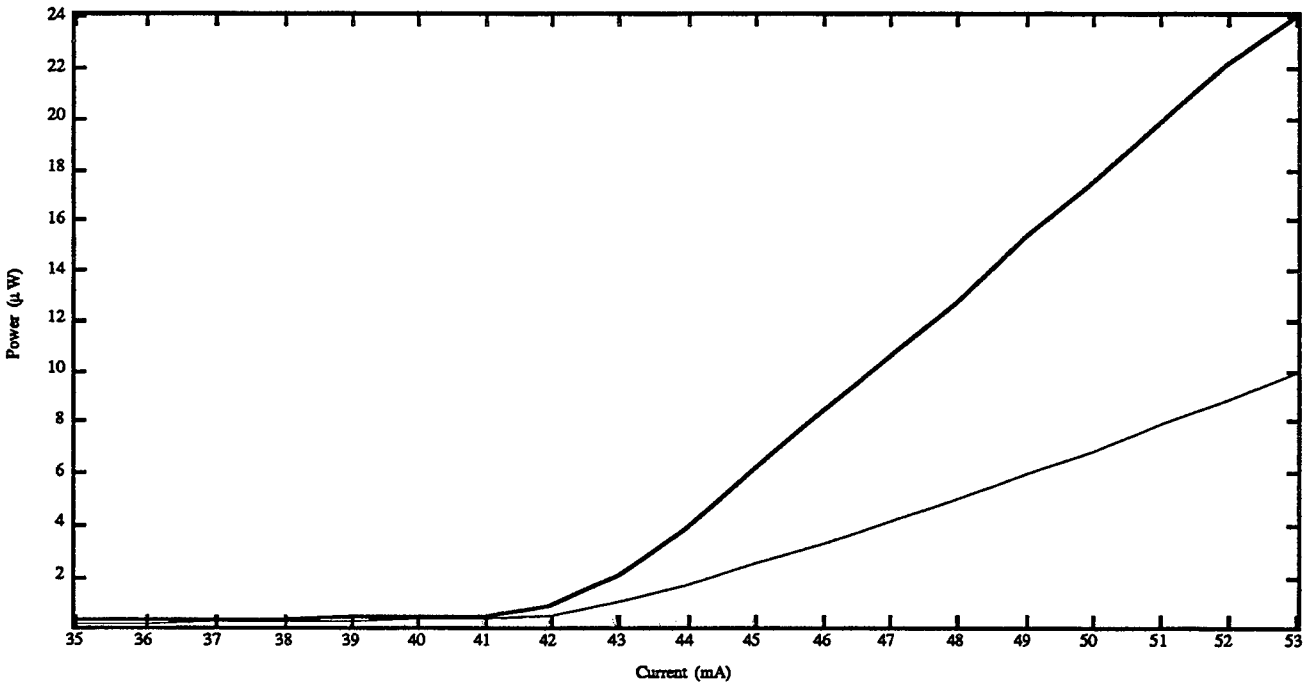

Fig. 4. Plot of the laser diode current vs. output power for the two polarization eigenstates

SOLAR THERMAL PROPULSION FROM CONCEPT TO REALITY

Karl J. Iliev

Antelope Valley High School
44900 N Division
Lancaster, CA 93535

Final Report for:
High School Apprentice Program
Phillips Laboratory
Edwards Air Force Base, CA

Sponsored by:
Air Force Office of Scientific Research
Bolling Air Force Base, Washington DC

and

Phillips Laboratory
Edwards Air Force Base, CA

August 1996

SOLAR THERMAL PROPULSION FROM CONCEPT TO REALITY

Karl J. Iliev
Antelope Valley High School

Abstract

Solar thermal propulsion's multiple facets were studied and its application was looked at briefly. The efficiency and capability of select solar propulsion components were tested. During my brief tenure, several small projects were begun, some completed. A calorimetry experiment tested the power output of the existing rigid concentrator. The process of constructing and testing an inflatable concentrator for slope errors and its power output was initiated. Slope errors will be measured using laser ray tracing techniques. A shutter was designed to quickly allow or block the passage of light onto the test subject in order to take more accurate measurements. Finally, different absorber, thruster, and propellant types and combinations were studied. Phillips Laboratory has been testing several different components in various important areas over the past 13 years. The ground tests will eventually provide enough information to build flight hardware. This culmination into several flight tests is the next step to reality of solar thermal propulsion.

SOLAR THERMAL PROPULSION FROM CONCEPT TO REALITY

Karl J. Iliev

Introduction

A solar thruster uses the sun's radiant energy to produce kinetic energy. Since the sun's heat is free, solar thermal propulsion may one day be a desirable form of orbit transfer for satellites. It creates thrust by collecting and focusing the sun's powerful rays into an absorber using a concentrator. The absorber collects the heat and transfers it to the fuel. The heated fuel expands and is forced through a nozzle. Because of the particles being forced out the aft end, the rocket is pushed forward with the same amount of force, or thrust. This, Newton's Third Law, is the basis of rocket science. The result of the conversion and expansion (no combustion) is efficient thrust created from a relatively lightweight and reusable vehicle.

Concentrator

The differences between the space-applicable, inflatable concentrator and the rigid concentrator in the laboratory were observed. Although rigid concentrators are great for testing in the lab, a much easier space deployable system is needed to make solar propulsion a viable and workable concept in space. In space weight and volume requirements can be met with lightweight and packageable inflatable concentrators. Inflatables are cheaper to produce than older forms of mechanically erected systems. Before flight, the testing of these inflatables for deployment capability, structural strength, and concentration efficiency must be performed to assure reliability. During this summer, time was dedicated to the testing the concentration of the inflatable verses that of the rigid concentrator to determine if this design packageability and reinflation was as proposed by the contractor.

Construction of the rigid concentrator in the lab included using 228 spherically shaped mirrors angled to simulate an off-axis paraboloid. In combination with a heliostat, or solar furnace, absorbers and thrusters are tested. The

heliostat is a series of flat mirrors, all lying on the same plane, that directs the sunlight into the lab and onto the concentrator. This allows us to work inside away from the uncomfortable and harmful to the delicate concentrator earth elements. Lab personnel manufactured this concentrator to have a 10,000 to 1 geometric concentration ratio, and to focus the light into a focal point 3.2 inches in diameter. When the concentrator was first tested for optical accuracy the RMS slope error was rated at 3 mrad and the assigned power was approximately 24.7 kW during the winter. It was tested again this summer to determine the degradation, but not to the same extent. A simple calorimetry experiment found the power output to be 18.21 kW during this summer, although a laser ray tracing wasn't performed to discover slope accuracy as before. To measure power, a calorimeter was easily made from an insulated ten gallon fishtank filled with darkened water to absorb the heat. A stirrer maintained uniform temperature throughout the tank. The insulation stopped most heat loss and helped give us more accurate readings. The temperature of the water remained almost constant for quite a while after the sun was covered, further showing the effectiveness of the insulation. The power was found by measuring the change in heat over a period of time.

Similar rigid concentrators may be made available for space flights and testing, although they are heavy and hard to build. It is not recommended, or even feasible, to use such a rigid concentrator in space. Therefore a lighter more packageable concentrator must be developed. Phillips Laboratory, Edwards, has the opportunity to be first to ground test an inflatable concentrator. The space application of these highly accurate concentrators requires them to be inexpensive, compact, light, and self deployable. This is the purpose of developing and testing inflatable concentrators. They are low in cost because they are easier to develop and to produce, in addition to the low launch cost due to low mass, and less time and people needed to deploy it. A space-applicable inflatable concentrator will generally be an off-axis elliptical section of a paraboloid because the incident light entering a paraboloid is concentrated onto one spot if the light shines directly on the projected minor diameter. Two of these paraboloidal sections are used to increase the performance of the system. The nature of these off-axis paraboloids requires them to be off to the sides, not only because of the necessity to move the system in any direction at

any time, but also to allow for the rocket plume to exhaust without any interference. The most simple designs look like a clam shell or a lens. They are simple because they are composed of a transparent canopy seamed together around the perimeter to a reflector. The first film, closer to the sun, would be as clear as possible to allow most of the light to hit the second film. The second film would be the reflective surface that concentrates the light into a focal point. As stated earlier, two of these ellipses concentrate light into two absorbers. An inflatable torus and three inflatable or foam-rigidized beams help support each concentrator and help them to keep their shape. There are also foam inflated and rigidized reflectors in development.

The trick is to construct a concentrator with a feasibly small slope accuracy error and surface error. They must also be large enough to focus the required amount of energy into the heat exchanger of absorber. In space, this would mean deploying a concentrator over 100 feet in projected diameter with slope accuracy error less than 2 mrad RMS. In a perfect world the reflective surface would be a single piece, but for now existing concentrators are seamed and gored. They consist of several strips of reflective material seamed together radially on-axis, like the spokes on a wheel. The reflector is tailored together just as a football is sewn together from several flat pieces. This tailoring causes weak points in the overall strength as well as surface and slope errors. It is very difficult to create an off-axis paraboloid's curvature in only one piece, but it is possible with the new spray casting on mandrels approach. In constructing our seamed and gored, clam shell concentrator, we first set up an ellipse shaped airtight pool in order to pull a vacuum. The vacuum pulled the reflective film into its correct off-axis paraboloidal shape. Then we will attach a clear film to the top of the reflective film and inflate. The reflector will be attached to the torus and then the torus to a stand. This will allow us to test the torus strength and capability to sustain the elliptical shape. If the torus works here on Earth, it may work in space due to the fact that there is one less unit of gravitational force in space. We will also be able to test the ellipse's optical output with similar experiments to the earlier calorimetry experiment mentioned above, and laser ray tracing experiments. Finally with the existing test stand, thrusters can be tested with this new technology.

Shutter

One problem during the testing of the concentrator with calorimeters or thrusters involves the accurate reading of data. A shutter of some type is required to instantly obstruct or unobstruct the sunlight from shining onto the test object. This allows us to more accurately gage temperature and time without other variables changing. For example during the fishtank calorimetry experiment, we calculated power by measuring heat vs. time. To accurately do this, the experiment had to begin and end at marked times. This is accomplished with a shutter that can quickly open and close. The shutter, while open, allows for all of the light to completely illuminate the test object, but when closed, isolates the test object from light. The lab setup includes a heliostat that directs the sunlight through a door onto a concentrator and then onto the test stand. The mechanical sliding door between the heliostat and the concentrator is functional but is very slow because of its size, but fortunately allows all of the light through when open. A shutter is required to withstand the heat of the extra light long enough for the door to close. The shutter may be placed anywhere in the lab setup. This may include allowing the light to hit the concentrator at all times and placing the shutter between the concentrator and test stand. A shutter there would have to endure more intense light on a smaller area. However, if it is placed near the heliostat it would have to be large, and heavy, to block all of the light. A shutter in either position would need to be collapsible and able to move quickly. The larger, heavier model would be hard to move, but the smaller model would have to collapse into less space.

The lab's new design is of the smaller, more durable type. The design is similar to Venetian blinds. Using several sheets of stainless steel tied together to be able to rotate into position in synchronous fashion. It was able to withstand high temperatures for a long enough time to allow the door to open and close. Sheets of stainless steel were strung together twice on each end through slots. Two of these cables were used as draw strings, while the other two were used as spacers. The draw strings are threaded through the middle of each side of each plate. The spacer cables attached at one corner of each side allow the weight to cause the plates to lie almost vertically when deployed. There are some problems. The plates will not lie flat because of interference caused by the draw

strings. Slotting the holes reduced this problem by creating more room and less friction. The horizontal placement of the plates also causes friction and results in the need of great force to retract the shutter. Currently the shutter is manually operated, but eventually the shutter will be automated. Other problems included heat radiating from the sheets of steel. The heat might have disturbed the temperature readings within the tank since the shutter was so close to the tank. Also there were some friction problems associated with the sheets deploying and retracting modes. Although the vanes were not completely shut or flat, letting some light through, the readings were adequate: a sudden increase in temperature after the shutters were opened and a level slope on the graph of temperature vs. time after the shutters were closed indicated the problem of the radiating heat. These readings showed the shutter worked satisfactorily, however.

Thruster

The thruster is composed of an aperture to let light through, and a heat exchanger or absorber. The heat absorber's main function is to conduct the radiant thermal energy through the wall of the heat exchanger, then transfer the heat to a propellant. It would be ideal if the propellant gas absorbed all of the heat without an exchanger. Unfortunately the gas is transparent to sunlight for our intents and purposes and most radiation passes through it. Some means of heat exchange is needed; the solar energy must be absorbed by an exchanger both in contact with the solar energy and the propellant. Two of these best types of absorbers are being tested and streamlined for flight tests. The first type, Black Body Cavity Absorbers, consists of an insulated tubelike cavity with a wall both in contact with the light and the fuel. Sometimes running the cold fuel through the cavity regeneratively cools the absorber cavity, to prevent the thruster from melting. The temperature is limited by the heat absorptivity of the absorber and the temperature the materials can withstand. The second type, the Volumetric Absorber, traps the solar energy inside the thruster behind a window. To impart this energy into the fuel, either porous material is placed in the chamber or small particles are placed in the propellant for heat exchange purposes. The major disadvantage of the this system could be the weight of the absorbent particles. If more particles are added, or bigger particles are used, more energy can be absorbed and therefore more heat can be

obtained. This creates an increase in thrust, but the added weight will lower the Isp (specific impulse) if the particles escape out the nozzle. A high temperature means that the Isp will also be high, to a point. Hydrogen gas can absorb great amounts of heat, possibly increasing Isp. A lighter material can solve the increased weight problem. Another way may be to induce the dissociation of the fuel because two H particles are lighter than one H2 particle. Hydrogen dissociation starts occurring at approximately 3800K. This high temperature (3000-4000K) is what gives solar propulsion a higher Isp than chemical propulsion. Solar propulsion requires only one propellant. This is another reason a solar propulsion system is lightweight; the concept requires no oxidizer, as opposed to chemical propulsion. Hydrogen is best suited as fuel because of its low molecular weight and its heat transfer capabilities. Hydrogen will be used as inflatant for the concentrator for the same reasons it's used as propellant.

Conclusion

As early as 2010 the government and private companies may be using this cheap and efficient upper stage as a means of orbit transfer. As of today, solar propulsion performance is between chemical and electric propulsion. Solar propulsion creates a higher, more efficient Isp than chemical propulsion; however it is capable of less thrust and takes longer to transfer payloads from Low Earth Orbit to Geosynchronous Equatorial Orbit (10-60 days). Because of the higher Isp, solar propulsion can carry more payload with less fuel. Electric propulsion may surpass solar propulsion in Isp efficiency, but it is incapable of creating high thrust. Therefore electric propulsion trip times are very long (180-300 days).

Since solar thermal propulsion is flexible, trip times can be varied to carry more payload in longer time, or less payload faster. As you can see, more industry will be turning towards solar thermal propulsion as it develops, because of its higher efficiency, lower cost, and better adaptability to missions needs. The concept has nearly become reality.

SOLAR THERMAL PROPULSION
FROM CONCEPT TO REALITY

Karl J. Iliev

References

1. Baxter, Alan Personal Interview. Edwards Air Force Base, California, July 1996. Phillips Laboratory, Edwards Air Force Base, California

2. Brandt, Rex Personal Interview. Edwards Air Force Base, California, July 1996. Phillips Laboratory, Edwards Air Force Base, California

3. Chenault, Stephanie Personal Interview. Edwards Air Force Base, California, July 1996. Phillips Laboratory, Edwards Air Force Base, California

4. Gierow, Paul Personal Interview. Edwards Air Force Base, California, July 1996. Phillips Laboratory, Edwards Air Force Base, California

5. Holmes PhD, Michael R. Personal Interview. Edwards Air Force Base, California, July 1996. Phillips Laboratory, Edwards Air Force Base, California

6. Jensen, Andrea Personal Interview. Edwards Air Force Base, California, July 1996. Phillips Laboratory, Edwards Air Force Base, California

7. Laug, Kristi THE SOLAR PROPULSION CONCEPT IS ALIVE AND WELL AT THE ASTRONAUTICS LABORATORY, Phillips Laboratory (AFMC) Edwards AFB, CA, 26 November 1993 revision.

8. Partch PhD, Russell Personal Interview. Edwards Air Force Base, California, July 1996. Phillips Laboratory, Edwards Air Force Base, California

9. Powell, Orin "Rusty" Personal Interview. Edwards Air Force Base, California, July 1996. Phillips Laboratory, Edwards Air Force Base, California

10. Sisk, Joel Personal Interview. Edwards Air Force Base, California, July 1996. Phillips Laboratory, Edwards Air Force Base, California

11. Smith, Julie Personal Interview. Edwards Air Force Base, California, July 1996. Phillips Laboratory, Edwards Air Force Base, California

12. Stephens, John Personal Interview. Edwards Air Force Base, California, July 1996. Phillips Laboratory, Edwards Air Force Base, California

SOLAR THERMAL PROPULSION
FROM CONCEPT TO REALITY

Karl J. Iliev

Acknowledgments

I have enjoyed working at Phillips Laboratory, Edwards AFB. Over the past two years my knowledge of the multiple careers in technology has become more apparent to me. I have learned how an engineer works and the tasks of contractors. I also had the opportunity to share engineering experiences. The more I work with technology the more interesting the field appears. I would like to thank the Research and Development Laboratory (RDL) High School Apprenticeship Program and Phillips Laboratory, Edwards AFB for making these experiences possible. I will cherish the support and friendship from my coworkers for the rest of my life.

Combined Effects of Gravity and Geomagnetic Field on Crystal Growth

Caroline H. Lee

Lexington High School
251 Waltham Street
Lexington, MA 02173

Final Report for:
High School Apprentice Program
Phillips Laboratory

Sponsored by:
Air Force Office of Scientific Research
Bolling Air Force Base, DC 20332

and

Phillips Laboratory
Hanscom Air Force Base, MA 01731

August 1996

Combined Effect of Gravity and Geomagnetic Field on Crystal Growth

Abstract

A space experiment was conducted in Shuttle Discovery in 1988 to investigate the gravitational effect on crystal growth. The observations, described briefly in the Chemistry textbook (Kotz and Purcell, "Chemistry and Chemical Reactivity," 1991) I studied last semester, show that crystals grew uniformly throughout the solution and also uniformly on a membrane at the center of the container. By contrast, in similar experiments performed on Earth, crystals did not grow uniformly in the solution nor on the membrane. However, it remained unexplained why crystals are able to grow uniformly in a rather weak gravitational field. Motivated by the space shuttle experiment, I have carried out some experiments in laboratory on crystal growth. The design of my experiments is based on a hypothesis that the growth of crystals is affected by not only gravity but also the geomagnetic field. A solenoid, that is, a long helical coil with many turns, was made to produce magnetic fields with magnitudes comparable to the local Earth's magnetic field. Changing the applied currents in the solenoid varies the intensities of the produced magnetic fields. Containers with chemical solutions were placed near the center of the solenoid to grow crystals. Two kinds of chemicals, aluminum potassium sulfate and monoammonium phosphate, were used to study the combined effect of gravity and the geomagnetic field on the growth of crystals with metallic elements and non-metallic elements, respectively. The preliminary results of my experiments have confirmed the hypothesis. The uniformity of the crystal growth and the size of the grown crystals can indeed be controlled by the combined effect of gravity and the magnetic field. My hypothesis supported by my experiments can explain well the observations of previous shuttle and laboratory experiments described in the Chemistry textbook. My future continued experiments will consider other important parameters such as the chemical density and the room temperature for a quantitative study of crystal growth under the effect of gravity and a controllable magnetic field.

1. Motivation

As mentioned in the Chemistry textbook (Kotz and Purcell, 1991) studied in my junior year at the Lexington High School, crystals grown in space showed clearly that space-grown crystals were different from those grown on Earth (DeLucas et al., 1986; Kelter et al., 1987; Singh and Glicksman 1987; Citteriio et al., 1988; Clifton and Owens, 1988), but why they were different was a matter of speculation. Under the NASA's Space Shuttle program, and experiment to see how crystals would grow in the absence of a strong gravitational field was conducted in Shuttle Discovery in 1988 (Scaife et al., 1990).

The apparatus used in the experiment consisted of four interconnected chambers [see figures 1 (a) & 1(b)]. The two ended chamber held lead acetate and potassium iodide solution, and the two inner chambers were filled with deionized water, and were separated by a cellulose membrane. When the valves separating the end and middle chambers were opened, the reactants migrated to the inner chambers. Iodide anions passed through a membrane faster than the lead cations; thus, lead iodide crystals formed on the membrane facing into the lead acetate solution.

In the experiment done on the Discovery flight, lead iodide crystals formed uniformly over the surface of the membrane and throughout the solution in the middle chamber [see Figure 1 (a)]. This is very different form the behavior on Earth, where the crystals grow only at the vertical membrane and then only on the bottom half of the membrane [see Figure 1 (b)]. However, it remains unexplained why crystals are able to grow uniformly in a rather weak gravitational field.

Motivation

(a) 1988 Shuttle Discovery Experiments

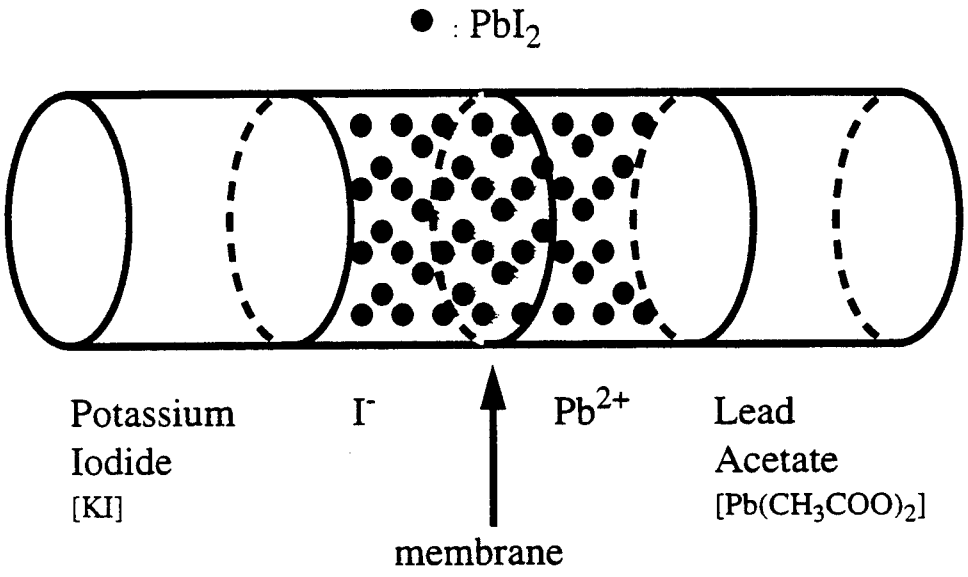

(b) Same Experiments in Laboratory on Earth

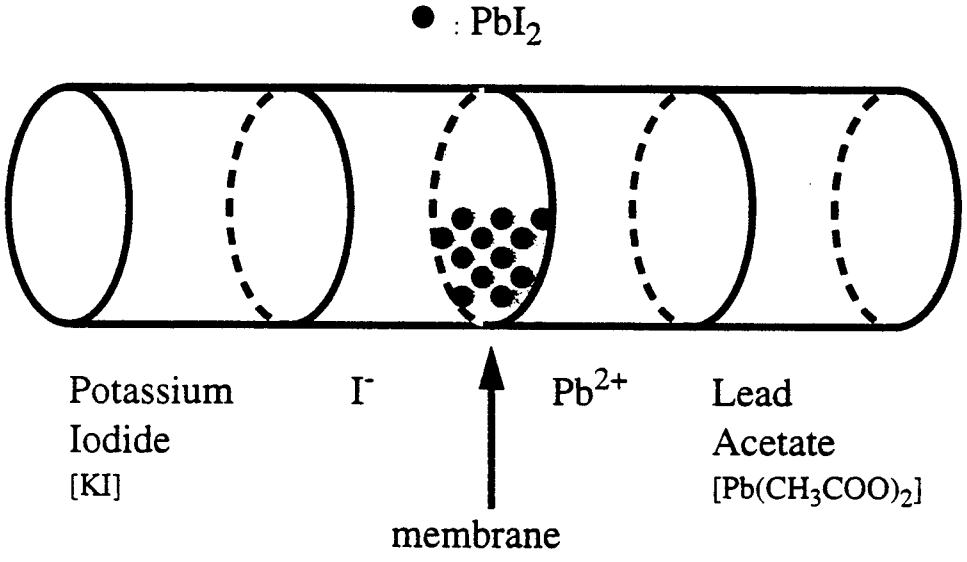

FIGURE 1.

2. Hypothesis/ A Theory

The solutions prepared for crystal growth contains anions and cations that are charged particles. In the presence of the gravitational field (**g**) and geomagnetic field (**B**), anions and cations move along and in opposite to the g x B direction [see Figure 2], respectively. This combined effect of gravity and the geomagnetic field, not considered by previous researchers, may be very important for crystal growth.

The expression for the g x B drift speeds of ions is given by mg/qB, where m and q denote the mass and electric charge of ions, respectively. At the altitude (~ 300 km) of a space shuttle, the B-field still has 87% of its value on Earth. The g-field, by contrast, is reduced drastically by several orders of magnitude, because under a circular orbit of the shuttle, the gravitational field is almost canceled by the centrifugal force.

Based on this hypothesis, we can expect that the combined effect of gravity and the geomagnetic field does not move anions and cations in solutions significantly in space shuttles, though this effect may be prominent in laboratory on Earth. Consequently, crystals can grow uniformly throughout the solution and on the membrane as observed in the Shuttle Discovery experiments. By contrast, the g X B effect prevents crystals from growing uniformly in the solution on Earth except on the membrane that hinders the motion of anions and cations due to the g X B drifts.

I have designed and carried out concept-proof experiments as described below to corroborate the theory.

A Theory

- **g x B Drifts of Charged Particles**
- **Drift Velocities**

$$V_q = mg \times B / qB^2$$

(Downward)

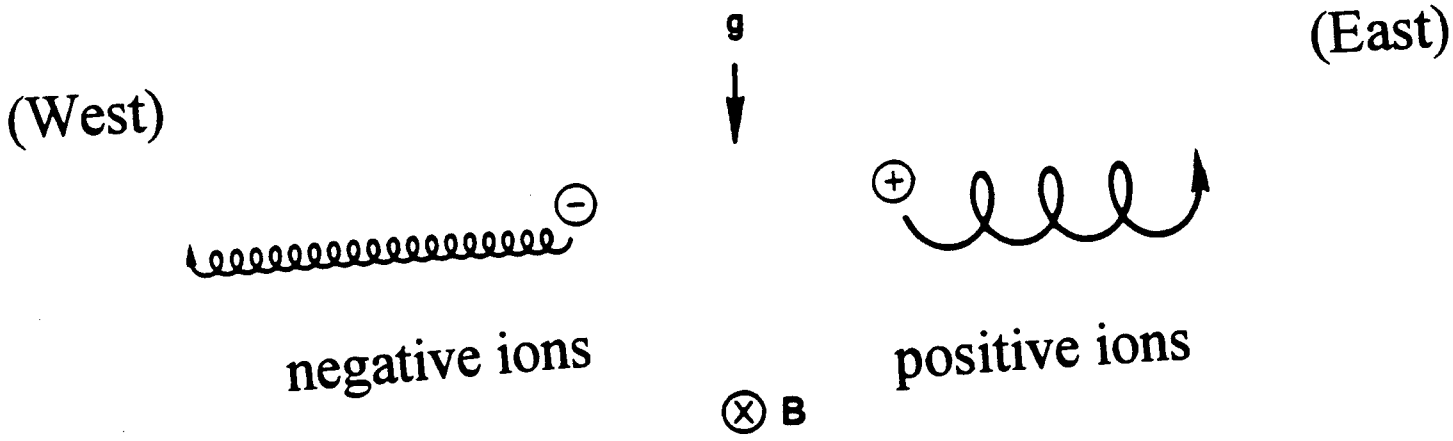

(To the North)

FIGURE 2.

3. Experiments

To test the combined effect of gravity and the geomagnetic field on crystal growth, I would need to adjust gravity and magnetic field in my laboratory experiments on Earth. While I cannot change gravity, I can easily produce relatively uniform magnetic field with intensities comparable to the Earth's magnetic field using a solenoid. The solenoid is a long helical coil with many turns. Currents generated by a power generator flow in the solenoid to produce relatively uniform magnetic field near the center of this long coil [see Figure 3].

With the help of a compass, I aligned the solenoid along the north-south direction so that the magnetic fields produced inside the solenoid will coincide with the Earth's magnetic field approximately. Placing a container with either aluminum potassium sulfate or monoammonium phosphate solution inside and near the center of the solenoid, I did a series of experiments with different intensities of magnetic fields.

As mentioned earlier, I intend to produce magnetic fields with intensities comparable to that of the Earth's magnetic field. The experiments I have carried out so far center on the studies of crystal growth under (1) zero magnetic field, (2) the background Earth's magnetic field, (3) twice the Earth's magnetic field, and (4) three times of the Earth's magnetic field. The condition for zero magnetic field was achieved as follows. Placing the compass inside and near the center of the solenoid, I adjusted the power generator to produce a magnetic field that is equal to but in the opposite direction of the Earth's magnetic field. When the needle of the compass began to wander, this

FIGURE 3.

indicated that the superposition of the background Earth's magnetic field and the current-produced magnetic field produced a zero magnetic field environment for my crystal growth experiments. A gauss meter was also used to measure the magnetic field intensities inside the solenoid.

4. Results

The experimental results for growth of the aluminum potassium sulfate and the monoammonium phosphate crystals are discussed separately here:

(I.) Aluminum potassium sulfate crystals

For the crystal growth outside the solenoid under the background Earth's magnetic field, I could clearly observe the crystals growing and note the following features. After the aluminum potassium sulfate powder dissolved in boiled distilled water, crystals began to grow on the surface of the solution and at the bottom of the containers in the shape of tiny needles. I attribute this as the evidence and consequence of anions (aluminum ions and potassium ions) and cations (sulfate ions) motion under the g x B effect.

The surface of the solution is the interface between the crystal solution and the air, and the bottom of the container is that between the crystal solution and the container. Anions and cations move toward the east and the west, respectively, under the g x B

effect. These positive and negative ions experienced friction at the interfaces, namely, the surface of the solution and the bottom of the container, where these drifting ions could be slowed down and accumulated to grow crystals.

This interpretation is supported by my observations of other experiments. Under the zero magnetic field condition, crystals grew on the bottom of the container, but they nearly did not grow on the surface of the solution. In the absence of the g x B, crystals uniformly formed in the solution and, because of gravity, they deposited at the bottom of the container. Crystals, growing under twice or three times of the Earth's magnetic field, did not start to grow on the surface of the solution either. It was presumably because the friction at the air-solution interface could not slow down the ions' motion significantly under a stronger g x B effect.

The most striking g x B effect has been seen from the crystal growth under stronger magnetic fields, especially in my experiments with three times of the Earth's magnetic field. As shown in Figure 4, many small crystals grown under the background Earth's magnetic field or zero magnetic field formed relatively uniformly at the bottom of the container with sizes less than one centimeter. By contrast, only a few (or just a single) much larger crystals grew under stronger magnetic fields.

Under three times of the Earth's magnetic field, crystals were always seen to grow against the wall of the container, clearly indicating that strong g x B motions of ions in the crystal solution were hindered by the wall for crystal growth. In one experiment, large crystals grew nearly symmetrically with respect to the magnetic field against the wall.

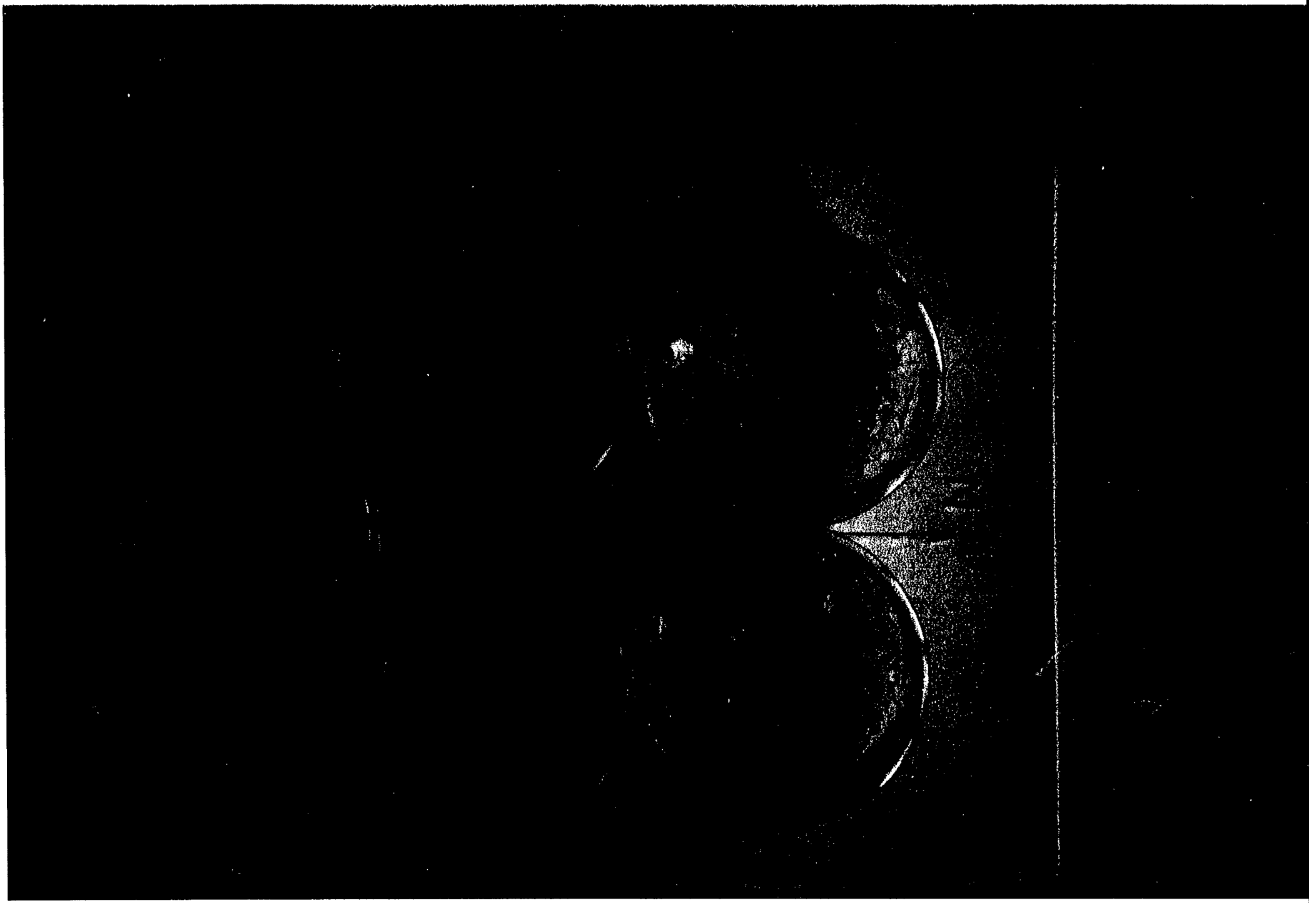

FIGURE 4.

(II) Monoammonium phosphate crystals

The growth of monoammonium phosphate crystals also exhibited similar characteristic features seen in the growth of aluminum potassium sulfate crystals. Crystals grew relatively uniformly at the bottom of the container under zero magnetic field, while discrete larger crystals formed against the wall of the container under stronger magnetic fields, especially under three times of the Earth's magnetic field. Enhanced yield was generally seen in the growth of these crystals.

However, a distinctive difference between the growth of these two crystals under three times of the Earth's magnetic field was noted. While aluminum potassium sulfate crystals only grew against the wall of the container, the monoammonium phosphate crystals could also extend to grow away from the wall at the bottom of the container. My explanation is that anions (hydrogen and ammonia ions) in the monoammonium phosphate solution have much less mass than anions (aluminum and potassium ions) in the aluminum potassium sulfate solution. Therefore, hydrogen and ammonia ions experience less gravitational force (that is, mass times gravity) and then less the g x B effect than aluminum and potassium ions. Note that the g x B effect is proportional to mass of the charged particle.

5. Further Research

I plan to continue this research for a more quantitative analysis of the combined effect of gravity and geomagnetic field for my Physics course project in my senior year at the Lexington High School. For instance, in experiments on the growth of aluminum potassium sulfate crystals, sometimes several large pieces of crystals grew, but sometimes just a single crystal was seen to grow. I suspect that the concentration and inhomogeneity of crystal solution and perhaps the room temperature may control the yield of the grown crystals.

Acknowledgements. I would like to thank Dr. Shu Lai of Phillips Laboratory at Hanscom Air Force Base for his interest and support. I also appreciate that M.I.T. Plasma Fusion Center provided me with experimental apparatus for my experiments.

Bibliography

Citterio, O.; Bonelli G.; Conti, G.; Hattaini, E.; Santambrogio, E; Sacco, B.; Lanzara, E.; Brauninger, H; Buckert, W. Applied Optics, 27, 1470-1475, 1988.

Clifton, K.B.; Owens, J.K., Applied Optics, 27, 603-609, 1988.

DeLucas, L.J.; Bugg, C.E.; Suddath, F.L.; Snyder, R.; Naumann, R.; Broom, M.B.; Pusey, M.; Yost, B.; Herren, B., Polymer preparation, American Chemical Society, Polymer Chemistry, 28, 383-384, 1987.

Kelter, P.B.; Snyder, W.B.; Buchar, C.S., Journal of Chemistry Education, 64, 228-231, 1987.

Kotz, J.C.; Purcell, K.F., Chemistry and Chemical Reactivity, 2nd Edition, Saunders College Publishing, 1991.

Nigli, S.; Chadha, G.K.; Trigunayat, G.C.; Bagai, R.K., Journal of Crystal Growth, 79, 522-526, 1986.

Scaife, C.W.J.; Cavoli, S.R.; Blanton, T.N.; Morse, M.D.; Sever B.R.; Willis, W.S.; Suib, S.L., Chemical Materials, 2, 777-780, 1990.

Singh, N.B.; Clicksman, M.E., Materials Letters, 5, 453-456, 1987.

AN INVESTIGATION OF CATALOGING PROCEDURES FOR POINT SOURCES IN THE GALACTIC PLANE

Maureen D. Long

Chelmsford High School
200 Richardson Rd.
Chelmsford, MA 01863

Final Report for:
High School Apprentice Program
Phillips Laboratory

Sponsored by:
Air Force Office of Scientific Research
Bolling Air Force Base, DC

and

Phillips Laboratory

August 1996

AN INVESTIGATION OF CATALOGING PROCEDURES FOR POINT SOURCES IN THE GALACTIC PLANE

Maureen D. Long
Chelmsford High School

Abstract

The Infrared Astronomical Satellite (IRAS), which flew in 1983, conducted a near-complete infrared survey of the sky at wavelengths of 12, 25, 60, and 100 μm. From this data, several infrared source catalogs were compiled, including the Point Source Catalog. One region of the sky that presented a problem during analysis of data was the galactic plane, a "confused" region. Point source extraction of the galactic plane region at 12 and 25 μm was performed using high-resolution techniques. We are transforming this data into catalogued form. This process involves eliminating repeats and spurious sources, setting signal-to-noise thresholds and other minimum criteria, and finally merging the 12 and 25 μm source lists into a final catalog. This project involved analyzing the data in several ways to determine what improvements to current cataloging processes could be made, and then making these improvements.

I. Introduction

A. *The Infrared Astronomical Satellite*

The Infrared Astronomical Satellite (IRAS) was a satellite mission conducted jointly by NASA of the United States, NIVR of the Netherlands, and SERC of the United Kingdom {5}. Over 96% of the sky was surveyed in four wavelength bands: 12, 25, 60, and 100 μm. It was launched in January of 1983 and had finished its mission by November of that year {1}. Several catalogs of sources of infrared emission have been published. The original catalog, the IRAS Point Source Catalog (PSC), was first released in 1984 and contains over 250,000 reliable point sources.

B. *High Resolution Analysis of Confused Regions*

The point source extraction algorithms used to produce the Point Source Catalog and other similar catalogs produce incomplete data for regions that are clutter backgrounds for sensor systems {3}. Therefore, confused regions had not been completely cataloged at the time of publication of the PSC. The galactic plane is one such confused region. Kennealy et al. provide a graphic depiction of this in Figure 1, a plot of all sources fainter than 1.0 jansky. The lack of sources in the galactic plane demonstrates that the PSC is indeed incomplete in the region of the galactic center.

The Geophysics Directorate at Phillips Lab, Hanscom Air Force Base, MA sponsored an effort to re-process the data in this region. This effort was led by the Space and Atmospherics Division at the Mission Research Corporation (MRC) located in Santa Barbara, CA. In addition, R. Gonsalves of Tufts University provided consultation, and the University of Wyoming performed validation and verification of the results {3}.

In order to completely catalog the galactic plane, a processing technique was developed by MRC utilized 2-D image representations of the IRAS data, rather than the 1-D scans used in the PSC {3}. A complete discussion of the extraction techniques used is beyond the scope of this paper, but the technique was

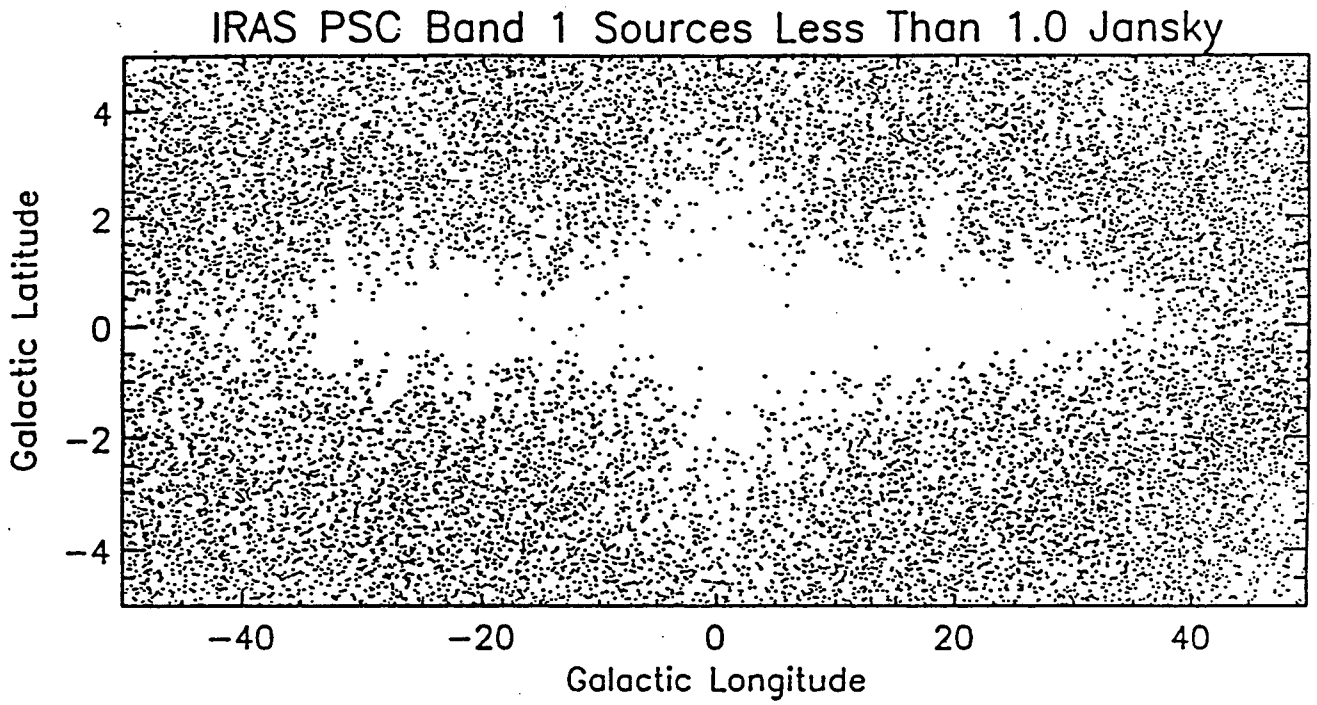

Figure 1
IRAS PSC Sources < 1 jansky in the Galactic Center

[High Resolution Descriptions of IRAS 12 and 25 Micron Confused Regions (1994)]

successful in extracting point sources in the galactic plane. A preliminary list of point sources was produced. This list is actually made up of six separate source lists: three separate hours-confirmed lists in each of the two wavelength bands.

C. *Cataloging Methods*

In order to create a catalog out of the six source lists provided, several processes must be performed. Firstly, regions of overlap in the survey must be merged to eliminate repeated sources in a process known as the platemerge. (This overlap occurs because of the way the two-dimensional plates were processed. The plates, which were 6° on a side, were processed as four quadrants, each 3.5° on a side {3}, as shown in Figure 2. This processing method caused overlap in the source lists. In fact, it is possible for a single source to appear as many as four times in the lists due to this overlap.) Secondly, the three different HCON (hours-confirmed)

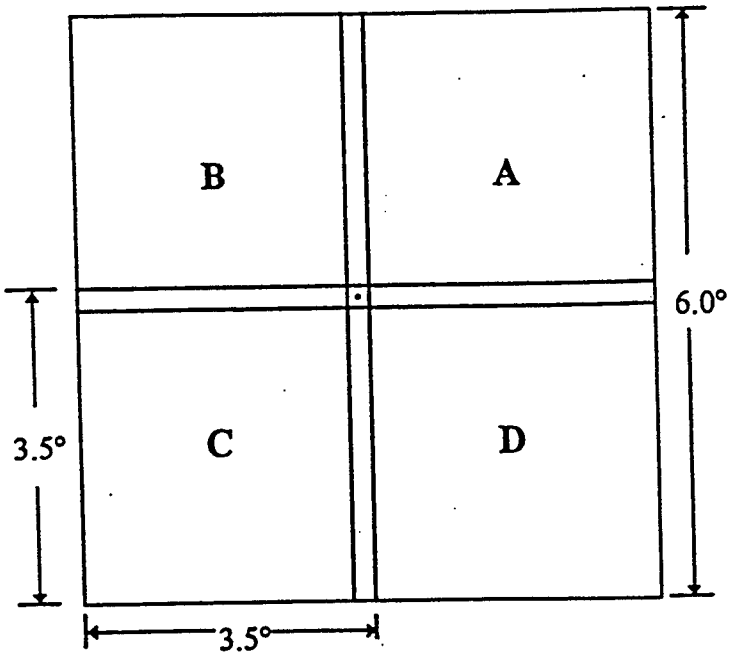

Figure 2
Definition of Quadrant plates relative to IPAC archival plates. MRC processes these plates in 3.5 degree quadrants, causing the overlap shown.

[High Resolution Descriptions of IRAS 12 and 25 Micron Confused Regions (1994)]

images must be merged into one. Thirdly, the source lists for the 12 and 25 μm bands must be merged to create a single, final source list.Preliminary versions of programs to perform all of these tasks have been created. For my project, I have analyzed the effectiveness of and the best ways to use these algorithms, and have made modifications to improve both their reliability and their completeness.

D. *Programming Tools*

The programs that I have written and modified, as well as several routines I wrote to produce graphs for data analysis, were written in Interactive Data Language (IDL). IDL is a "complete computing environment for the interactive analysis and visualization of data" {2}. IDL's mathematical and, especially, graphic capabilities made it ideal for the purposes of my project.

II. The Project

A. *Preliminary Data Analysis*

To begin my project, I focused on utilizing the graphing capabilities of IDL to create graphs of different types constructed from the data. The purpose of this was twofold: firstly, it enabled me to become familiar with IDL in general and, more specifically, IDL's graphics routines, but it also allowed me to familiarize myself with the data. This in turn allowed me to make informed decisions about the scope and direction of my project.

One of the series of graphs that I first worked on was a series of histograms. I used a data file containing sources that had been HCON-merged and platemerged, but not yet bandmerged. I took a sample consisting of the first sixty thousand sources in each band. I restricted the sample to this size because of the large size of the data file and the memory problems associated with reading large quantities of data from the source lists. I then constructed histograms of flux and signal-to-noise ratio for each band and for both bands combined - a total of six graphs in all. (See Figs. 3-8). Next, I was asked to pick one of my graphs, the histogram of flux for both bands combined, and focus on it. I then created cumulative histograms for this category, experimenting with different binsizes and log-log as well as linear-linear plots. (See Figs. 9-14). All of these graphs were created by IDL graphics routines that I wrote.

B. *Bandmerge Version 1 Analysis*

After creating graphs that presented a graphical view of the HCON-merged and platemerged source lists, I turned my attention to the bandmerge. The purpose of the bandmerge is to take the two separate 12 and 25 μm source lists and merge them into one, final list {6}. The bandmerging program used for this project searches for matches by position only and does not take flux or any other values into account. One of the variables involved in the bandmerge is the search radius - the maximum distance a potential match can be to a source and still be considered a match. The original bandmerge program had been run with a search radius of

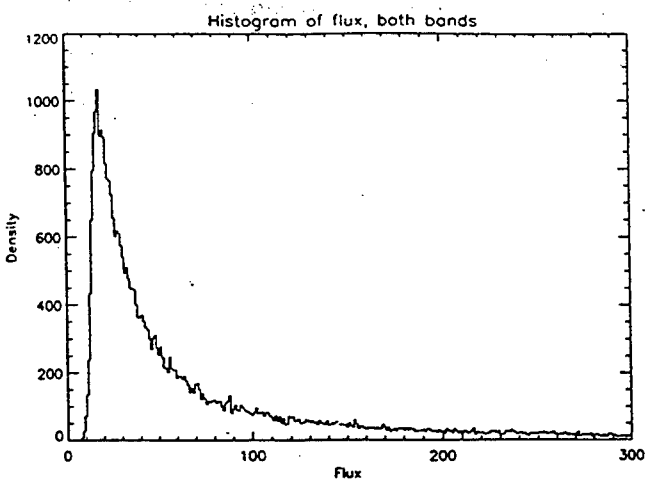

Figure 3

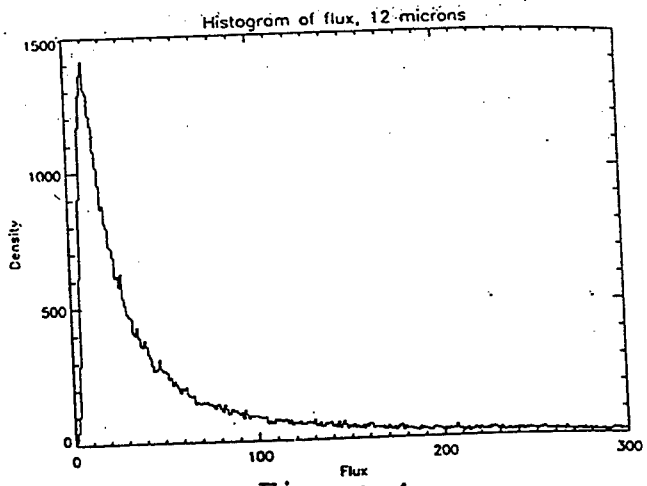

Figure 4

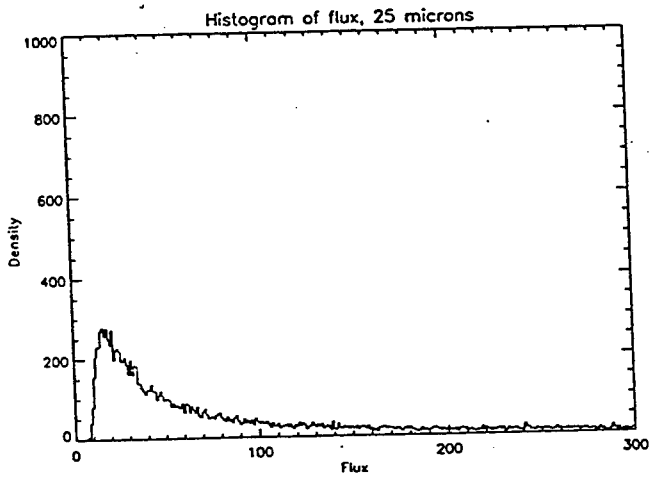

Figure 5

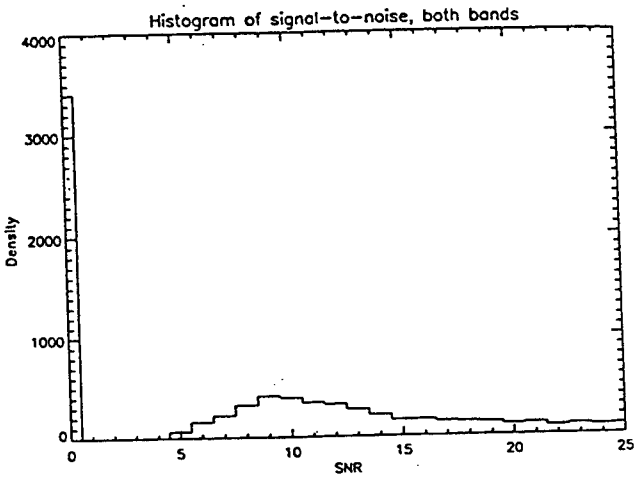

Figure 6

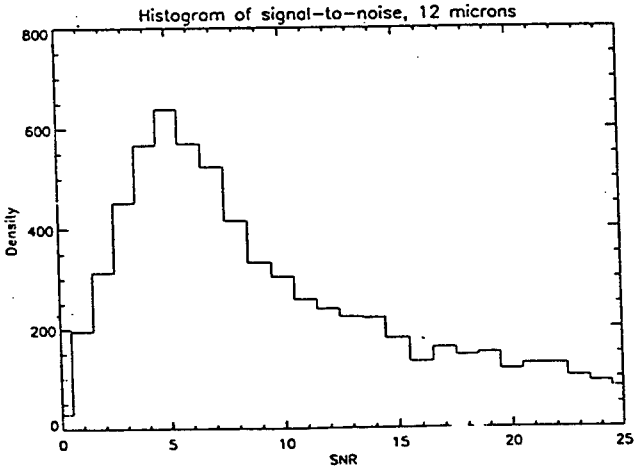

Figure 7

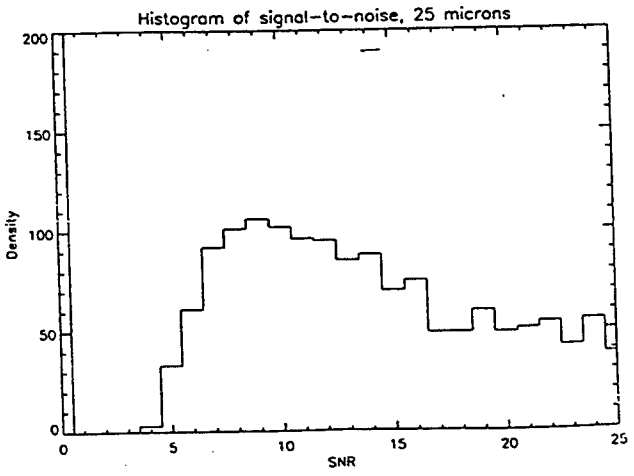

Figure 8

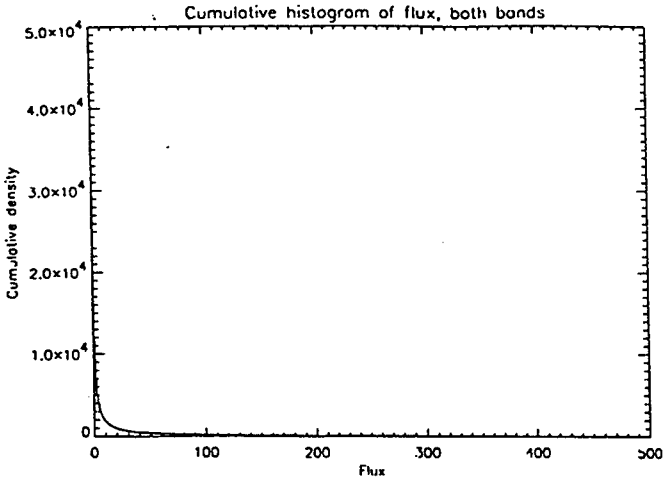

Figure 9 Binsize of 1.0

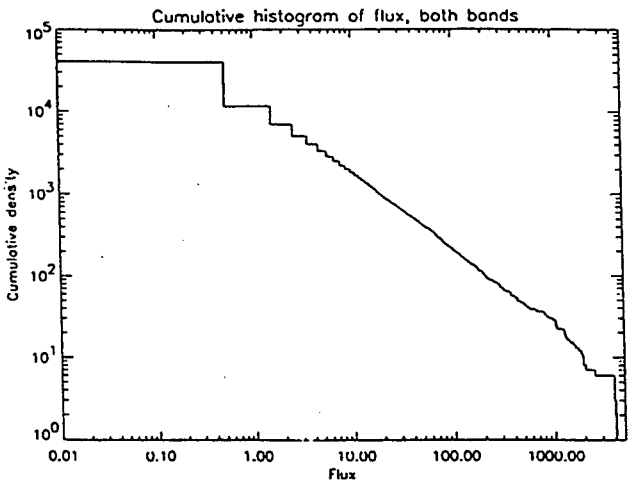

Figure 10 Binsize of 1.0

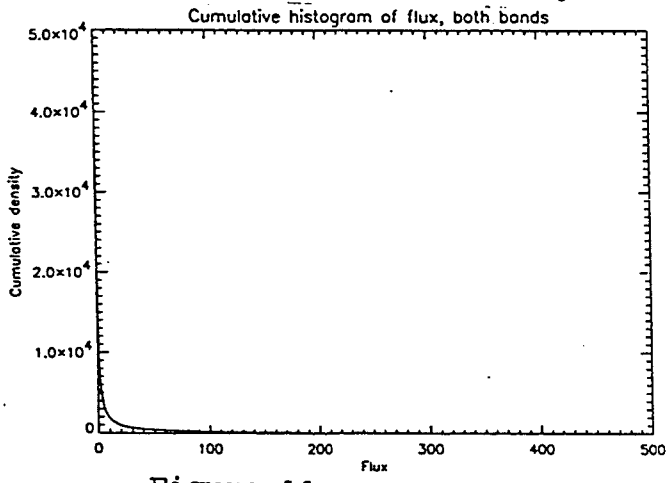

Figure 11 Binsize of 0.1

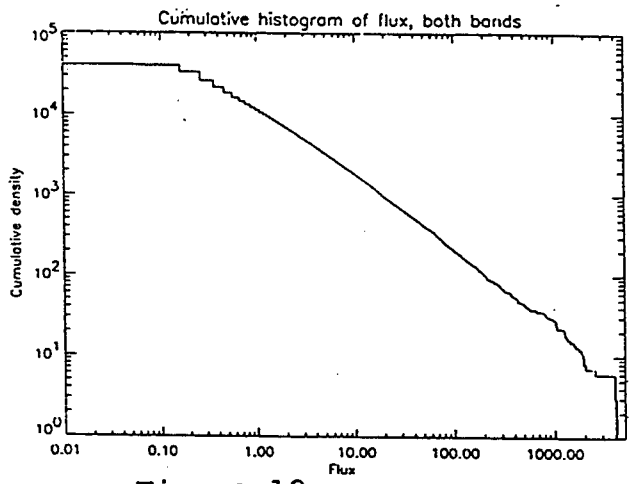

Figure 12 Binsize of 0.1

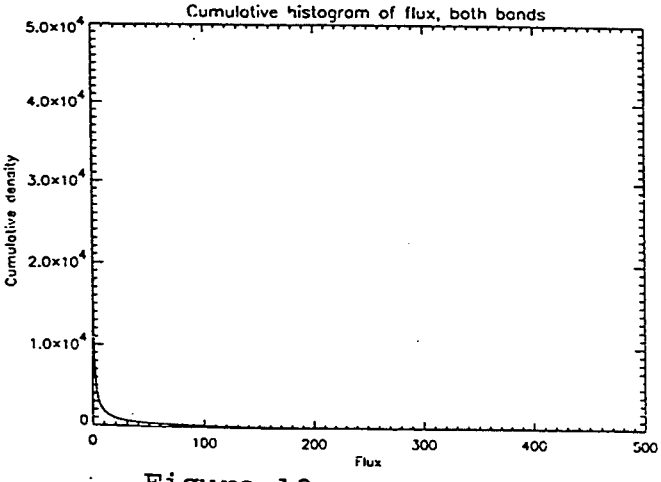

Figure 13 Binsize of 0.01

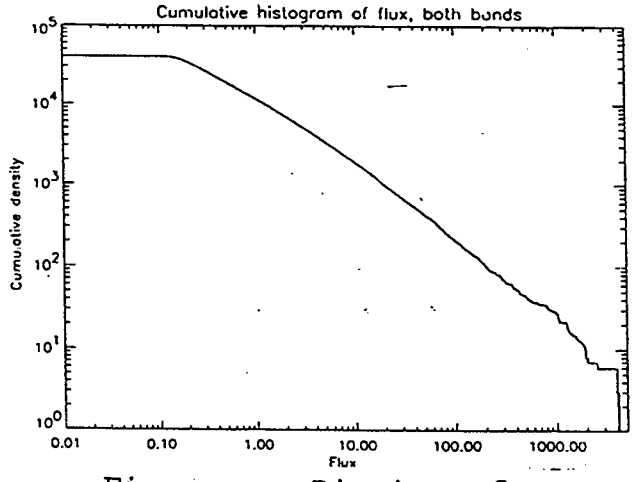

Figure 14 Binsize of 0.01

45 arcseconds. My task was to run the bandmerge for a variety of search radii to determine the "best" radius to use. In choosing the optimal search radius, two factors must be balanced: reliability and completeness. If the search radius is too small, some correct matches will not be made. This will ensure high reliability, but the completeness of the catalog would be compromised. However, if the search radius is too large, many random matches will be made. A high level of completeness will be achieved, but the reliability will be low. Searching for an optimal radius involves balancing these two factors.

Over a period of several days, I ran the bandmerging program with different radii. The minimum radius used was 15 arcseconds. This value was chosen because it is equal to the size of a pixel on the scans used to extract the sources. Obviously, any lower value would have no practical significance. An upper value of 900 arcseconds was chosen because the width of the detectors on the satellite made a higher value insignificant. Any additional matches made at a search radius above 900 arcseconds would probably be random.

When I finished running the programs, I had for each search radius the number of matches made by the bandmerging algorithm. (See Table 1). Now it remained to find an optimal search radius. A look at the graph of the number of matched sources versus the radius for the first eight data points (see Fig. 15) strongly suggests a square-root relationship. If this is true, then the formula for the number of matched sources is equal to:

$$\#\text{ of matched sources} = C_0 * \text{ search radius},$$

where C_0 is a constant. We can therefore calculate the value of the constant for each of the data points, and hopefully we can find an ideal value for the constant. And, if we calculate the ideal number of matched sources by multiplying the ideal constant by the square root of each radius, we can find the ideal search radius.

Originally, we had hypothesized that the value of the constant, C_0, would approach a single value as the search radius grew larger. However, this was not the case. The values of C_0, which are summarized in Table 1, started at 9480.03 for 15 arcseconds. The values then climbed steadily, and reached a maximum value of 13528.98 at 60 arcseconds. The values then steadily decreased to 6750.47 for the maximum radius of 900 arcseconds. Fig. 16 is a graph of ideal and actual numbers of matched sources using 13528.98, the maximum value, for the ideal constant. Fig. 17 is a graph of ideal and actual values using the minimum value of C_0, 6750.47, which occurs for the maximum radius of 900 arcseconds.

Data for Bandmerge Version 1 for different radii

Table 1

Radius (arcseconds)	# of matched sources	C_0
15	36,716	9,480.03
30	67,980	12,411.39
45	89,478	13,338.59
60	104,795	13,528.98
75	116,133	13,409.88
90	125,008	13,177.00
105	132,208	12,902.18
120	138,103	12,607.02
150	147,542	12,046.75
200	160,489	11,348.29
400	188,017	9,400.85
600	196,692	8,029.92
800	201,043	7,107.94
900	202,514	6,750.47

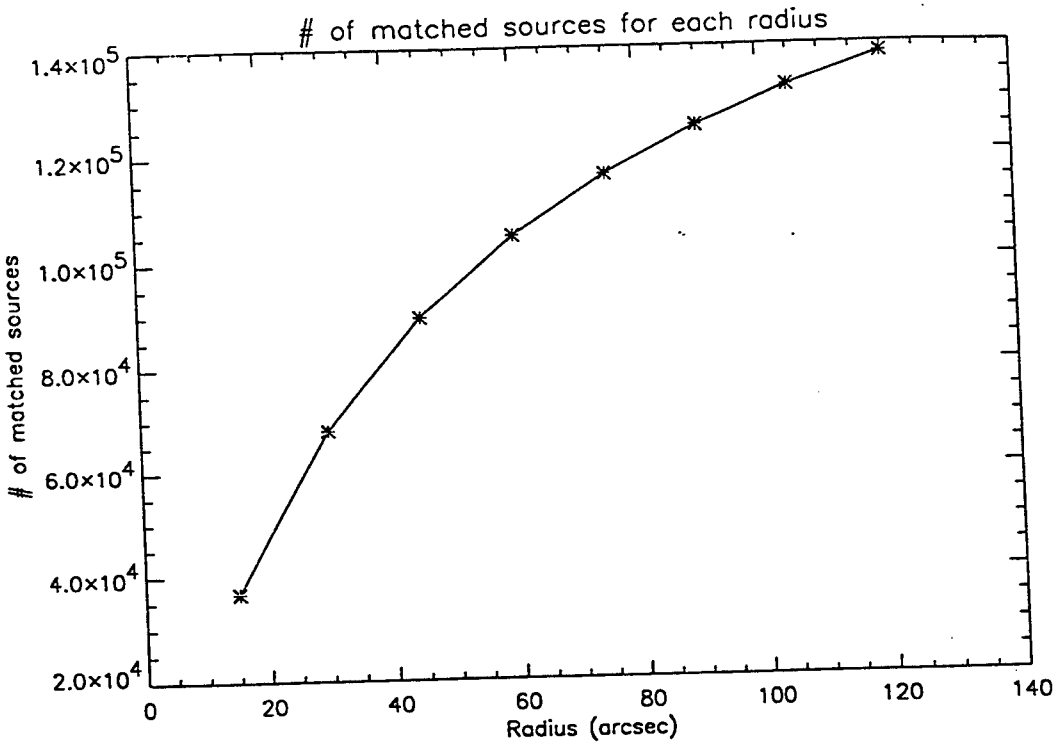

Figure 15

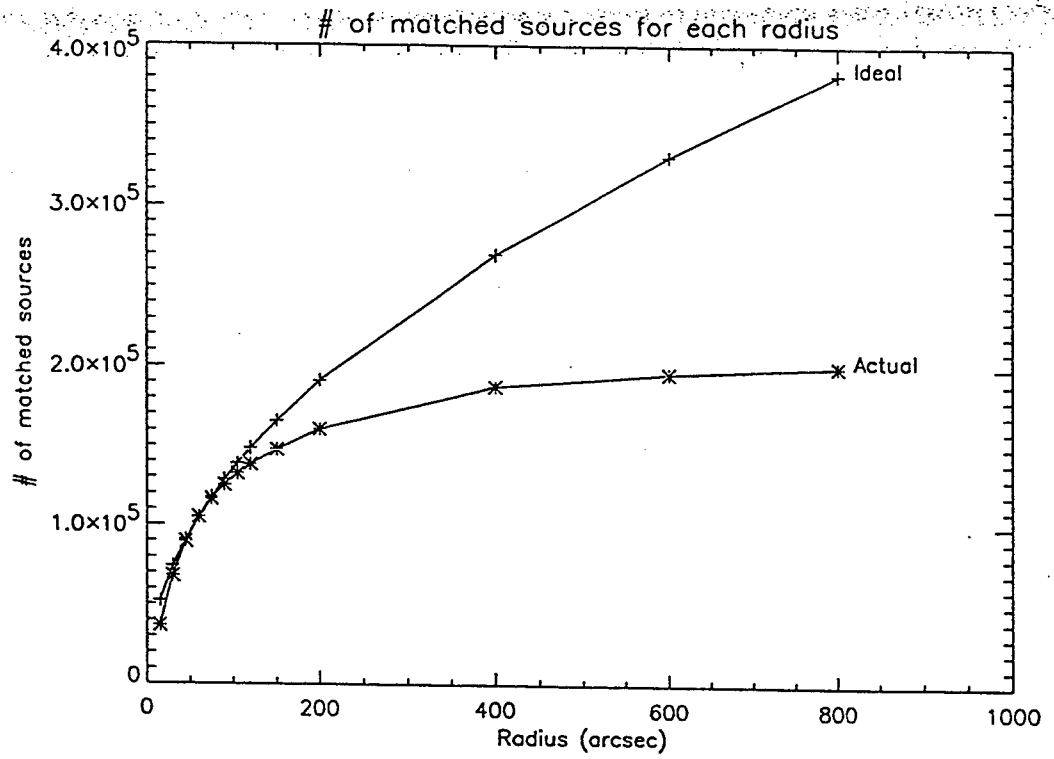

Figure 16

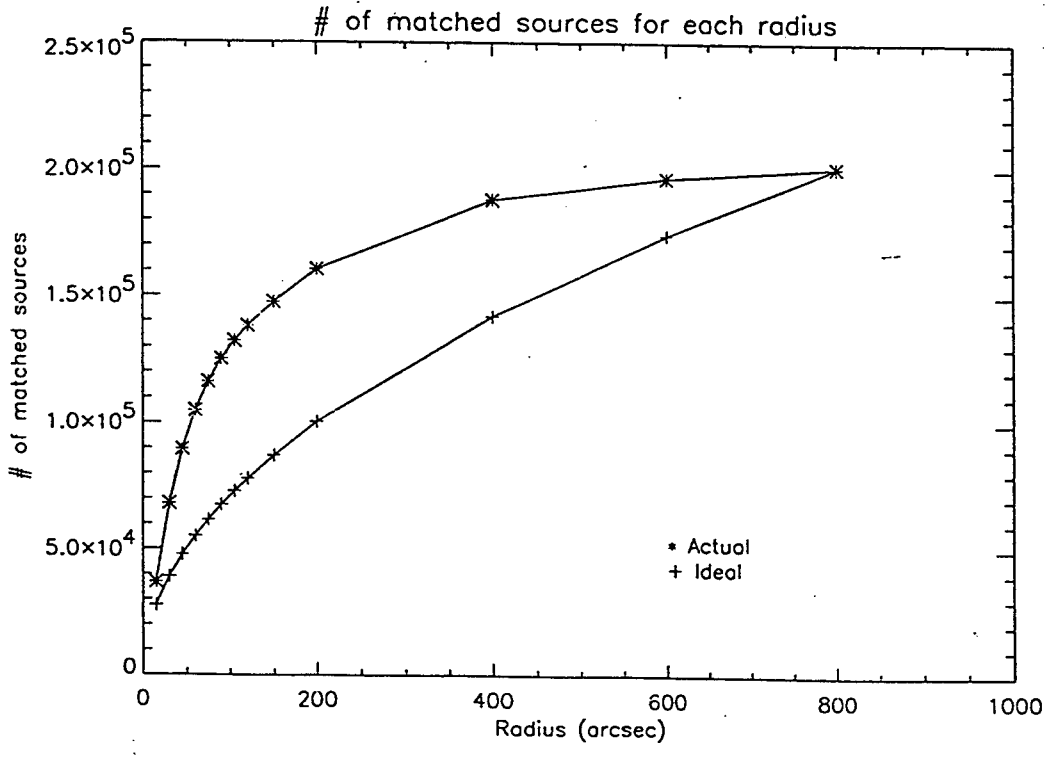

Figure 17

C. *Modification of Bandmerge Version 1*

The next stage of my project involved actually modifying the program that performed the bandmerge. To do this I first had to analyze the bandmerge code, determine what (if any) improvements could be made, and finally make those improvements to the program.

1. *The Original Bandmerge*

The original bandmerge code operates on a fairly simple principle. The objective of the code is to search within the radius specified around each 12 μm source and match it to the closest 25 μm source within the window. Once these matches are made, a new source list is compiled so that the matches are each represented as a single source. This process refines the position of each source as well as eliminating sources detected in only one band.

This method does present a problem, however. If there is more than one 25 μm source within the search radius of a given 12 μm source, the matches made will depend on the order in which the 12 μm sources are processed. For example, consider Fig. 18. Source 2, a 25 μm source, and source 3, a 12 μm source, are extremely close together and should be matched together as a single source. Source 1 and source 4, since they occur in different bands and are well within the search radius, should also be merged together. If source 3 is processed before source 1, this will indeed happen. The problem will arise if source 1 is processed before source 3. In this instance, the program will search for the closest 25 μm source to source 1, which in this case is source 2. Therefore, source 1 and source 2 will be matched together and sources 3 and 4, because they are so far apart, will remain unmatched. Therefore, when a situation arises such as the one presented in Fig. 18, sources will be matched incorrectly about fifty percent of the time.

2. *The Modified Bandmerge*

In order to correct this problem, I needed to create an algorithm that would match sources correctly no matter what order the sources were processed in. A simple solution is the following: once a 25 μm source is

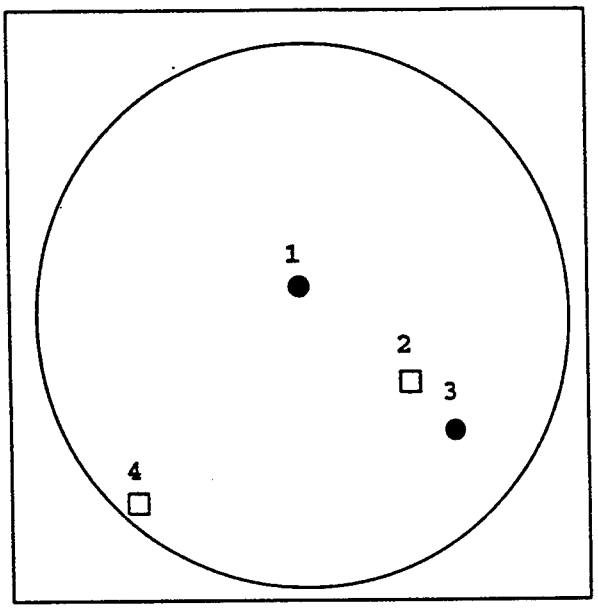

Figure 18

● 12 micron source

□ 25 micron source

○ represents search radius

found to match to a 12 μm source, the program then searches for the nearest 12 μm source (excluding the original source) that could be matched to the 25 μm source. If no match is found, the first two sources are matched and the program proceeds. If another source within the search radius is found, the distance between the original 12 μm source and the 25 μm source and the distance between the 25 μm source and the second 12 μm source are compared. The two sources that are closer are then matched. If the 25 μm source is matched to the 12 μm source originally under consideration, the program proceeds. If it is matched to the second 12 μm source, the program attempts to find another 25 μm source in the window to match to the original source. This process is repeated for all 12 μm sources. For the example given in Fig. 18, this algorithm will make the correct matches no matter what order the 12 μm sources are processed in. Although this algorithm seems to be a fairly

simple extension of the original algorithm, the code required quite extensive modifications to perform the change.

III. Results

A. *Optimal Search Radius for Bandmerge*

The task of balancing reliability and completeness in the process of cataloging the IRAS data is formidable. Some catalogs strive for reliability at the expense of completeness; others emphasize completeness and sacrifice reliability. The problem of selecting a search radius for the bandmerge is an example of this dilemma.

The final decision of what search radius to use will be made by others who are working on this catalog. By running the bandmerge for different search radii and analyzing and graphing the data I collected, I have helped contribute to this effort. The information I have collected hopefully will help them in their decision-making process.

B. *Success of the Modified Bandmerging Algorithm*

In order to test the new bandmerging program, I ran this program with a search radius of 15 arcseconds, the minimum radius used in the tests of the original bandmerge. By looking at the data for the matches made by the program, I have determined that my algorithm does indeed work as planned - the matches are made accurately, and several matches are made by the new method. However, I would estimate that situations such as that described above, in which the original bandmerging algorithm would make incorrect matches, only occur in about 1% to 2% of all matches made. Therefore, although the changes made were significant and do improve the accuracy of the bandmerge, they only impact about 1% of all matches.

I was surprised to learn that my algorithm made fewer matches than the original algorithm. The original bandmerge found 36,716 matches for a search radius of 15 arcseconds, as shown in Table 1. My program made about 35,000 matches for this radius. However, I do not think any firm conclusions about the

effectiveness of the changes made can be drawn from this data. I hypothesize that although fewer matches were made, the matches that were eliminated were eliminated in favor of other, closer matches.

One drawback to the new bandmerging algorithm is the huge amount of time it takes to run. The original bandmerge took two to three hours to run for any given search radius. My program, on the other hand, took nearly forty hours to run for a given radius. Not only does this run time make debugging, testing, and analysis difficult, but it also makes the improved algorithm less practical than the original algorithm. One further improvement that could be made to this program is an effort to decrease run time.

Another improvement on the program that could be made is to add a recursive feature so that a situation like that depicted in Figure 19 would not arise. In Figure 19, sources 3 and 4 should be matched together, sources 1 and 2 should be matched together, and source 5 should be left unmatched. However, my algorithm would match together sources 2 and 3 and would then match 1 and 5, leaving source 4 unmatched.

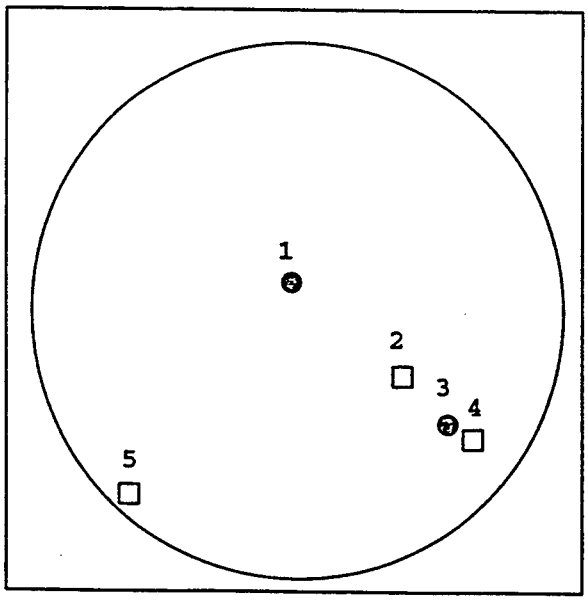

Figure 19

One way to fix this problem would be to add a recursive function that would continue to find a closer source for each and every source examined. However, situations like this one are extremely rare, and the added processing time that this change may make this change impractical, as the extra run time would outweigh the benefits of the change.

IV. Conclusion

This summer, I have had the opportunity to work on a small part of a large-scale project. My efforts have contributed to the Phillips Lab effort to catalog the galactic plane. No specific inferences or conclusions can be drawn from my work, but the data analysis I performed and the programs I wrote and modified will assist others at Phillips Lab in their efforts to completely catalog the galactic plane.

V. References

1. Beichman, C. A. et al. Infrared Astronomical Satellite (IRAS) Catalogs and Atlases: Explanatory Supplement. NASA Reference Publication, 1988.

2. IDL User's Guide. Research Systems, Inc., Boulder, CO, 1995.

3. Kennealy, R. M. et al. High Resolution Descriptions of IRAS 12 and 25 Microns Confused Regions. Phillips Laboratory Directorate of Geophysics, Hanscom AFB, MA, 1994.

4. Kleinmann, S. G. et al. Explanatory Supplement to the IRAS Serendipitous Survey Catalog. Infrared Processing and Analysis Center (IPAC), 1986.

5. Lawrence, A. (Ed.) Comets to Cosmology: Proceedings of the third IRAS Conference. Editor's Preface. Lecture Notes in Physics Series, Springer-Verlag, Berlin, 1987.

6. Moshir, M. et al. Explanatory Supplement to the IRAS Faint Source Survey. IPAC, 1989.

INSTRUMENTATION AND DATA ACQUISITION

Ruben E. Marin

Littlerock High School
10833 East Avenue R
Littlerock, CA 93543

Final Report For:
High School Apprentice Program
Phillips Laboratory, Edwards AFB, CA

Sponsored by:
Air Force Office of Scientific Research
Bolling Air Force Base, DC

and

Phillips Laboratory, Edwards AFB, CA

August 1996

INSTRUMENTATION AND DATA ACQUISITION

Ruben E. Marin

Littlerock High School

Abstract

This research was conducted at Area 1-120, Phillips Laboratory, Edwards Air Force Base. It is currently the United States Air Forces Large Engine and Component Test Facility. It has been in operation for about 40 years and has seen the evolution of the American space program. Now in the dawn of a new age, this area is calm and undergoing improvements. This paper will focus on the new instrumentation, methodology and data acquisition systems being installed in 1-120, those that will make a difference in the way things are done here and the change it will make in today's Defense and Aerospace industries.

INSTRUMENTATION AND DATA ACQUISITION

Ruben E. Marin

Littlerock High School

Area 1-120 is the Air Force's Large Engine and Component Test Facility at Phillips Laboratory, Edwards Air Force Base. Their tests until now have been mostly research and development for defense purposes. Now in the 1990's they are focusing their objective to mostly test and evaluation for industrial purposes and achieving its goals for a new purpose: Meeting today's modern stringent demands. It's shift from defense research and development to industrial test and development shows Phillips Laboratory's adaptation in an evolving economic climate. With the advent of new technology and the need for faster, better, stronger and thriftier propulsion systems, the Aerospace industry can take advantage of the limitless possibilities that the new Area 1-120 offers. Phillips Laboratory can handle newer, more powerful and sophisticated equipment, conduct tests using its strict guidelines and superior methodology and conduct them at a distance from the home factory that is far shorter than most other California or National sites.

1-120 has three test stands: 1A, 2A and 1B. 1B is currently out of operation and 1A and 2A are being renovated to meet modern specifications and are scheduled to be fully operational within the next couple of months. These stands are being equipped with advanced technology and new equipment to ensure that tests are done smoothly, accurately, safely and cost-efficiently.

Both test stand 1A and 2A burn fuels called CRYOPROPELLANTS. These cryopropellants, Liquid Hydrogen (LH2) and Liquid Oxygen (LOX) provide fuel for large engines. These propellants provide excellent power, results, cost-efficiency and produce environmentally-safe water in the form of steam.

Rocket engine testing is a very long, complicated and technical process. Engineers can earn masters degrees and men and women can work long, hard hours in unforgiving conditions just to setup up for a test (Fortunately, this report will only cover the basics). Just like building a car is not just one welder and parts, other

aspects go into a good, successful test along with instrumentation and data acquisition. Safety, operations, management, control, mechanical and electrical engineering, design, computer systems administration and simple common sense all contribute through teamwork to produce satisfactory results. But, for purposes here, the research will center on: Control, Instrumentation and Data Acquisition.

Control:

Virtually everything in Instrumentation is controlled by the Allen-Bradley Control System. The Allen-Bradley Control System is programmed, monitored and administered from a remote location in a control room. The Allen-Bradley Control System uses PC's, touch-screens to control every valve, switch, meter, gauge on the test stands. Instruments on the test stands relay their information back to the control center where it is monitored. One of its functions is to "watch' for dangerous situations. It can shut down any test automatically should it become hazardous.

Instrumentation:

The Allen-Bradley Control System controls every piece of equipment that it is programmed to run, yet without precise instruments, the control system would fail possibly leaving very catastrophic results. Instruments used to measure data can very in size from many feet and tons to millimeters and ounces.

Since listing ALL instruments used would comprise an entire book, a quick introduction to instruments will work perfectly.

Pressure Transducer:

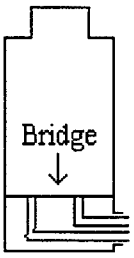

Electricity is almost like a liquid. It flows across the path of lest resistance. A Wheatstone Bridge is simplly four wires bridged by resistors on a diaphragm. As pressure enters the pressure transducer, the diaphragm is distorted causing a shift in resistance. Pressure is measured by the amount of voltage flowing through certain wires

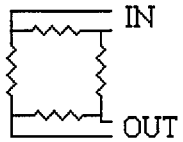

Wheatstone Bridge

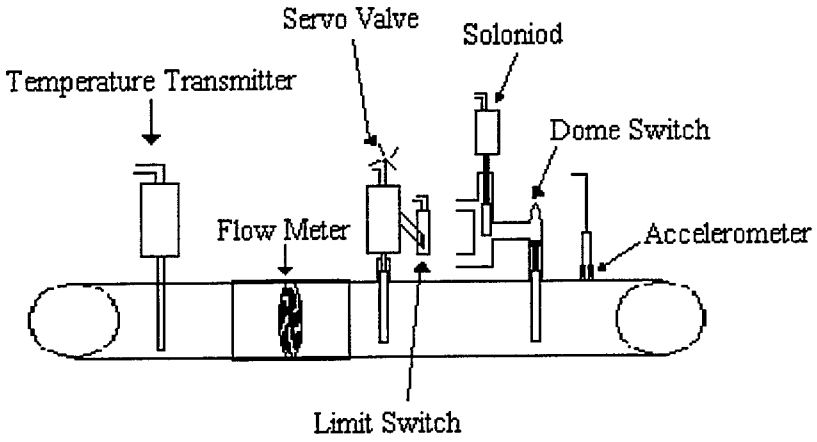

A temperature transmitter measures temperature in the amount of voltage that is read back. Two dissimilar metals, when exposed to different temperatures give different resistances. This constant curve of resistance is what rocket scientists use in measuring voltage and, therefore, measuring tempurature.

A flow meter simply measures flow, granted that it has been accurately calibrated. Should there be an unwanted change in pressure, a servo valve might remedy the problem. A servo valve is a remote operated valve. It sometimes may depend on a limit switch to operate and "tell" it how much needs to be opened or closed.

A soloniod opens or closes a switch remotely. This switch controlls air flow into a chamber. This chamber, a dome switch raises or lowers a valve according to pressure.

An accelerometer measures vibration. Since an engine can literally shake itself to pieces, vibration needs to be kept to a minimum. Accelerometers usually give their readings to a Vibration Measurement System. This system can stop a test at any time should there be a problem.

INSTRUMENTATION AND DATA ACQUISITION

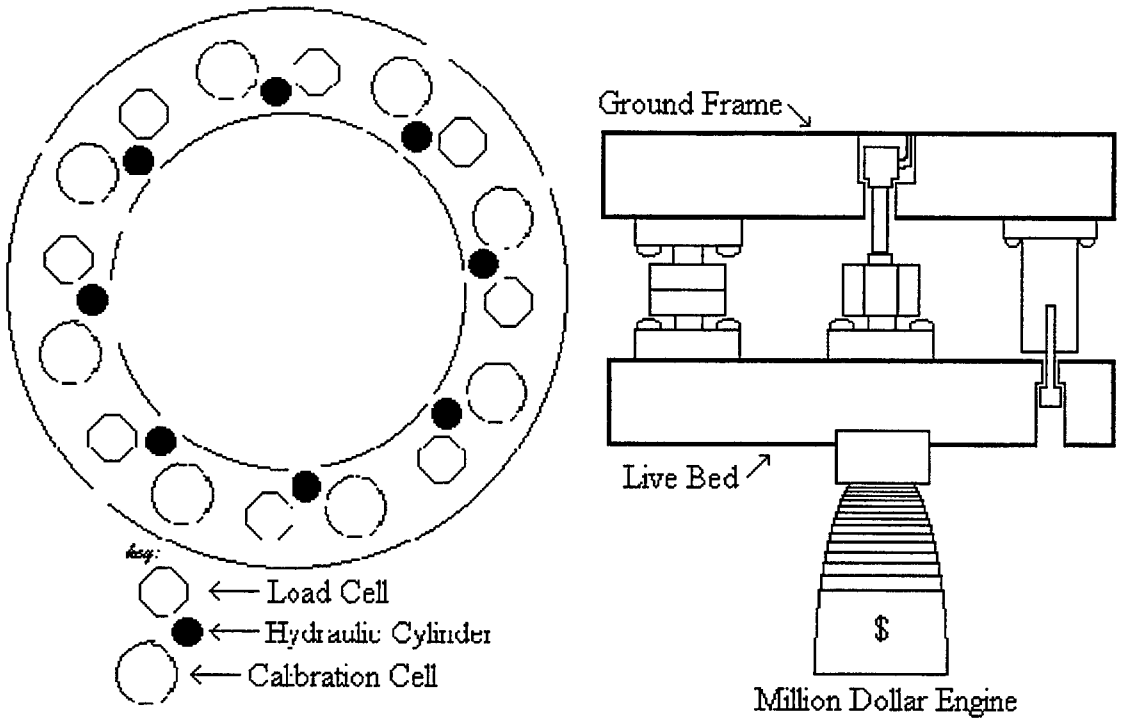

The Thrust Measurement System (TMS) for Area 1-120 is manufactured by Integrated Aerosystems. It is probably the largest and most sophisticated instrument used. The TMS consists of two 180 inch "rings" which are termed "Ground Frame" (top) and "Live Bed" (bottom). These two "rings" are pressed together during a test firing are their tension is measured and transmitted by a LOAD CELL. There are eight as suggested above.

All instruments need to be calibrated every once-in-a-while just as teeth need to be checked up and a car needs to be tuned. Load cells are no different. Integrated Aerosystems has their TMS so completely efficient and self-contained, it never has to be taken to a shop for calibration. Prior to test firing, load cells and the Live Bed may have excess weight, stress, strain and pressure that could hinder results and place a margin of error upon the load cells. Controlled by a PC in the control room, the calibration process begins. HYDRAULIC CYLINDERS, eight of them in suggested places above, each pull the Live Bed with a force of 200,000 foot-pounds. This combined pull of 1.6 million foot-pounds is registered by eight CALIBRATION (cal) CELLS. Cal cells relay their information to the control room computer, compare their accurate readings to the variable load cell readings, and a new standard is set. This practically eliminates a margin of error from the load cells. Once this procedure is done, the cal cells unlock from the "rings" and take themselves out of the thrust measurement equation.

Data Acquisition:

Only half of the instruments readings are sent to the ABCS. The other half go to the Data Acquisition System (DAS). The DAS is manufactured by Cyber Systems. The DAS, also known as the "Cyber", receives data and records it digitally. Its sends its information through fiber-optic lines to a control room where it can be monitored there. It is a new machine with state-of-the-art technology that is one of the many improvements being made to Area 1-120.

Unfortunately, the Cyber can only read and convert so fast. Instruments like accelerometers send their information at speeds that are too fast for the Cyber to read and convert. Fortunately, a Vibration Measurement system is being put into place and will aid in the accurate measurement and quality of a test. Other instruments with high-speed data go to FM recorders. These recorders offer superior recording ability with little speed limitation. Later, the FM tape can be played back for analysis, review and retrospect.

FERROELECTRIC LIQUID CRYSTALS FOR SATELLITE COMMUNICATIONS PHASE II

Fawn R. Miller

Manzano High School
12200 Lomas Blvd., NE
Albuquerque, NM 87112

Final Report for:
High School Apprentice Program
Phillips Laboratory

Sponsored by:
Air Force Office of Scientific Research
Bolling Air Force Base, DC
and
Phillips Laboratory

August 1996

15-1

FERROELECTRIC LIQUID CRYSTALS FOR SATELLITE COMMUNICATIONS PHASE II

Fawn R. Miller
Manzano High School

Abstract

This two year project studied the nature and operation of liquid crystals in a variety of different phases. Ferroelectric liquid crystal modulators were evaluated for use in satellite laser communications. The performance of the ferroelectric liquid crystal was measured previously by ON-OFF modulation techniques of a laser beam. Measurements were taken from 10 to 500 hertz and results indicated potential future applications.

The ferroelectric liquid crystals are capable of handling a moderate data rate. To achieve this data rate consistently, the ferroelectric liquid crystals must stay at a constant temperature. Many studies were conducted on how to cool the ferroelectric liquid crystals. The temperature controlling mechanisms created proved the crystals could be a productive satellite communication modulator.

Ferroelectric Liquid Crystals for Satellite Communications Phase II

Liquid crystals have been used in technology for only a few years. Today, Liquid Crystal Display (LCD) technology is used in wrist watches, pocket calculators, aircraft, and many devices that transfer alphabetic and numerical information to the user. Recently, liquid crystal technology has been tested for use in satellite communications.

Liquid crystals have been experimented with because they switch from transparent to opaque at fast speeds, effectively modulating a laser beam. A large laser on the ground could be used to illuminate a satellite. The light hitting the satellite would pass through a liquid crystal and then be reflected back to the ground. The data from the satellite would be used to create a modulation pattern for the liquid crystal. The reflected, modulated laser beam would be received on the ground by a telescope where an optical detector would be used to retrieve the satellite data.

The Phillips Laboratory has been working on laser communications technology for many years and recent laser technology advances make this appear to be a feasible alternative to RF systems. With the new discoveries of laser communications on satellites, the liquid crystal appears to be an effective device to be used to transmit data from the satellite. This laser and liquid crystal technology team up to give many advantages to data transmission. Some advantages include:

-Low weight of the satellite

-Little power is needed on satellite because there are no moving parts to be operated

-The setup is fairly simple

-The transmitting is more secure because the laser transmits to a smaller area

-There is still a moderate data transmitting rate

Ferroelectric Liquid Crystals (FLC's)

Liquid crystals are unlike ordinary crystals nor ordinary liquids, they have a classification of their own. Yet, they have some characteristics of both solid crystals and liquids.

In liquids, such as water, the molecules run into each other and move around. In a solid crystal, such as ice, the molecules are no longer free to move, they are arranged regularly and oriented in the same direction. Liquid crystals consist of rod-shaped organic molecules about 25 Angstroms (10^{-10} meters) in length. See Figure 1. These molecules are free to move around, as in an ordinary liquid, but they all point in the same direction, like in a solid crystal.

Figure 1. Ferroelectric Crystal Molecule.

There are several types of liquid crystals. The orientation order of the

constituent molecules characterizes the nematic phase liquid crystal. The molecular orientation (and hence the material's optical properties) can be changed by having an electric current applied to it. When the crystal has no charge applied to it, the nematic LC has a cloudy appearance or is blocked. The state changes and appears to melt when the plate has a charge put to it. Thus, the plate clears up and can be looked through. The nematic phase can be controlled by an electric current. The effect of the current is an opening and shutting of the liquid crystal. Nematics are (still) the most commonly used phase in liquid crystal displays (LCD's).

The smectic phases, which are found at lower temperatures than the nematic, form well-defined layers that can slide over one another like soap. The smectics are thus positionally ordered along one direction. In the Smectic A phase, the molecules are oriented along the layer normal, while in the Smectic C phase they are tilted away from the layer normal. These phases, which are liquid-like within the layers, are illustrated in Figure 2. Unlike nematic liquid crystal technology, FLC devices are not voltage tunable, they have only two states.

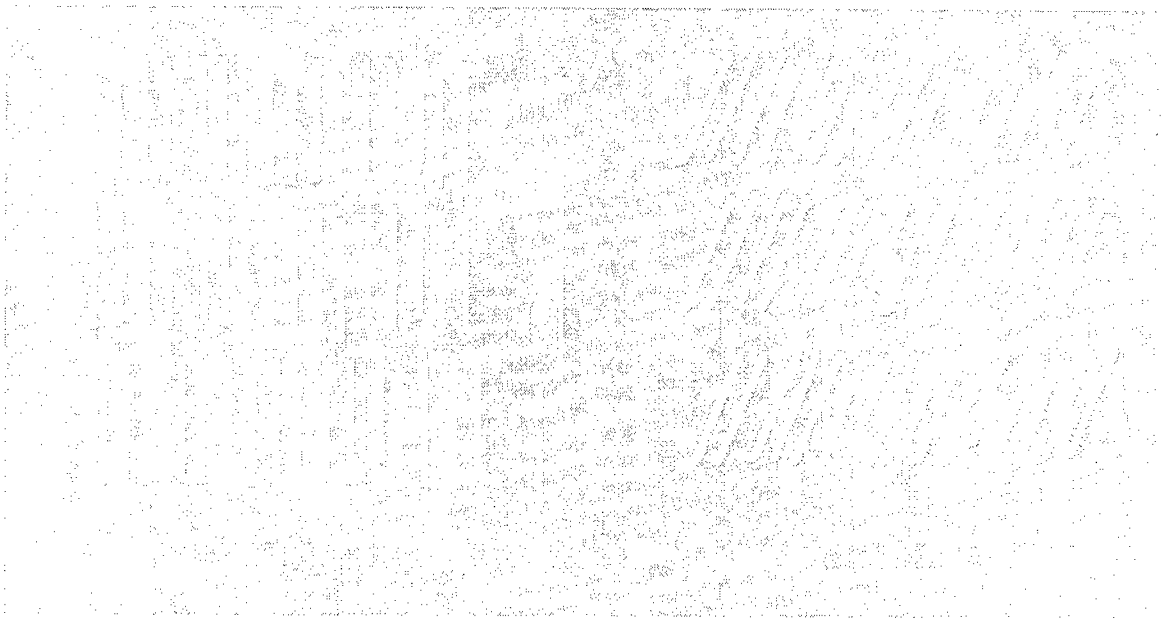

Figure 2. Orientation of Smectic Phases.

Liquid crystal's states can be changed by having an electric current applied to it. The LC has a cloudy appearance or is blocked when no current is applied to it. Then when a current is applied, the crystal appears to melt, and the plate clears up and can be looked through. The nematic phase can be controlled by an electric current. The effect of the current is an opening and shutting of the liquid crystal.

The FLC is only about a micrometer thick. The FLC is covered by two glass plates on both sides of it. The glass is then coated with a transparent conducting material, usually indium tin oxide (ITO). Two voltage wires are connected to this conducting material and the current sent to the glass effects the FLC's stage. Control of the FLC is straight forward, to hold the FLC "open" or "closed," five volts is applied between the leads. To change the state of the FLC, the polarity of the voltage is

reversed.

The FLC tends to heat rapidly with the laser light flowing through it, and the voltage being applied constantly. The FLC does not function properly when it gets too hot. The heat can cause the crystal to "melt" and the damaged crystal cannot be used again properly.

The laser diode used to transmit the data, can also get very hot, and needs to be keep at a constant temperature of 31 degrees Celsius. The studies of the previous two summers were to determine how fast the FLC could be opened and shut while keeping the FLC and the laser diode at a constant, cool temperature.

Experiment

The setup used was as follows: A polarized Helium Neon (HeNe) laser was put at one end of the setup. A neutral density filter was placed where the laser light went through it to act as an attenuator. The laser beam then passed through the ferroelectric liquid crystal (FLC) modulator and finally, the beam went into a detector. The information from the detector went to a computer and was stored on a program called LabView. A function generator was connected to the FLC and to the computer program. The generator sent an electric current to the FLC to open and shut it.

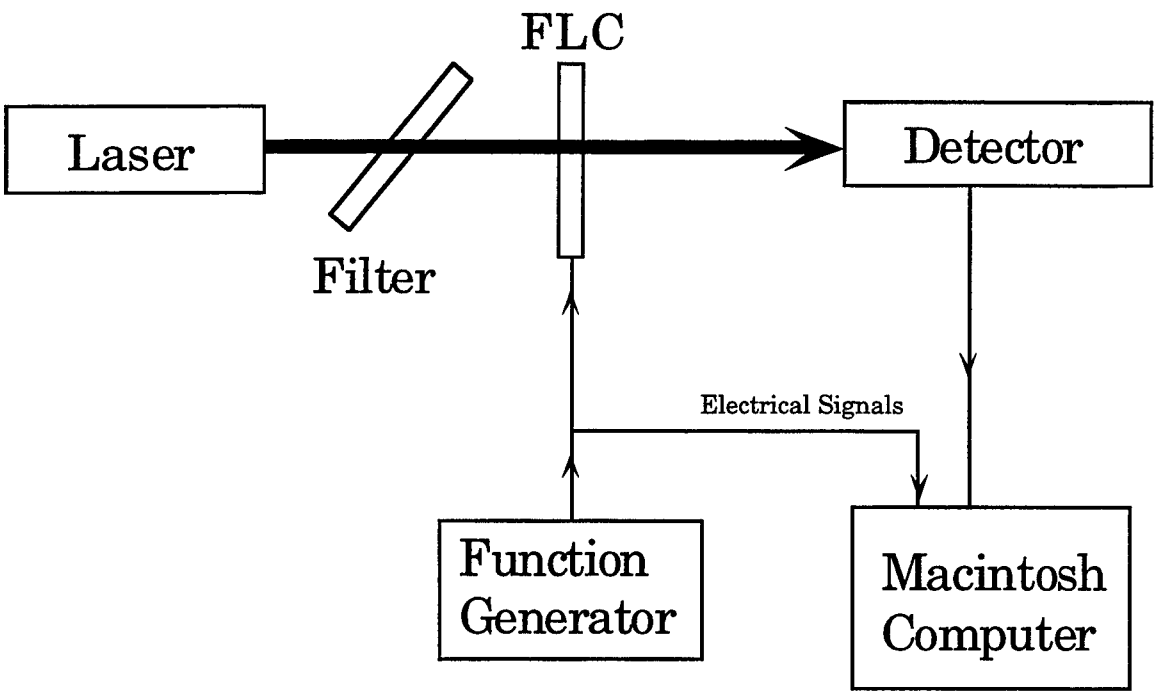

Figure 3. Experiment Schematic

The laser was covered with two temperature controllers, and was placed on a large heat shrink. The heat shrink was surrounded by two fans, and the whole system successfully cooled the laser.

The FLC was covered in an insulated box with temperature controllers attached to the sides. All of the equipment was controlled by VI's from LabView.

The information received by the detector and the electric current sent to the FLC was also sent to the computer on two different channels. The program that picked up the two channels on the computer was LabView. This program displayed the data and stored it. In LabView, a VI (virtual instrument) had to be programmed to do what was necessary before data could be displayed and stored.

We used a Macintosh computer for data acquisition and analysis. Data entered the computer through a 12-bit analog-to-digital converter card using a program called LabView. Within LabView we created an object oriented program, called a virtual instrument or VI. This was used to read two channels of data at 1000 data points a second and store the data to disk. After data acquisition, we were able to plot the data to determine the performance of the FLC.

Results

The results were recorded in a square wave frequency. Since the square wave has a tall boxy look, it is easy to tell how much laser light, or information, is going through the FLC at different speeds. Again, the effect wanted is totally open and completely shut at the fastest speed. The slowest test (10 Hz) showed the FLC opened and closed almost completely; about 95% open and 95% shut.

The fastest test was at 500 Hz and the response was about 10% open and 10% shut. The results that were taken from the FLC testing were reasonable, but hopefully can be improved.

The FLC and the laser temperature controllers were hard to make, but after many tests and experimenting, the cooling mechanisms worked. Some of the VI's from LabView did not read the temperature, so we had to devise a circuit board of our own to control and read the exact temperature.

Conclusion

The ferroelectric liquid crystal technology is hopefully going to have an effective use in satellite technology. The FLC has many advantages over other laser or RF communication techniques on the satellite. The FLC can receive information from a large angle. The FLC is also fairly inexpensive, around $150 for each modulator. The total estimated weight of the communication system with the FLC, is less than 10 pounds. Another large benefit of using the FLC and the laser is the smaller area it transmits to on the ground, making it more secure for Air Force applications.

The use of liquid crystals is a fairly new technology and the AFOSR research program has allowed my work with this new and upcoming technology. The knowledge of an unexplored field of technology is very beneficial. The ideas that can come to this technology are endless. The use of lasers and ferroelectric liquid crystals on satellites have a future of improvement and success.

The tests on temperature controlling this year, were very successful. The "test run" of the experiment is scheduled to fly in September 1996. The United States Air Force Academy is providing a balloon for the flight at Phillips Laboratories.

This summer, my process of learning about what was wrong in an experiment, correcting it, and doing something to fix the problem, was very beneficial to all areas of my study and knowledge.

References

Halliday, David, and Robert Resnick, Physics, John Wiley & Sons, 1978.

Pedrotti, Frank L., and Leno S. Pedrotti, Introduction to Optics, Prentice-Hall, 1987.

WWW pages from the Clark Research Group at the University of Colorado at Boulder.

Fergason, James L., Liquid Crystals, Scientific American, 1964. pp.77-82, 85.

Patel, J.S., and Goodby, J.W., Properties and Applications of Ferroelectric Liquid Crystals, Optical Engineering, May 1987. pp.373-384.

Writing Diagnostic Software for Photoluminescence Studies

Lewis P. Orchard

Sandia Preparatory School
532 Osuna Rd. NE
Albuquerque, NM 87113

Final Report for:
High School Apprentice Program
Phillips Laboratory

Sponsored by:
Air Force Office Apprentice Program
Bolling Air Force Base, DC

and

Phillips Laboratory

August 1996

Writing Diagnostic Software For Photoluminescence Studies

Lewis P. Orchard
Sandia Preparatory School

Abstract

Our project was to study the wavelength emissions from optically pumped semiconductor emitters. To study the wavelengths we fired a twenty watt Yag CW laser onto the sample and recorded the fluorescence using a monochrometer. Viewing the emissions from the emitter allowed us to answer our primary question, which was to find out if the sample lased. Armed with this information we were able to evaluate the effectiveness of the emitter.

Writing Diagnostic Software for Photoluminescence Studies

Lewis P. Orchard

Introduction-

The study of semiconductor lasers is a blossoming area of research throughout the scientific community. The commercial uses of a semiconductor lasers are practically endless. The semiconductor laser already performs numerous tasks to raise our standard of living. Some of the more common uses include; laser pointers, CD players, and a myriad of medical devices. In the future we can expect semiconductor lasers to play a greater part in each of our lives in devices such as; new communication technology, eye safe laser radar, and molecular spectroscopy detectors for gas leaks.

New emitters are under constant development. Characterizing and testing semiconductor lasers allows developers to envision the full range of technologies which can be created from an increasing understanding and control of these lasers.

Our project was to optically pump semiconductor lasers. Our goal was to find out if the emitters lased and determine the frequency spectrum of the output power being produced.

Methodology-

To excite the emitter we optically pumped the semiconductor emitter. To do this we fired a 20 watt CW YAG laser onto the emitter. We viewed the spectrum by using a monochrometer. In order to get the emitter to lase we found it necessary to chill it down. We accomplished this by using a cryostat to cool the sample temperature to between 77 - 300 Kelvin. One of the obstacles was obtaining and manipulating the data provided by the monochrometer, on a computer. My primary responsibility was writing the program

that would both control the experiment and digitize and manipulate the data.

Discussion of the problem-

The program I wrote is in HTBasic. My program began with a function that could move the monochrometer to any wavelength the user wanted to view. When the user is ready to run a scan he/she could break from the opening function and enter the main program. After the opening function the program required some information so that it could automate the experiment and record the operating parameters such as; beginning wavelength, ending wavelength, grating number, YAG power level, slit entrance width, slit exit width, pulse width, duty cycle, clocking, step size, scan rate, and temperature. After the user inputs this information my program then removes the backlash and moves the monochrometer to the beginning wavelength. Then the program reads the voltage from the (boxcar or lock-in depending on which is being used) and moves the monochrometer to the next wavelength along the spectrum. Then the program dumps the data into a file and plots the data to the screen. After the scan ends, the program has the option of plotting or printing the graph.

Results-

Example A is a spectrum scan from the a sample over a 1200nm region. In this scan, the sample is not lasing, but you can see the fourth harmonic of the YAG coming from the laser. Example B is a standard output of my code. In this example the output of the scan information is in the upper left-hand corner. As you examine the plot you see the first spike that the sample generated. The sample in this example is lasing. As you continue across the spectrum, the second spike is that of the YAG's fourth harmonic (the laser that we are pumping the semiconductor emitter with). Example C is a closer look at the sample's lasing peak. This view of the lasing peak is only 100 nm across.

Conclusions-

Throughout my internship my key responsibility was to generate the software that would run the experiment and manipulation the data. I managed to complete this project, perfect it, and add innumerable features for reading and manipulating the data.

Appendix A

Graphs

Filename is: c:\data\19Jul96.1

Yag power level (Amp): 25
LOCK-IN scale= 10
Slit Width Enterence (Microns): 1
Exit: 1
Pulsewidth (microsec) = : 167
Duty cycle (%): 5
Clocking (deg.): 0

Y-axis scale value: 2
Starting wavelength(nm): 3800
Ending wavelength(nm): 5000
Stepsize (nm): 3
Scanrate (nm/min: 500
Temperature = 150
Grating #: 3

NRL

Thinned @ 150μ

EXAMPLE A

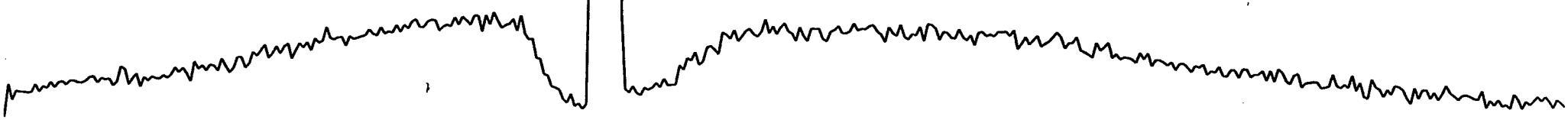

Filename is: c:\data\23Jul96.3

Yag power level (Amp): 30
LOCK-IN scale= 10
Slit Width Enterence (Microns): 1.5
Exit: 1.5
Pulsewidth (microsec) = : 168
Duty cycle (%): 5
Clocking (deg.): 0

Y-axis scale value: 2
Starting wavelength (nm): 3800
Ending wavelength (nm): 5000
Stepsize (nm): 3
Scanrate (nm/min: 50
Grating #: 3
Temperature 150

16-8

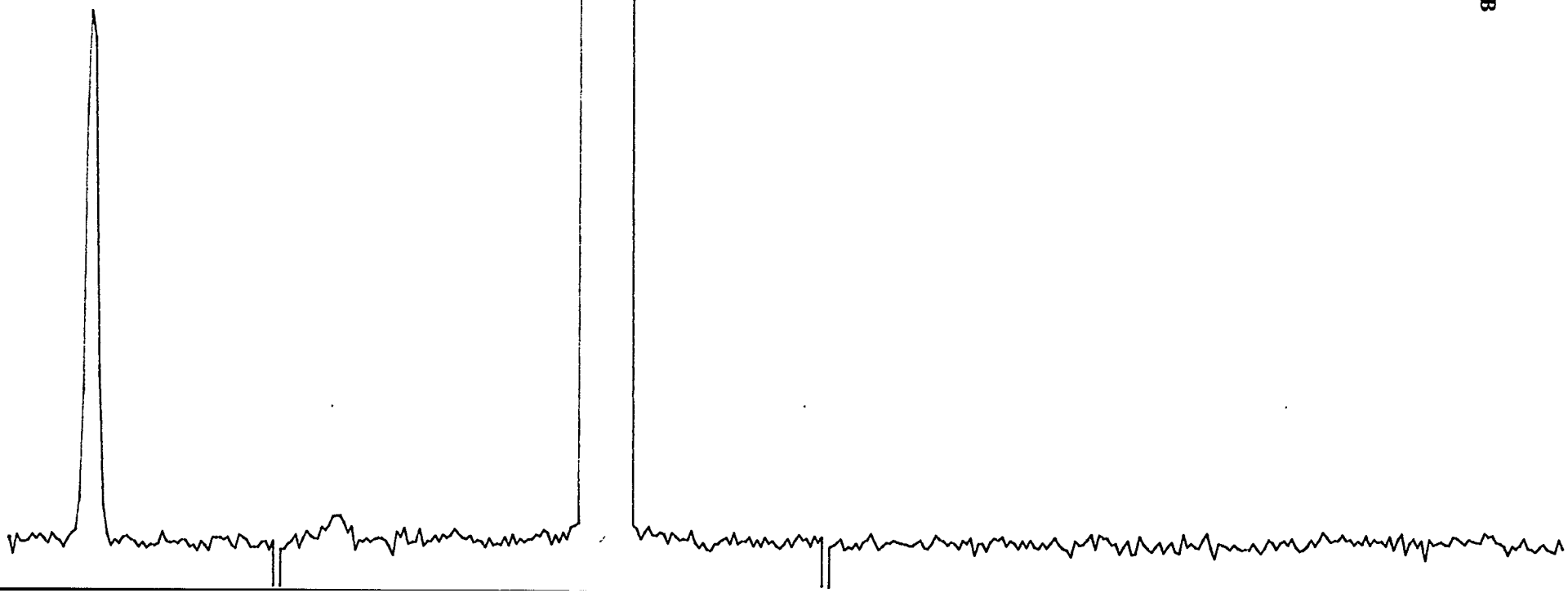

EXAMPLE B

Filename is: c:\data\23Jul96.5

Yag power level (Amp): 30
LOCK-IN scale= 10
Slit Width Enterence (Microns): 1
Exit: 1
Pulsewidth (microsec) = : 167
Duty cycle (%): 5
Clocking (deg.): 0

Y-axis scale value: 2
Starting wavelength (nm): 3800
Ending wavelength (nm): 3900
Stepsize (nm): 1
Scanrate (nm/min: 500
Grating #: 3
Temperature 150

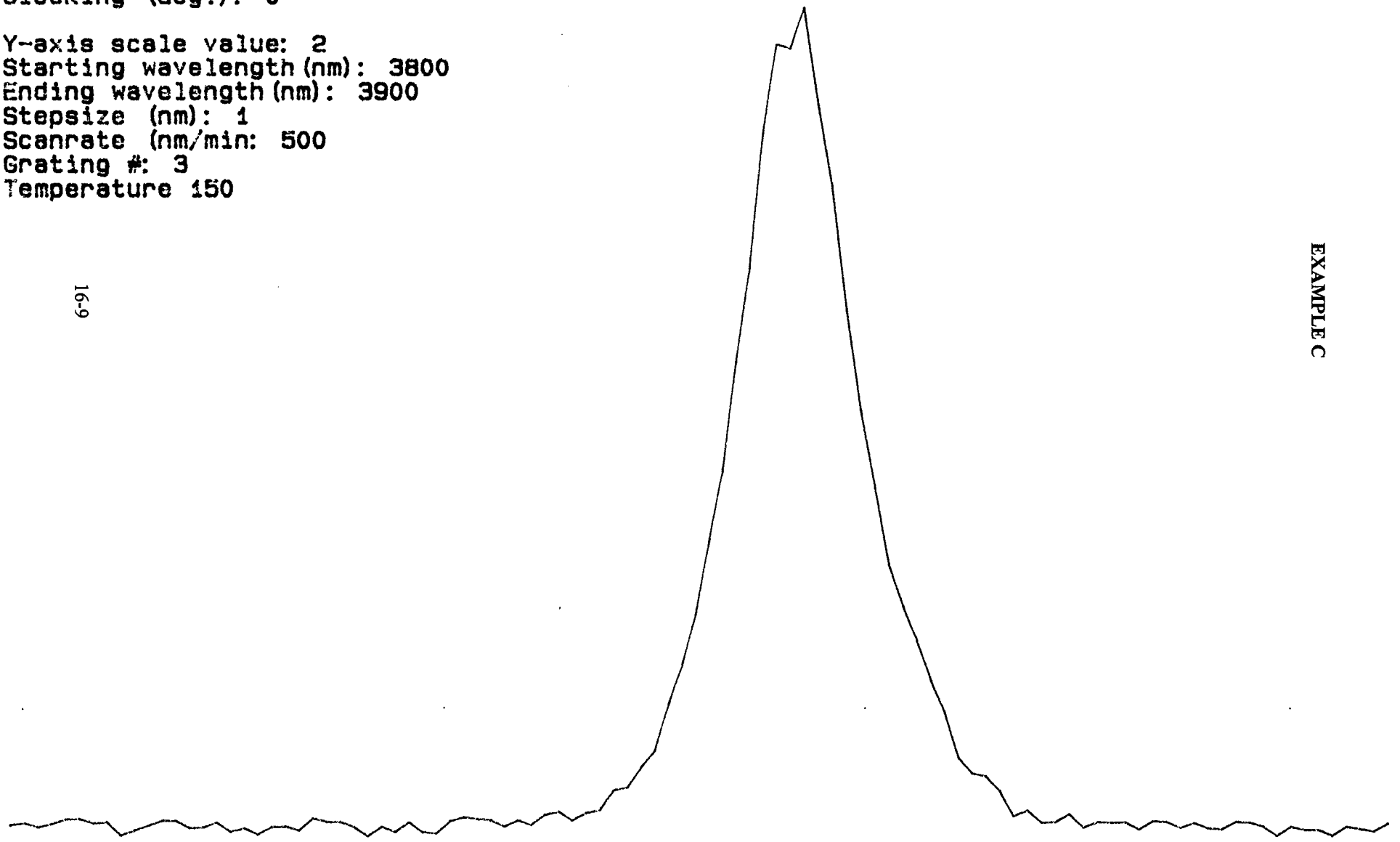

EXAMPLE C

Appendix B

Code

```
10   REM Program for acton monomiter
20 CLEAR SCREEN
30 RESET 7
40 ASSIGN @Out TO 711;EOL CHR$(13)   !CHR$(13)=RETURN
50 ASSIGN @Loc TO 716
60 ASSIGN @Plt TO 705
70 ASSIGN @Prt TO 10
80 Count1=0
90 Ret$=CHR$(13)
100 Runnum=Runnum+1
110   REM ****************************************************************
115 OUTPUT @Loc;"SB2=1"
120 PRINT "This part of the program moves the monomiter to a spicific wavelength."
130 LOOP
140   REM Begins the operitive loop
150 INPUT "Enter the wavelangth you want to go to.  (-1 to exit)",I$
160 IF I$="-1" THEN I=-1
170 EXIT IF I=-1
180 I$=I$&".0"
190 PRINT I$
200 OUTPUT @Out;I$&" GOTO"
210!WAIT 2
220    REM ***************
230!Stat=SPOLL(711)
240!PRINT Stat
250!IF Stat<>1 THEN GOTO 200
260    REM ***************
270 END LOOP
280   REM ************************************************************************
290   REM Sets up grating
300 CLEAR SCREEN
310 PRINT "The available gratings in the monochromator are:"
320 PRINT "Grating 1 = 600 groove/mm;   1 micron blaze"
330 PRINT "Grating 2 = 300 groove/mm;   2 micron blaze"
340 PRINT "Grating 3 = 150 groove/mm;   4 micron blaze"
350 PRINT
360 PRINT
370 INPUT "Would you like to change the gratings (y/n) ?",Ans$
380 IF Ans$="yes" OR Ans$="Yes" OR Ans$="YES" OR Ans$="Y" OR Ans$="y" THEN
390   REM ****changing the grating****
400 INPUT "Change Grating (1-3)",Ans2
410 OUTPUT @Out;Ret$
420 OUTPUT @Out;Ans2
430 OUTPUT @Out;"GRATING"
440 OUTPUT @Out;Ret$
450   REM INPUT "Press any key when the Grating has changed",Smile
460 WAIT 1
470   REM *****************
480 Stat=SPOLL(711)
490 IF Stat<>0 THEN GOTO 480
500   REM *****************
510 END IF
520   REM ****************************
```

```
530 CLEAR SCREEN
540   REM ************************************************************
550   REM setting up key info
560 INPUT "Enter the beginning wavelength in nm.",Beg
570 INPUT "Enter the final wavelength to be scaned.",Final
580 INPUT "Input the step size to the nearest .01nm.",Step
590 INPUT "Input the Yag power level.",Yag
600 INPUT "What is the Loc-in or Boxcar scale",Boxsc
610 INPUT "What is the Rep rate?(Hz)",Pulse
620 INPUT "What is the Duty cycle",Duty
630 INPUT "What is the Clocking?",Deg
640 INPUT "What is the Slit Entrance?(mm)",Slit
650 INPUT "What is the Silt Exit?(mm)",Slit2
660 INPUT "What is the Grating number?",Grat
670 INPUT "What is the temperature?(K)",Temp
680 IF Step<=1 THEN
690 Scan=CINT(200*Step)
700 END IF
710 IF Step>1 THEN
720 Scan=50
730 END IF
740 PRINT "The time between monochromator steps is";100*(Step/Scan)
750 INPUT "Do you want to change the scanrate (y/n)?",Ans3$
760   REM ******************
770 IF Ans3$="yes" OR Ans3$="Yes" OR Ans3$="YES" OR Ans3$="Y" OR Ans3$="y" THEN
780   REM *********
790 INPUT "Input the new scan rate in nm/min (.1-200nm/min)",Scan
800 PRINT "The time between monochromator steps is";100*(Step/Scan)
810 INPUT "Do you want to change this to a new scanrate(y/n):",Ans4$
820 IF Ans4$="yes" OR Ans4$="Yes" OR Ans4$="YES" OR Ans4$="Y" OR Ans4$="y" THEN
830 GOTO 790
840 END IF
850   REM *********
860 OUTPUT @Out;Ret$
870 OUTPUT @Out;Scan
880 OUTPUT @Out;"NM/MIN"
890 OUTPUT @Out;Ret$
900 END IF
910   REM *****************
920 INPUT "Enter the number of averages at each step",Nave
930!Beg=CINT(10*Beg)/10
940!Final=CINT(10*Final)/10
950 Numstep=CINT(ABS((Final-Beg)/Step))
960 ALLOCATE Data(Numstep+1)
970 PRINT "Scaning from";Beg;"to";Final;"."
980 PRINT "There will be";Numstep;"points."
990 INPUT "HIT ANY KEY TO CONTINUE...",Smile
1000 CLEAR SCREEN
1010   REM ************************************************************
1020   REM Removing backlash
1030 PRINT Beg
1040!A$=VAL$(INT(100*(Beg-1)+.5)/100)
1050!IF POS(A$,".")=0 THEN A$=A$&".00"
```

```
1060!G$=A$[POS(A$,"."),LEN(A$)]
1070!IF LEN(G$)=2 THEN A$=A$&"0"
1080 Go$=VAL$(Beg-1)
1090!PRINT Go$
1100 Go$=Go$&".0"
1110!PRINT Go$
1120!Go$=Go$&" goto"
1130 OUTPUT @Out;Go$&" GOTO"
1140 OUTPUT @Out;Ret$
1150 WAIT 4
1160 A$="10.0 NM/MIN"
1170 OUTPUT @Out;A$
1180 OUTPUT @Out;Ret$
1190!B$=VAL$(INT(100*Beg+.5)/100)
1200!IF POS(B$,".")=0 THEN B$=B$&".00"
1210!G$=B$[POS(B$,"."),LEN(B$)]
1220!IF LEN(G$)=2 THEN B$=B$&"0"
1230 B$=VAL$(Beg)
1240 B$=B$&".0"
1250 B$=B$&" NM"
1260 OUTPUT @Out;B$
1270 OUTPUT @Out;Ret$
1280!B$=VAL$(INT(10*Scan+.5)/10)
1290!IF POS(B$,".")=0 THEN B$=B$&".0"
1300!B$=B$&"NM/MIN"
1310 OUTPUT @Out;Scan
1320 OUTPUT @Out;"NM/Min"
1330 OUTPUT @Out;Ret$
1340 Wavelength=CINT(Beg)
1350    REM ****************************************************************
1360 PRINT "Wavelength should be reset to (nm)";Wavelength
1370 X0=Beg
1380 X1=Beg
1390 X2=Final
1400 Y0=-.2
1410 Y1=-.2
1415 WAIT 9
1420 INPUT "What is the maximum intensity value?",Y2
1430 INPUT "How many scans do you want to take?",Numscans
1440    REM ************************************************************
1450 REM FOR Scan=1 TO Numscans
1460 Count=Scan+1
1470    REM ***************************
1480 Runnum$=VAL$(Runnum)
1490 Date$=DATE$(TIMEDATE)
1500 Filename$=Date$[1,2]&Date$[4,6]&Date$[10,11]&"."&Runnum$
1510 Make$="c:\data\"&Filename$
1520    REM **************
1530 ON ERROR GOTO 1580
1540 ASSIGN @File TO Make$;FORMAT ON
1550 Runnum=Runnum+1
1560 GOTO 1470
1570    REM **************
```

```
1580 CREATE Make$,Numstep
1590 ASSIGN @File TO Make$;FORMAT ON
1600 OUTPUT @File;"YAG current level:";Yag
1610 OUTPUT @File;"Scanrate (nm/min):";Scan
1620    REM **************
1630    REM ************************************************************
1640    REM **************
1650!OUTPUT @Loc;"OUTX 1"
1660!PRINT "1"
1670 FOR N=0 TO Numstep
1680 Avg=0
1690    REM *****
1700 FOR J=1 TO Nave
1710 OUTPUT @Loc;"?1"
1711!OUTPUT 716;"?1"
1720!PRINT "2"
1730!PRINT "1"
1740 ENTER 716;Dat
1750!PRINT "2"
1760 Avg=Dat+Avg
1770 NEXT J
1780    REM *****
1790 Count1=Count1+1
1800 Avg=Avg/Nave
1810!CLEAR SCREEN
1820    REM ****************************************
1830!OUTPUT @Loc;"SENS ?"
1840!ENTER @Loc;Sens
1850!PRINT "here"
1860!SELECT Sens
1870!CASE 7
1880!  Avg=Avg/.00000005
1890!CASE 8
1900!  Avg=Avg/.00000001
1910!CASE 9
1920!  Avg=Avg/.00000002
1930!CASE 10
1940!  Avg=Avg/.0000005
1950!CASE 11
1960!  Avg=Avg/.000001
1970!CASE 12
1980!  Avg=Avg/.000002
1990!CASE 13
2000!  Avg=Avg/.000005
2010!CASE 14
2020!  Avg=Avg/.00001
2030!CASE 15
2040!  Avg=Avg/.00002
2050!CASE 16
2060!  Avg=Avg/.00005
2070!CASE 17
2080!  Avg=Avg/.0001
2090!CASE 18
```

```
2100!  Avg=Avg/.0002
2110!CASE 19
2120!  Avg=Avg/.0005
2130!CASE 20
2140!  Avg=Avg/.001
2150!CASE 21
2160!  Avg=Avg/.002
2170!CASE 22
2180!  Avg=Avg/.005
2190!CASE 23
2200!  Avg=Avg/.01
2210!CASE 24
2220!  Avg=Avg/.02
2230!CASE 25
2240!  Avg=Avg/.05
2250!CASE 26
2260!  Avg=Avg/.1
2270!END SELECT
2280    REM ****************************************
2290!PRINT "3"
2300!CLEAR SCREEN
2310!ALLOCATE Data(Numstep)
2320!PRINT "smile"
2330 Data(Count1)=-Avg
2340!PRINT "smile"
2350 Per=Count1/Numstep
2360!PRINT "smile"
2370 Per=100*Per
2380!PRINT Per;"% COMPLETED"
2390!CLEAR SCREEN
2400 Wavelength=Wavelength+Step
2410 OUTPUT @Out;Ret$
2420!PRINT "5"
2430!B$=VAL$(INT(100*Wavelength+.5)/100)
2440!IF POS(B$,".")=0 THEN B$=B$&".00"
2450!G$=B$[POS(B$,"."),LEN(B$)]
2460!IF LEN(G$)=2 THEN B$=B$&"0"
2470!B$=B$&"goto"
2480 Wavelength$=VAL$(Wavelength)
2490 Wavelength$=Wavelength$&".0"
2500!PRINT "5"
2510 OUTPUT @Out;Wavelength$&" GOTO"
2520 WAIT 3
2530!next N
2540    REM ************************
2550!FOR Count5=1 TO Numstep
2560 OUTPUT @File;(Step*N)+Beg;", ";Data(N)
2570!NEXT Count5
2580    REM ************************
2590 IF N=1 THEN
2600 CLEAR SCREEN
2610 Count6=0
2620 VIEWPORT 0,160,40,140
```

```
2630 WINDOW 0,Numstep,0,Y2
2640 PEN 1
2650 FRAME
2660 END IF
2670 Count6=Count6+1
2680!PEN 2
2690 PEN 2
2700 IF N=1 THEN PLOT 1,Data(1),-2
2710!FOR Count4=1 TO Numstep
2720 PLOT N,Data(N),1
2730!NEXT Count4
2740 IF N=1 THEN
2750 PRINT TABXY(0,19),Make$
2760 PRINT TABXY(0,20),"Beginning wavelength (nm) = ";Beg;"  Ending wavelength=";Final
2770 PRINT TABXY(0,21),"The step size is";Step;"  Scanrate = ";Scan
2780 PRINT TABXY(0,22),"Averages = ";Nave
2790 PRINT TABXY(0,23),"y-axis max value = ";Y2
2800 END IF
2810 NEXT N
2820 INPUT "Would you like to invert the graph?(Y/N)",Invert$
2830 IF Invert$="Yes" OR Invert$="YES" OR Invert$="Y" OR Invert$="yes" OR Invert$="y" THEN
2840 FOR Count2=1 TO Numstep
2850 Data(Count2)=-1*Data(Count2)
2860 NEXT Count2
2870 CLEAR SCREEN
2880 Count6=0
2890 VIEWPORT 0,160,40,140
2900 WINDOW 0,Numstep,0,Y2
2910 PEN 1
2920 FRAME
2930 Count6=Count6+1
2940 PEN 2
2950!PEN 7
2960 PLOT 1,Data(1),-2
2970 FOR Count4=1 TO Numstep
2980 PLOT Count4,Data(Count4),1
2990 NEXT Count4
3000!IF N=1 THEN
3010 PRINT TABXY(0,19),Make$
3020 PRINT TABXY(0,20),"Beginning wavelength (nm) = ";Beg;"  Ending wavelength=";Final
3030 PRINT TABXY(0,21),"The step size is";Step;"  Scanrate = ";Scan
3040 PRINT TABXY(0,22),"Averages = ";Nave
3050 PRINT TABXY(0,23),"y-axis max value = ";Y2
3060 GOTO 2820
3070 END IF
3080 INPUT "Enter 1 to print, enter 2 to plot and enter 3 to exit.",Out
3090 SELECT Out
3100 CASE 1
3110   Esc$=CHR$(27)
3120   Endline$=CHR$(13)
3130   Lterm$=CHR$(3)
3140   End$=CHR$(13)&CHR$(3)
3150   OUTPUT @Prt;Esc$;"E"
```

```
3155   OUTPUT @Prt;Esc$;"&l1O"
3160   OUTPUT @Prt;Esc$;"%0B"
3170!PLOTTER IS 10,"HPGL"
3180!GOTO 2510
3190   OUTPUT @Prt;"IN;"
3200   OUTPUT @Prt;"SP1;"
3210   OUTPUT @Prt;"SC";Beg;",";Final;",0,";Y2
3220!  OUTPUT @Prt;"PU;";Beg;",0;PD;";Final;",0"
3230!  OUTPUT @Prt;"PU;";1;",";Data(1)
3240!  OUTPUT @Prt;"PU"
3250   OUTPUT @Prt;"PA";Beg;",0;"
3260!  OUTPUT @Prt;"PD"
3270   FOR Nprint=1 TO Numstep
3280   Npr=Nprint*Step+Beg
3290   OUTPUT @Prt;"PD";Npr;",";Data(Nprint);";"
3300!  OUTPUT @Prt;"PD;"
3310   NEXT Nprint
3320    OUTPUT @Prt;"SC;"
3330   OUTPUT @Prt;"PU;"
3340   OUTPUT @Prt;"PA80,7500;"
3350   OUTPUT @Prt;"LBFilename is:";Make$;Endline$
3360   OUTPUT @Prt;"";Endline$
3370   OUTPUT @Prt;"Yag power level (Amp):";Yag;Endline$
3380   OUTPUT @Prt;"LOCK-IN scale=";Boxsc;Endline$
3390   OUTPUT @Prt;"Slit Width Enterence (Microns):";Slit;Endline$
3400   OUTPUT @Prt;"  Exit:";Slit2;Endline$
3410   OUTPUT @Prt;"Pulsewidth (microsec) = :";Pulse;Endline$
3420   OUTPUT @Prt;"Duty cycle (%):";Duty;Endline$
3430   OUTPUT @Prt;"Clocking (deg.):";Deg;Endline$
3440   OUTPUT @Prt;"";Endline$
3450   OUTPUT @Prt;"Y-axis scale value:";Y2;Endline$
3460   OUTPUT @Prt;"Starting wavelength(nm):";Beg;Endline$
3470   OUTPUT @Prt;"Ending wavelength(nm):";Final;Endline$
3480   OUTPUT @Prt;"Stepsize (nm):";Step;Endline$
3490   OUTPUT @Prt;"Scanrate (nm/min:";Scan;Endline$
3500   OUTPUT @Prt;"Temperature = ";Temp;Endline$
3510   OUTPUT @Prt;"Grating #:";Grat;End$
3520   OUTPUT @Prt;Esc$;"%0A"
3530   OUTPUT @Prt;Esc$;"E"
3540 GOTO 3080
3550   CASE 2
3560!PLOTTER IS 705,"HPGL"
3570!GOTO 2510
3580!  PEN 3
3590   Endline$=CHR$(13)&CHR$(3)
3600   OUTPUT @Plt;"IN;"
3610   OUTPUT @Plt;"SP2;"
3620   OUTPUT @Plt;"SC";Beg;",";Final;",0,";Y2
3630!  OUTPUT @Plt;"PU";Beg;",0;PD";Final;",0"
3640!  OUTPUT @Plt;"PU";1;",";Data(1)
3650   OUTPUT @Plt;"PA";Beg;",0;"
3660   FOR Nprint=1 TO Numstep
3670   Npr=Nprint*Step+Beg
```

```
3680   OUTPUT @Plt;"PD";Npr;",";Data(Nprint);";"
3690   NEXT Nprint
3700   OUTPUT @Plt;"SP3;"
3710   OUTPUT @Plt;"SC"
3720   OUTPUT @Plt;"PU"
3730   OUTPUT @Plt;"PA60,7720;"
3740   OUTPUT @Plt;"LBFilename is:";Make$;Endline$
3750   OUTPUT @Plt;"PA60,7545;"
3760   OUTPUT @Plt;"LB";Endline$
3770   OUTPUT @Plt;"PA60,7370"
3780   OUTPUT @Plt;"LBYag power level (Amp):";Yag;Endline$
3790   OUTPUT @Plt;"PA60,7195;"
3800   OUTPUT @Plt;"LBLOCK-IN scale=";Boxsc;Endline$
3810   OUTPUT @Plt;"PA60,7020;"
3820   OUTPUT @Plt;"LBSlit Width Enterence (Microns):";Slit;Endline$
3830   OUTPUT @Plt;"PA60,6845;"
3840   OUTPUT @Plt;"LB  Exit:";Slit2;Endline$
3850   OUTPUT @Plt;"PA60,6670;"
3860   OUTPUT @Plt;"LBPulsewidth (microsec) = :";Pulse;Endline$
3870   OUTPUT @Plt;"PA60,6495;"
3880   OUTPUT @Plt;"LBDuty cycle (%):";Duty;Endline$
3890   OUTPUT @Plt;"PA60,6320;"
3900   OUTPUT @Plt;"LBClocking (deg.):";Deg;Endline$
3910   OUTPUT @Plt;"PA60,6145;"
3920   OUTPUT @Plt;"LB";Endline$
3930   OUTPUT @Plt;"PA60,5970;"
3940   OUTPUT @Plt;"LBY-axis scale value:";Y2;Endline$
3950   OUTPUT @Plt;"PA60,5795;"
3960   OUTPUT @Plt;"LBStarting wavelength(nm):";Beg;Endline$
3970   OUTPUT @Plt;"PA60,5620;"
3980   OUTPUT @Plt;"LBEnding wavelength(nm):";Final;Endline$
3990   OUTPUT @Plt;"PA60,5445;"
4000   OUTPUT @Plt;"LBStepsize (nm):";Step;Endline$
4010   OUTPUT @Plt;"PA60,5270;"
4020   OUTPUT @Plt;"LBScanrate (nm/min:";Scan;Endline$
4030   OUTPUT @Plt;"PA60,5095;"
4040   OUTPUT @Plt;"LBGrating #:";Grat;Endline$
4050   OUTPUT @Plt;"PA60,4920;"
4060   OUTPUT @Plt;"LBTemperature";Temp;Endline$
4070!  OUTPUT @Plt;Esc$;"%OA"
4080   OUTPUT @Plt;"PG"
4090 GOTO 3080
4100 CASE 3
4110!PLOTTER IS CRT,"INTERNAL"
4120 END SELECT
4130!MOVE X1,Y1
4140!DRAW X2,Y1
4150!Num=(X2-X1)/2
4160    REM ********************
4170!IF Num=INT(Num) THEN
4180    REM **********
4190!FOR Q=X1 TO X2 STEP 2
4200!MOVE Q,Y1
```

```
4210!DRAW Q,(Y1+.02)
4220!NEXT Q
4230    REM **********
4240!END IF
4250    REM ********************
4260!INPUT "Do you want to run another scan?(Y/N)",Ans$
4270!IF Ans$="YES" OR Ans$="Yes" OR Ans$="yes" OR Ans$="Y" OR Ans$="y" THEN
4280!   GOTO 10
4290!END IF
4300 END
```

The Use of Reverberation Chambers for Susceptibility Testing on Airplane Electronics

Seth B. Schuyler

Sandia Preparatory School
532 Osuna Rd
Alb., NM, 87113

Final Report for:
High School Apprentice Program
Phillips Laboratory

Sponsored by:
Air Force Office of Scientific Research
Bolling Air Force Base, DC

and

Phillips Laboratory

July, 1996

The Use of Reverberation Chambers for Susceptibility Testing on Airplane Electronics

Seth B. Schuyler
Sandia Preparatory School

Abstract

New and more efficient means of gathering important electromagnetic susceptibility data have been found. The system has been automated to increase efficiency. Now it is easier to find the electromagnetic frequencies that will cause a piece of electronics to malfunction. This will allow smaller industries to test for susceptibility creating a more electromagnetic compatible world.

The Use of Reverberation Chambers for Susceptibility Testing on Airplane Electronics

Seth B. Schuyler
Sandia Preparatory School

Introduction:

Modern Airplanes are controlled or aided by electronics. These electronics, however, can be affected by electromagnetic waves. Such effects could render the plane uncontrollable, which would have disastrous results. Shielding the electronics in metal containers would stop the electromagnetic waves, but shielding all the electronics from all the frequencies would add too much weight to the plane. The chassis does help to shield, but the waves can enter through seams, antennas and the cockpit glass. Thankfully, not every frequency effects a piece of electronics equipment, so the amount of shielding can be minimized if the sensitive frequencies are known.

Methodology:

In order to find the sensitive frequencies of a particular piece of equipment, it must be operated while electromagnetic waves are passed into it. When it stops functioning normally, then a sensitive frequency and or power level has been found. There are three methods for putting electromagnetic waves into the equipment: direct injection, anechoic chamber, and reverberation chamber. Direct injection is achieved by attaching the signal generator, through an amplifier, into the equipment with a wire. This method is inexpensive and fast, but it is still inaccurate. The main problem is finding good points to test. Direct injection is sill in the development stages. In the anechoic chamber, the electromagnetic waves are directed into the equipment from an antenna. This is much more realistic than direct injection, and is accepted as the most accurate testing method. The down fall of this method is the time it takes to set it up for each angle that the researcher wants to test. The reverberation chamber was designed to make the testing process faster. It is set up similar to the anechoic chamber, but instead of absorbing the excess electromagnetic energy, it reflects it back. The purpose of reflecting is to generate an even field of energy around the sample equipment. This tests every angle of incidence simultaneously, saving a great deal of time. Within the chamber there are "hot" and "cold" spots, (Areas of high or low electromagnetic intensity.) caused by constructive and destructive interference of the waves. To minimize this effect, the chamber is stirred,

either mechanically with a metal paddle wheel, or electronically with Gaussian White Noise.

Results:
The reverberation method is simple enough to be put under the control of a computer. The computer uses the GPIB to control the noise generator, the signal generator, the amplifiers, and the data analyzer to run tests and generate data. The computer's speed and relative low expense are great advantages during this process. The data is stored on disk, so it can be more easily fed into a simulator, or be analyzed. The computer controller was programmed by Capt. Thomas Loughry. The original was DOS based, but a Windows version is being written using LabWindows. The revised edition will be more user-friendly, and more easily modified for each specific task. This makes the testing of electronics even simpler, leading to more accurate testing of critical airplane parts.

Conclusion:
With the advent of new testing method, and the use of computers, the entire testing process has been made more effective. Now the commercial world can, and is making use of it. Car companies are testing car computers with cellular phone frequencies to keep them from interfering with each other. (Electromagnetic Compatibility) This will mean more reliable products, and safer transportation in the future.

References:

Pozar, *Microwave Engineering.*

Condon and Odishaw. Handbook of physics. 2nd edition. New York: McGraw-Hill. 1967.

Loughry, Thomas A. *Frequency Stirring: An Alternative Approach to Mechanical Mode-Stirring for the Conduct of Electromagnetic Susceptibility Testing.* Phillips Laboratory, Kirtland AFB, NM. PL-TR--91-1036. 1991.

A STUDY OF THE CHARACTERIZATION IN SEMICONDUCTOR LASERS

William D. Shuster

Albuquerque Academy High School
6400 Wyoming Blvd. NE
Albuquerque, NM 87109

Sponsored by:
Air Force Office of Scientific Research
Bolling Air Force Base, DC

and

Phillips National Laboratories

August 1995

A STUDY OF ALPHA FACTOR IN SEMICONDUCTOR LASERS

William D. Shuster
Albuquerque Academy High School

Abstract

The characterization of semiconductor diode lasers is an important event that must happen in order to get a efficient laser. A laser properly characterized gives off a beam that is even and energy efficient. If semiconductor lasers are to be used they must output a beam that is coherent are gives off enough energy for practical uses. This can be accomplished through characterization.

AN EXPERIMENTAL SETUP FOR

CHARACTERIZATION OF SEMICONDUCTOR LASERS

William D. Shuster

Introduction

Semiconductor diodes have become an increasingly influential field in laser technology. Semiconductor lasers have been looked into for defense, compact disc technology, and medical applications. The Phillips Laboratory is involved in developing higher power semiconductor lasers that maintain good beam quality. A critical part of this development is in the electrical and optical characterization of the many cavity structures under consideration. The method of testing semiconductor lasers involves a series of tests, each giving specific data about the laser. The IV test is a preliminary test which is used to recognize weather or not the diode is efficient as a diode. The test graphs amperage over volts(see fig #1). The first test is a graph of laser power output verses pulsed current, this test is performed on most lasers, it tells us if the diode lases as well as how efficient the power output is the steeper the graph the more efficient the laser is. The pulsed current test gives peak energy performance at a certain amount of amperage. The second of the tests that a diode is put through is the power output verses continuous current test. This test performs much the same way as the pulsed current test however instead of measuring peak power this test measures average power this test also puts a great deal more stress on the diode then the pulsed current test. This test gives much more information about the power output of the laser under stressful conditions. (see fig #2) The third test is a far field scan of the laser. The scan moves a sensor in an arc of the tester's choosing across the beam of the laser. The sensor takes measurements and graphs it's measurements by power output over angle. This test helps us to find out if the diode's laser beam is a nice single lobe or broken into several lobes. Multiple lobed far-field patterns are not as useful for most applications. The last test a near field far field scan is used to see if the diode's cavity is properly formed. An improper cavity will be jagged while a properly formed cavity will be rectangular in shape.

Methodology

Over the course of my stay at Phillips Laboratories I constructed means for conducting the aforementioned tests. I used a form of computer communication known as IEEE or GBIP which allowed for the computer to be connected to various instruments. This allowed every attached instrument to be controlled by the computer through a computer language called HTB386. The pulsed current test was already programmed when I arrived at the laboratories, however I was given the task of programming the other two tests. The continuous current test was programmed despite problems with instrument communication which were eventually solved. The program consisted of many features which allowed it to be very user friendly while also solving the problem quickly and efficiently.(see appendix A) The far field scanning program was finished with much more ease then the continuous current program. This was largely due to lack of problems with instrument communication which plagued the continuous current program. Unfortunately a delay in the making of special mounts, for the far field scanner, delayed the construction of the far field scanner until after my departure from the laboratory. (see fig #3) The program however is working and is fully functioning. (see appendix B) The near field far field scanner was never in working order the plotter that is designed to work with the program failed in the simplest of tasks and no reason was ever found for why. The program was unable to be salvaged and I decided to continue with the next problem. The final problem was collecting data so as to calibrate the programs and instruments. I calibrated the programs by taking diodes that have been known to work and modified the program until the end results matched already known results. After I had done the calibration the programs were finished and ready to take measurements.

Results

The results of my work was a comprehensive automated system for studying the quality of the beam of semiconductor lasers. A system that can give multitudes of information about the particular semiconductor laser that the test are performed on. The system is quick and easy to use requiring minimum human interaction. The persons using the system can perform the tests altering every possible variable to look at different outcomes. The diode's can be tested quickly and efficiently with maximum data output.

Conclusion

The characterization of semiconductor lasers is very difficult process. A solution will only be found through many years of trial and error. Once a means to create a semiconductor laser with a powerful efficient beam the uses of

such a laser will be immense. However due to the difficult process of growing diodes it may be impossible to reliably create a efficient semiconductor laser without a easier method of growth.

Figure (1)

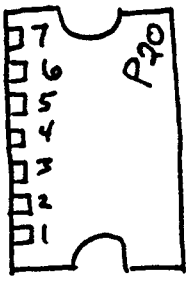

Bar P20
CD 1067
31 July 96

TEKTRONIX 571 Curve Tracer

SQW #1

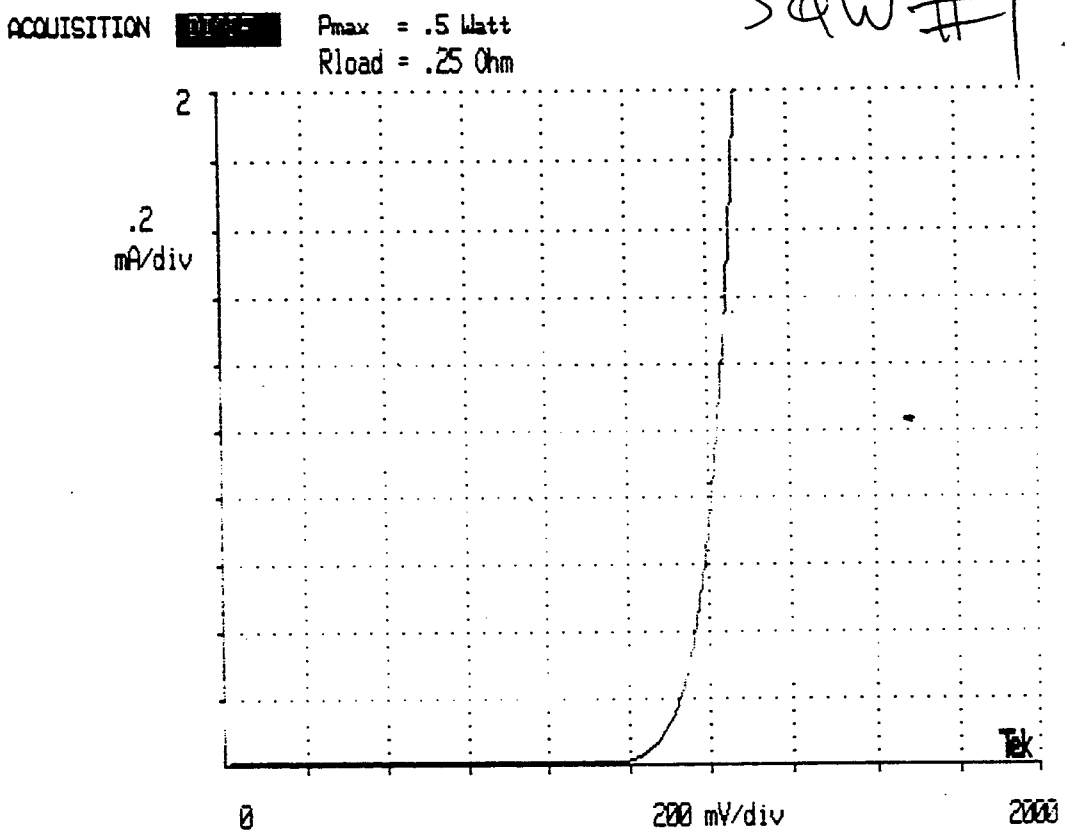

Screen copy (since power up) #9

Figure (2)

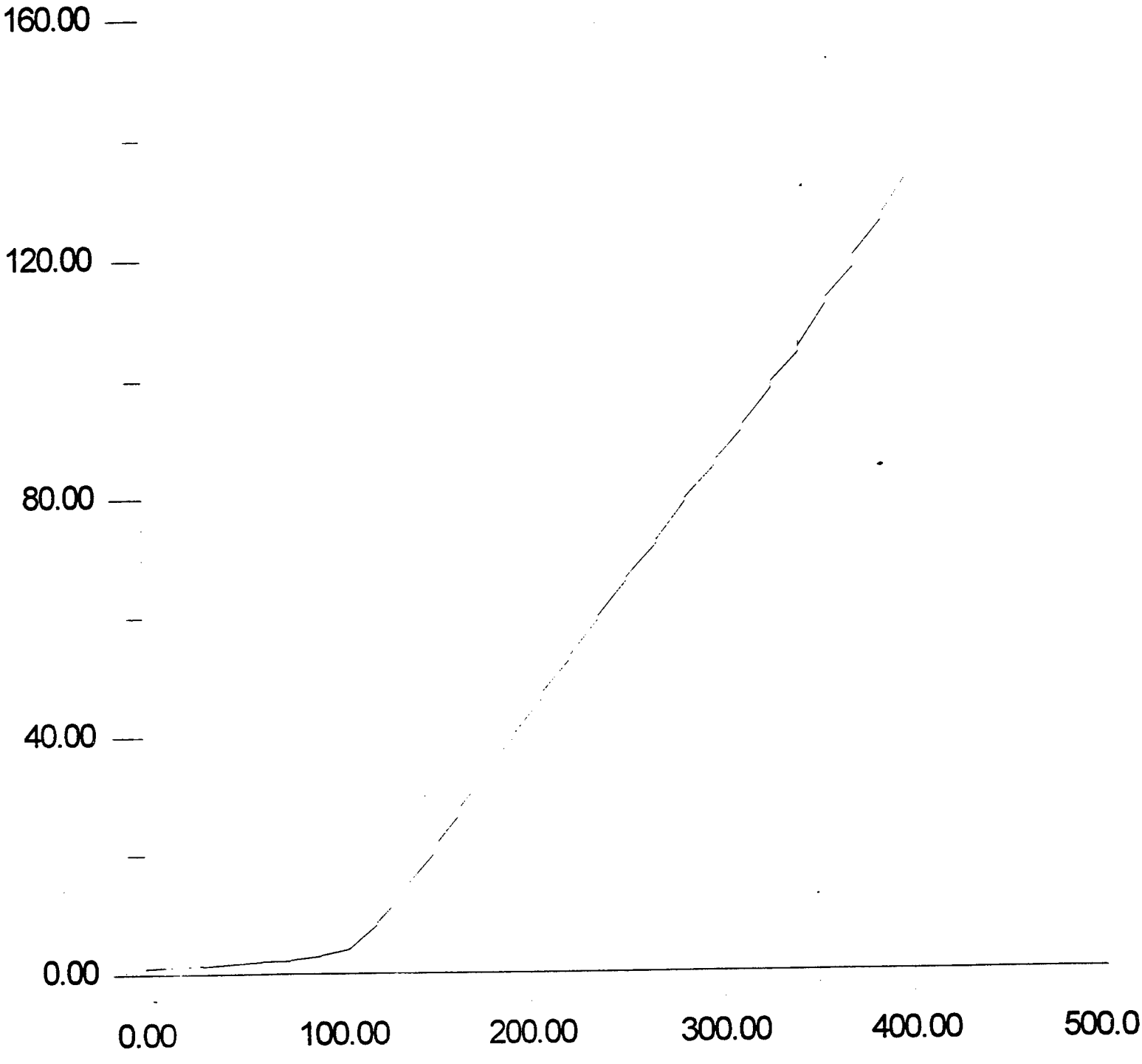

```
10    ! This program takes farfield scans stopping between
20    ! points to let mechanical vibrations settle.
30    CLEAR SCREEN
40    OFF TIMEOUT
50    Address=724
60    ALLOCATE Angle(2000)
70    ON ERROR GOTO 1260
80    DIM Ffdata(2000)
90    PRINT "";CHR$(142)
100   PRINT TABXY(10,10);"LASER DIODE FAR-FIELD MEASUREMENT PROGRAM";CHR$(138)
110   PRINT "";CHR$(130)&CHR$(138)
120   PRINT "Requires: HP 3478A multimeter, and"
130   PRINT "          Newport PMC200 motion controller";CHR$(128)
140   ON KBD GOTO 160
150   GOTO 140
160   CLEAR SCREEN
170   PRINT "";CHR$(142)
180   PRINT "Initial setup procedure:"
190   PRINT "1. Connect photodetector to the multimeter"
200   PRINT "2. Connect the PMC200 controller axis 1 to a model 496 rotation sta
210   PRINT "3. Manually set the zero of the PCM200 normal to the output facet"
220   PRINT "4. Go to setup and enable GPIB, with address 04"
230   PRINT "";CHR$(136)
240   ON KBD GOTO 270
250   GOTO 240
260   !menu
270   CALL Li_setup(Num_samps,Wait_time,Angmax,Max_power)
280   PRINT CHR$(136)
290   ON TIMEOUT 7,1 GOTO 1300
300   !looks for multimeter
310   OUTPUT Address;"meas:volt:dc?"
320   ENTER Address;Testing
330   OUTPUT Address;"DISP:TEXT 'I AM ALIVE'"
340   OFF TIMEOUT
350  ! LOCAL LOCKOUT 7
360   OUTPUT 704;"move1 0"
370   PRINT "*** Moving to initial position..."
380   I=0
390   !moves the actuators to inital postions
400   OUTPUT 704;"VEL1 05.0"
410   OUTPUT 704;"MOVE1 ";-Angmax
420   WAIT 2.0
430   OUTPUT 704;"*OPC?"
440   ENTER 704;Rsp
450   IF Rsp<>1 THEN GOTO 420
460   PRINT "*** Ready to begin..."
470   PRINT "*** Press [F2] to continue..."
480   PAUSE
490   CLEAR SCREEN
500   PRINT "*** Press any key to interrupt..."
510   ON KBD GOTO 1160
520   CALL Draw_screen(Angmax,Max_power)
530   Angle(I)=0
540   Ffdata(I)=0
550   MOVE -Angmax,6
560   ! ****Main data collection loop****
570   I=I+1
580   Angle(I)=0
590   Ffdata(I)=0
600   WAIT Wait_time
```

```
610   WAIT 1.5
620   Ffdat=0.
630   !gets measurements from multimeter
640   FOR J=1 TO Num_samps
650   OUTPUT Address;"meas:volt:dc?"
660   ENTER Address;Ff
670   Ffdat=Ffdat+Ff
680   NEXT J
690   Ffdata(I)=Ffdat/Num_samps*Max_power
700   !gets postion from actuators
710   ON TIMEOUT 7,.50 GOTO 1240
720   OUTPUT 704;"POS1?"
730   ENTER 704;Angle(I)
740   OFF TIMEOUT
750   !PRINT Angle(I),Ffdata(I)
760   Angle(I)=Angle(I)+0
770   OUTPUT 704;"JOG1 0.5"
780   !graphs line
790   PLOT Angle(I),Ffdata(I),-1
800   PEN 2
810   IF Angle(I)<Angmax THEN GOTO 570
820   OUTPUT 704;"STOP"
830   Numpts=I
840   PRINT ""
850   PRINT "data collection complete..."
860   PRINT ""
870   OFF KBD
880   INPUT "save data? (Y,N)",Yn$
890   IF Yn$="N" OR Yn$="n" THEN GOTO 1200
900   INPUT "FILE NAME?",Fln$
910   PRINT "****INSERT DISK IN DRIVE A..."
920   PRINT "****[F2] to continue..."
930   PAUSE
940   !look for disk in drive a and store data
950   ON ERROR GOTO 1020
960   PRINT "****STORING DATA ON DRIVE A..."
970   CREATE "A:"&Fln$,100
980   ASSIGN @Filepath TO "A:"&Fln$;FORMAT ON
990   PRINT "A:"&Fln$
1000  GOTO 1070
1010  !if no disk, store data on drive c
1020  OFF ERROR
1030  PRINT ERRM$
1040  INPUT "Try to store data again? (y/n)",Yynn$
1050  IF Yynn$="y" OR Yynn$="Y" THEN GOTO 900
1060  GOTO 1200
1070  OFF ERROR
1080  ! store data
1090  FOR K=1 TO Numpts
1100  OUTPUT @Filepath;Angle(K),Ffdata(K)
1110  NEXT K
1120  PRINT ""
1130  PRINT "**** Data storage complete..."
1140  WAIT 1.0
1150  GOTO 1200
1160  PRINT "PROGRAM INTERRUPT"
1170  ! return multimeter to local operation
1180  LOCAL Address
1190  OUTPUT 704;"STOP"
1200  CLEAR SCREEN
```

```
1210  INPUT "Do you wish to take another data set?",Yn$
1220  IF Yn$="y" OR Yn$="Y" THEN GOTO 90
1230  GOTO 1360
1240  OUTPUT 704;"*opc"
1250  GOTO 720
1260  PRINT "Error number is:"
1270  PRINT ERRM$
1280  GOTO 1360
1290  !looks for working multimeter
1300  INPUT "Problem finding multimeter do you have one? (y/n)",Yn$
1310  IF Yn$="n" OR Yn$="NY" THEN GOTO 1350
1320  INPUT "What is your multimeter's GPIB address?",Address
1330  IF Address<700 THEN Address=Address+700
1340  GOTO 290
1350  PRINT "You need a multimeter to use this program"
1360  END
1370  !*************************************************
1380  SUB Li_setup(Num_samps,Wait_time,Angmax,Max_power)
1390  CLEAR SCREEN
1400  Num_samps=3
1410  Wait_time=0
1420  Angmax=10
1421  Max_power=200
1430  PRINT TABXY(5,10);CHR$(142)
1440  PRINT TAB(10);"LI SETUP"
1450  PRINT CHR$(138)
1451  PRINT TAB(10);CHR$(141);"P";CHR$(138);"ower";TABXY(40,0);Max_power
1460  PRINT TAB(10);CHR$(141);"N";CHR$(138);"umber of samples- ";TABXY(40,0);Num_
1470  PRINT TAB(10);CHR$(141);"W";CHR$(138);"ait time between points ";TABXY(40,
1480  PRINT TAB(10);CHR$(141);"M";CHR$(138);"aximum angle ";TABXY(40,0);Angmax
1490  PRINT TAB(10);CHR$(141);"C";CHR$(138);"ontinue... "
1500  PRINT " "
1510  INPUT Optionx$
1520  SELECT Optionx$
1521  CASE "P","p"
1522  INPUT "Maximum power output (mW)...",Max_power
1530  CASE "N","n"
1540  INPUT "Number of samples ... ",Num_samps
1550  CASE "W","w"
1560  INPUT "Wait time (seconds) ... ",Wait_time
1570  CASE "M","m"
1580  INPUT "Maximum angle (degrees) ... ",Angmax
1590  CASE "c","C"
1600  GOTO 1630
1610  END SELECT
1620  GOTO 1430
1630  SUBEND
1640  !*************************************
1650  SUB Draw_screen(Angmax,Max_power)
1660  GCLEAR
1670  GRAPHICS ON
1680  WINDOW -Angmax,Angmax,0,Max_power
1690  PEN 1
1700  VIEWPORT 25,105,25,95
1710  FRAME
1720  LINE TYPE 3
1730  GRID Angmax/5,Max_power/10,-10,2,1,1
1740  CLIP OFF
1750  MOVE 0,0
1760  LINE TYPE 1
```

```
1770  CSIZE 3
1780  LORG 6
1790  LDIR 0
1800  LABEL "0"
1810  MOVE -Angmax,0
1820  LABEL -Angmax
1830  MOVE Angmax,0
1840  LABEL Angmax
1850  MOVE -Angmax-1,Max_power
1860  LABEL Max_power
1870  MOVE -Angmax,Max_power/2
1880  DEG
1890  LDIR 90
1900  LORG 4
1910  CSIZE 4
1920  LABEL "Average Power"
1930  LDIR 0
1940  LORG 6
1950  MOVE -Angmax/2,0
1960  LABEL "Angle"
1970  SUBEND
```

AXIAL ROTATION LASER MOUNT ASSEMBLY

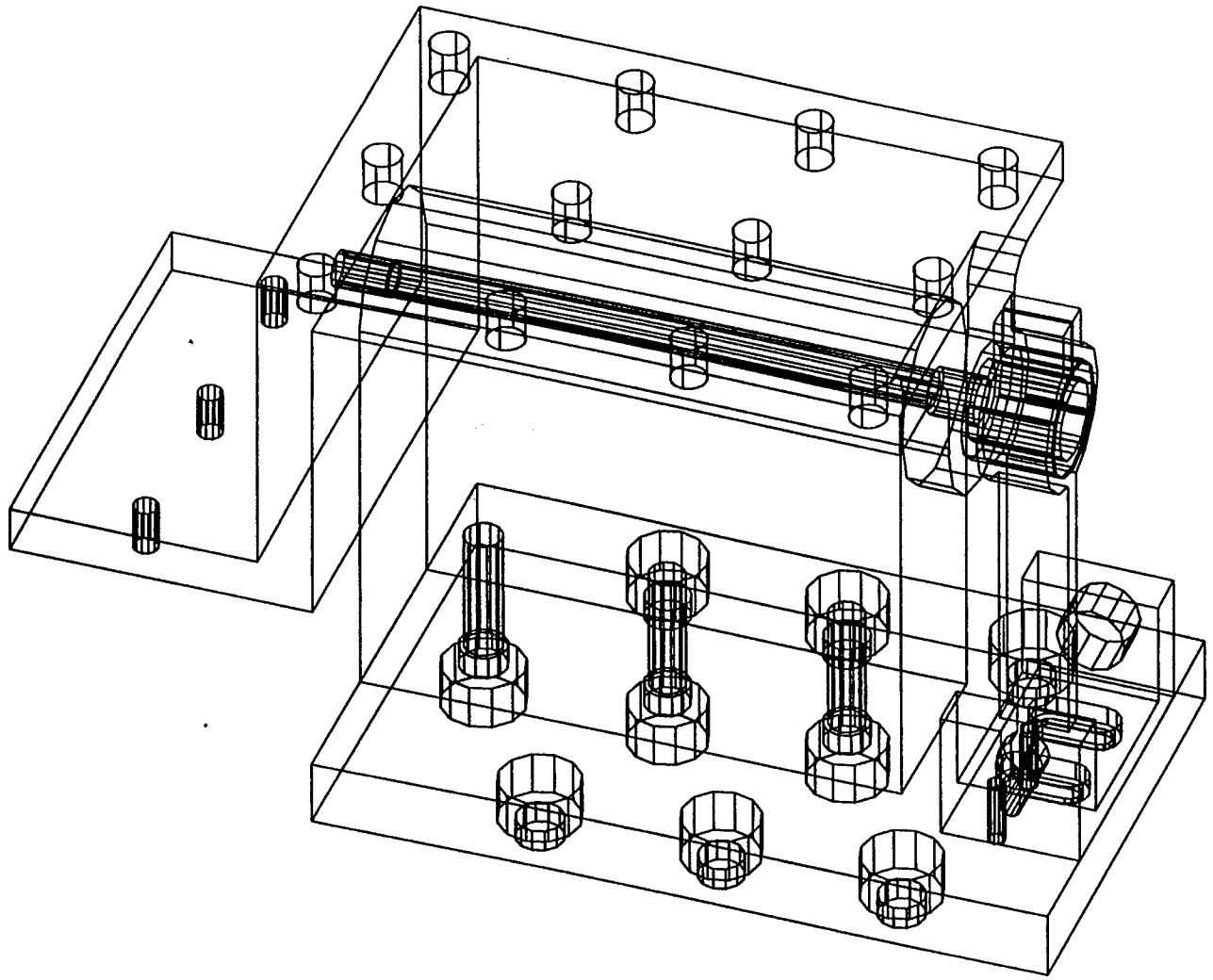

```
        10    CLEAR SCREEN
20    Chan=1
30    Cntrl=0
40    Vout10=0
50    V16$=IVAL$(Vout10,16)
60    Vout16$=V16$[2,4]
70    OUTPUT 706;Chan,Cntrl,Vout16$
80    PRINT CHR$(142)
90    PRINT TABXY(10,10);"LASER DIODE POWER vs. CURRENT MEASUREMENT PROGRAM"
100   PRINT "";CHR$(138)
110   PRINT TAB(12);"Requires: HP 34401A multimeter, GPIB address 724"
120   PRINT TAB(12);"          KEPCO Programmer, GPIB address 706"
130   PRINT TAB(12);"          KEPCO Power Supply"
140   PRINT ""
150   ON KBD GOTO 170
160   GOTO 150
170   CLEAR SCREEN
180   PRINT TAB(10);CHR$(142);"INITIAL SETUP"
190   PRINT "";CHR$(138)
200   PRINT TAB(10);"          Align the optical components to maximize signal"
210   PRINT TAB(10);"          Align beam with center of sensor"
220   PRINT TAB(10);"          Goto statistics menu on Labmaster"
230   PRINT ""
240   ON KBD GOTO 260
250   GOTO 240
260   Init$="Y"
270   Pwr_scale=25.7732    ! Watts/Volt
280   OPTION BASE 1
290   ON TIMEOUT 7,5 GOTO 1470
300   OUTPUT 724;"DISP:TEXT 'We ARE ALIVE'"
310   CALL Li_setup(Max_curr,Max_power,Duty_cycle,Num_pts,Num_samps,Range_fac,Wa
320   ALLOCATE Power(Num_pts),Curr_meas(Num_pts)
330   ON ERROR GOTO 420
340   Chan=1
350   Cntrl=0
360   Vout10=0
370   V16$=IVAL$(Vout10,16)
380   Vout16$=V16$[2,4]
390   OUTPUT 706;Chan,Cntrl,Vout16$
400   WAIT .2
410   !OUTPUT 9;"of a, on"
420   CALL Graph(Max_curr,Max_power)
430   !
440   ! *** main loop ***
450   !
460   Vstep=.0001
470   FOR I=1 TO Num_pts
480   !  Increments the current from the power supply
490      V=I*Vstep
500      Vout10=(V)*4096
510      V16$=IVAL$(Vout10,16)
520      Vout16$=V16$[2,4]
530      Chan=1
540      Cntrl=0
550      OUTPUT 706;Chan,Cntrl,Vout16$
560   ! Wait time before next reading
570   OUTPUT 9;"sr a"
580      WAIT 1
590      WAIT Wait_time
600     Vsumx=0
```

```
610   ! Get the voltage from the multimeter and
620   ! determine the average power output from
630   ! the power supply.
640     FOR B=1 TO Num_samps
650         CALL Nmulti(Valuex)
660         Vsumx=Vsumx+Valuex
670     NEXT B
680   !  Get the voltage from the labmaster and
690   !  determine the average power output from
700   !  the laser.
710      Vsum=0
720     !FOR B=1 TO Num_samps
730        CALL Multi(Value)
740        Vsum=Value+Vsum
750     !NEXT B
760     !Vsum=Vsum/3
770     Curr_meas(I)=Vsumx/10.00/Num_samps*1000
780      Duty_cycle=.01
790     Power(I)=Vsum*1000 !Vsum/Num_samps*Pwr_scale !*Range_fac/Duty_cycle
800   !  PRINT "I=",Curr_meas(I)," mA","    P=",Power(I)," mW"
810     DRAW Curr_meas(I),Power(I)
820   NEXT I
830   !  Save the LI curve to disk
840   Vout10=0
850   V16$=IVAL$(Vout10,16)
860   Vout16$=V16$[2,4]
870   OUTPUT 706;Chan,Cntrl,Vout16$
880 ! INPUT "PLOT DATA? (Y,N)",Yn$
890 ! IF Yn$="n" OR Yn$="N" THEN GOTO 980
900 ! K=1
905 ! OUTPUT 708;"SC0,";Max_curr;",0,';Max_power
910 ! OUTPUT 708;"PA0,0;"
911 ! OUTPUT 708;"tl100"
912 ! B=1
913 ! OUTPUT 708;"sp 1"
915 ! FOR B=1 TO 10
916 ! OUTPUT 708;"xt"
917 ! OUTPUT 708;"yt"
918 ! OUTPUT 708;"PA0,0;"
920 ! Plot_tick=Max_power/10*B
921 ! OUTPUT 708;"pa0,";Plot_tick
922 ! NEXT B
923 ! OUTPUT 708;"sp 2"
924 ! FOR K=1 TO Num_pts
950 ! OUTPUT 708;"PD";Curr_meas(K);",";Power(K)
960  !OUTPUT 708;"PD"
970 ! NEXT K
980   INPUT "SAVE DATA ? (Y,N)",Yn$
990   IF Yn$="N" OR Yn$="n" THEN GOTO 1380
1000  INPUT "FILE NAME?",Fln$
1010  CLEAR SCREEN
1020  PRINT "....INSERT DISK IN DRIVE A..."
1030  PRINT "....OTHERWISE DATA SAVED ON DRIVE C...."
1040  PRINT "HIT [ENTER] WHEN READY"
1050  INPUT Go
1060  !
1070  !look for disk in drive a and store data
1080  !
1090  ON ERROR GOTO 1180
1100  PRINT "STORING DATA ON DRIVE A"
```

```
1110  CREATE "A:"&Fln$,100
1120  ASSIGN @Filepath TO "A:"&Fln$;FORMAT ON
1130  PRINT "A:"&Fln$
1140  GOTO 1310
1150  !
1160  !if no disk, store data on drive c
1170  !
1180  OFF ERROR
1190  PRINT ERRM$
1200  PRINT "STORING DATA ON DRIVE C"
1210  ON ERROR GOTO 1260
1220  CREATE "C:\htb\"&Fln$,100
1230  ASSIGN @Filepath TO "C:\htb386\"&Fln$;FORMAT ON
1240  PRINT "C:\HTB386\"&Fln$
1250  GOTO 1310
1260  OFF ERROR
1270  PRINT ERRM$
1280  INPUT "Try to store data again? (y/n)",Yynn$
1290  IF Yynn$="y" OR Yynn$="Y" THEN GOTO 1000
1300  GOTO 1380
1310  OFF ERROR
1320  !
1330  ! store data
1340  !
1350  FOR K=1 TO Num_pts
1360  OUTPUT @Filepath;Curr_meas(K),Power(K)
1370  NEXT K
1380  PRINT "...PROGRAM COMPLETE..."
1390  INPUT "Would you like to run the program again? (y/n)",Yyynnn$
1400  ! Resets power supply to default settings
1410  IF Yyynnn$="n" OR Yyynnn$="N" THEN GOTO 1440
1420  DEALLOCATE Power(*),Curr_meas(*)
1430  GOTO 10
1440  GOTO 1490
1450  PRINT "PROGRAM INTERRUPT"
1460  GOTO 1490
1470  PRINT "   PROGRAM HALTED"
1480  PRINT "!!!!GPIB INACTIVE!!!!"
1490  END
1500  !
1510  !*****************************************
1520  !
1530  SUB Li_setup(Max_curr,Max_power,Duty_cycle,Num_pts,Num_samps,Range_fac,Wai
1540  CLEAR SCREEN
1550  Max_curr=300
1560  Max_power=200
1570  Num_pts=50
1580  Num_samps=3
1590  Wait_time=0.
1600  Curr_level=20
1610  Outp_state$="OFF"
1620  PRINT TABXY(5,10);CHR$(142)
1630  PRINT TAB(10);"LI SETUP"
1640  PRINT CHR$(138)
1650  Num_pts=INT(Max_curr/6)
1660  PRINT TAB(10);CHR$(141);"M";CHR$(138);"aximum current ";TABXY(40,0);Max_cu
1670  PRINT TAB(10);CHR$(141);"P";CHR$(138);"ower scale ";TABXY(40,0);Max_power
1680  !PRINT TAB(10);CHR$(141);"N";CHR$(138);"umber of data points";TABXY(40,0)
1690  PRINT TAB(10);CHR$(141);"S";CHR$(138);"amples ";TABXY(40,0);Num_samps
1700  PRINT TAB(10);CHR$(141);"W";CHR$(138);"ait time between points ";TABXY(40
```

```
1710  PRINT TAB(10);CHR$(141);"L";CHR$(138);"Current level";TABXY(40,0);Curr_lev
1720  PRINT TAB(10);CHR$(141);"X";CHR$(138);"Power on";TABXY(40,0);Outp_state$
1730  PRINT TAB(10);CHR$(141);"C";CHR$(138);"ontinue..."
1740  PRINT ""
1750  INPUT "",Optionx$
1760  SELECT Optionx$
1770  CASE "M","m"
1780  INPUT "Maximum current (mA) ... ",Max_curr
1790  CASE "P","p"
1800  INPUT "Maximum power plotted on graph ... ",Max_power
1810  CASE "N","n"
1820  INPUT "Number of data points ... ",Num_pts
1830  CASE "S","s"
1840  INPUT "Number of samples ... ",Num_samps
1850  CASE "W","w"
1860  INPUT "Wait time (seconds) ... ",Wait_time
1870  CASE "L","l"
1880  INPUT "Current Level (mA) ... ",Curr_level
1890  CASE "X","x"
1900  IF (Outp_state$="OFF") THEN
1910     Outp_state$="ON "
1920  ELSE
1930     Outp_state$="OFF"
1940  END IF
1950  CASE "C","c"
1960  GOTO 2100
1970  END SELECT
1980  IF (Outp_state$="OFF") THEN
1990  V=0
2000  ELSE
2010  V=Curr_level*.0000165
2020  END IF
2030  Vout10=V*4096
2040  V16$=IVAL$(Vout10,16)
2050  Vout16$=V16$[2,4]
2060  Chan=1
2070  Cntrl=0
2080  OUTPUT 706;Chan,Cntrl,Vout16$
2090  GOTO 1620
2100  SUBEND
2110  !
2120  !*********************************************
2130  !
2140  SUB Multi(Value)
2150  !OUTPUT 9;"pw? a"
2160  OUTPUT 9;"spa? a"
2170  ENTER 9;Value
2180  SUBEND
2190  !
2200  !*********************************************
2210  !
2220  SUB Graph(Max_curr,Max_power)
2230  VIEWPORT 25,105,25,95
2240  WINDOW 0,Max_curr,0,Max_power
2250  CLEAR SCREEN
2260  GRAPHICS ON
2270  PEN 1
2280  LINE TYPE 1
2290  FRAME
2300  LINE TYPE 3
```

```
2310  GRID Max_curr/10,Max_power/10,0,0
2320  CLIP OFF
2330  MOVE 0,-Max_power/100.
2340  LINE TYPE 1
2350  CSIZE 3
2360  LORG 6
2370  LABEL "0"
2380  MOVE Max_curr,-Max_power/100.
2390  LABEL Max_curr
2400  MOVE -Max_curr/100.,0
2410  LORG 8
2420  LABEL "0"
2430  MOVE -Max_curr/100.,Max_power
2440  LABEL Max_power
2450  MOVE -Max_curr/100.,Max_power/2
2460  DEG
2470  LDIR 90
2480  LORG 4
2490  CSIZE 4
2500  LABEL "Average Power (mW)"
2510  LDIR 0
2520  LORG 6
2530  MOVE Max_curr/2,-Max_power/100.
2540  LABEL "Current (mA)"
2550  MOVE 0,0
2560  PEN 2
2570  SUBEND
2580  !
2590  !*********************************************
2600  !
2610  SUB Nmulti(Valuex)
2620  OUTPUT 724;"MEAS:VOLT:DC?"
2630  ENTER 724;Valuex
2640  LOCAL 724
2650  SUBEND
```

FABRICATION OF A WIDE SPECTRUM IMPULSE RADIATING ANTENNA

Raj C. Singaraju

Albuquerque Academy
6400 Wyoming Blvd. NE
Albuquerque, NM 87109

Final Report for:
High School Apprenticeship Program
Phillips Laboratory at Kirtland Air Force Base

Sponsored by:
Air Force Office of Scientific Research
Bolling Air Force Base, DC

and

Phillips Laboratory

August 1996

FABRICATION OF A WIDE SPECTRUM IMPULSE RADIATING ANTENNA

Raj C. Singaraju
Albuquerque Academy

Abstract

This paper discusses the construction of a wide spectrum reflector antenna with an emphasis on transmission line design and construction, coax design and construction, and resistive termination of the transmission lines. The antenna created is an Impulse Radiating Antenna with a diameter of 45.7 cm and an F/D of .5. It is fed by two flat transmission lines which emerge from the side of the antenna and are connected in parallel at the focal point. The goal of this project is to create a fast rising, slow decaying voltage wave pulse, with an amplitude of 30 kV at the pulses apex. A pulse of this type creates a wide spectrum radiated field extending from roughly 500 MHz to 5 GHz.

FABRICATION OF A WIDE SPECTRUM IMPULSE RADIATING ANTENNA

Raj C. Singaraju

Introduction

In this paper we discuss the process for building a wide spectrum Impulse Radiating Antenna (IRA) . This type of antenna produces a dispersionless wide band pulse with a nearly flat radiated spectrum. This type of pulse has many practical uses in: electric warfare, enemy target identification and hidden object identification. The antenna discussed in this paper uses a parabolic reflector dish with a diameter of 45.7 cm and an F/D of .5. Power is supplied through two coaxial lines which emerge through a small hole at the base of the reflector an connect to two pairs of flat transmission lines at the focal point. Each pair of transmission lines are in parallel with and terminated by 400 ohms resistors at each end where the transmission lines intersect the reflector dish. Placing the two resistors In parallel produces a net impedance of 200 ohms along each of the coplanar transmission lines. An Impulse Radiating Antenna of this type is designed to produce a fast rising, slow decaying voltage wave pulse, with an amplitude of 30 kV at its apex. A pulse of this type creates a wide spectrum radiated field extending from roughly 500 MHz to 5 GHz.

Diagram 1

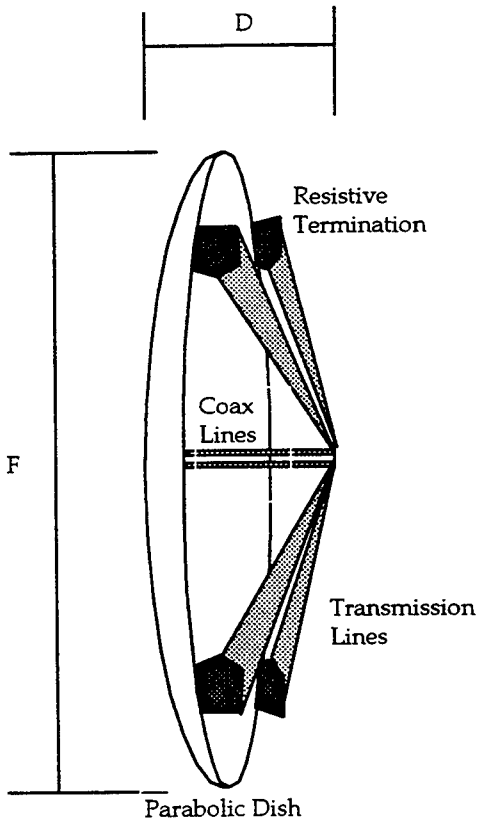

Side View

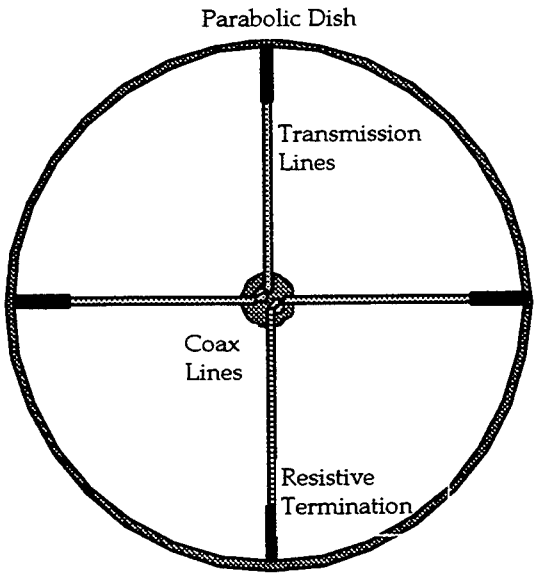

Frontal View

FABRICATION OF A WIDE SPECTRUM IMPULSE RADIATING ANTENNA

Raj C. Singaraju

Dish Selection

The first step in fabricating this antenna is to chose a suitable dish. We chose an aluminum spun reflecting dish with a diameter of 47 cm and a F/D of .5. The dish size is not critical, this size was chosen, because, it is small enough to be handled easily in the lab, yet large enough to work with.

Coax Design

The impulse is fed through two 100 ohm coaxial lines, with one pair of transmission fins connecting to each coax. Ideally the coax cable will supply power evenly to each set of fins creating an electric field as shown below. To obtain a stable electric field center conductor of the first coax is connected to one pair of fins, the center of the second coax is connected to the shielding of the of the first coax and the shielding of the second coax is connected to the other pair of fins (diagram 2). In this way charge will flow through one set of transmission lines and an opposite charge will flow down the other, creating a closed circuit at the antenna dish.

Diagram 2

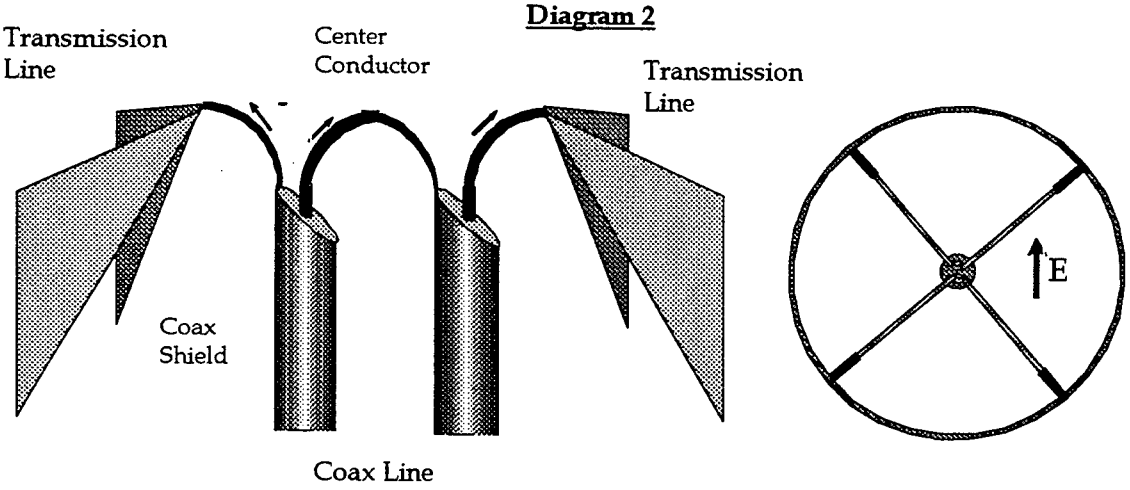

When alternating current travels at high frequencies along the coax shielding (as the negative charge does here) ; it only travels along the inside of the shield at a shallow skindepth.

Raj C. Singaraju

The outside becomes a separate path for the current to travel on, So current can travel up the inner wall of the coax shielding and down the outside. This problem occurs in this setup as well, where current can travel to the apex on the inside of the coax and back down the outside without having to travel along the transmission line. To prevent this from occurring ferrite cylinders are placed on the outside of the coax shielding. The ferrite acts as a high impedance resistor for current traveling down the outside to the coax shielding, while not significantly reducing current flow on the inner wall of the coax. Now with the ferrite in place the current travels through the transmission line because it is the path of least resistance

Transmission Line Design

The transmission lines consist of two pairs of flat triangular copper fins, with a transmission impedance of 400 ohms on each pair of fins. The two pairs are placed in parallel creating an effective impedance of 200 ohms. In addition each pair of fins are placed at 90° angels to each other. The fins are then attached to the at the edge of the dish and come together at the dished focal point, 22.9 cm above the base of the dish. The resistance of 400 ohm for each fin pair was chosen over 200 ohms, because 200 ohm fins are more than twice as wide. This increased width would interfere with the radiated signal.

Resistive Termination

Finally it is necessary to resistively terminate the ends of the transmission lines, this is done to prevent the signal from reflecting back to the focus. The pulse is initiated at the apex of the fins, it then travels down the transmission lines towards the dish. If the transmission lines are not resistively terminated the wave hits the dish reflects back up the fins to the coax cable. This echoed signal acts as a new pulse, doing the same thing as the initial pulse did, it travels down the transmission lines to the dish and bounces back up; this process continues on until the pulse dies out. As a result you get a series of progressively smaller pulses after the initial pulse. To prevent this from occurring a resistive substance is

placed at the end of the fins. If the resistance of the termination has the same impedance as the transmission lines, the initial pulse will travel down the transmission line, and through the resistor without noticing a change, however signals which bounce off the dish will be absorbed by the resistor.

In the initial assembly twenty 4 Kilo-ohm resistors were placed in parallel at each end of the transmission lines, because each end of the transmission line is in parallel with each other this produces a net resistance of 100 ohms. This was done not only to see if the resistive termination would dissipate the pulse, but also to see if the inductance caused by the resistor leads would have an effect on the antenna. To prevent this it was decided that a resistive sheet would be placed between the dish and transmission lines. As you can see by diagram 3, however, resistors at the ends of the transmission lines create a constant resistive termination greatly reduces ringing after the pulse.

The substance that will be placed between the fin and dish needs to have a uniform resistance. We selected ten substances to test ranging from carbon loaded plastic to space cloth. A simple ohm meter has very narrow leads, it will not measure the collective resistance across a sheet, so it is necessary to build a jig that allows the ohm meter to do so. The jig is a simple device, two copper plates on each side of the material clamp the material securely, This creates a solid electrical connection between the material and the copper. Then an ohm meter measures the resistance across the fabric

In order to determined how uniform the resistance of each substance is we measured shapes at different ratios. Since we were measuring resistance in ratios of ohms per square inch only relative dimensions are important, for example a 2" x 1" piece should have twice the resistance of a 1" x 1" piece. Rectangles of: 1" x 1" , 2" x 1", and .5" x 2.5" were cut out and their resistivity are measured. These measurements are then compared with calculated resistance based on the 1" x 1" square of fabric. (Table 1).

Raj C. Singaraju

Table 1

Fabric	1"*1" (1st half)	1"*1" (middle half)	1"*1" (last half)	average	% change
Carbon Paper	3.692	3.518	3.648	3.619	2.80%
Space Cloth 1	1.435	1.304	1.43	1.390	3.16%
Space Cloth 2	0.248	0.234	0.247	0.243	3.70%
ARC Cloth	1.908	1.824	2.124	1.952	8.10%
C 152	0.16	0.163	0.159	0.161	1.43%
C 354	0.162	0.162	0.151	0.158	4.63%
C 313	0.04759	0.05243	0.05074	0.050	5.30%
C 356	16.166	15.901	15.819	15.962	1.26%
Foam	58.09	59.11	74.3	63.833	14.09%
Rubber	0.245	0.231	0.262	0.246	6.11%

Fabric	2" * 1" estimate	2" * 1" actual	% error	.5" * 2.5" estimate	.5" * 2.5" actual	% error
Carbon Paper	7.239	6.238	13.82%	0.724	1.244	42%
Space Cloth 1	2.779	2.478	10.84%	0.278	0.346	20%
Space Cloth 2	0.486	0.424	12.76%	0.049	0.060	19%
ARC Cloth	3.904	4.002	2.45%	0.390	0.473	17%
C 152	0.321	0.324	0.82%	0.032	0.072	55%
C 354	0.317	0.328	3.46%	0.032	0.030	5%
C 313	0.101	0.12	16.24%	0.010	0.018	44%
C 356	31.924	34.56	7.63%	3.192	3.329	4%
Foam	127.667	102.14	19.99%	12.767	8.270	35%
Rubber	0.492	0.485	1.42%	0.049	0.086	43%

(Resistance in K)

After examining the resistance of these substances it was decided that none of them were in the range needed or uniform enough to be useful. So. in the final assembly 400 ohm resistive cards are be used. These are circuit cards coated with a resistive substance one side.

There is a problem with resistively terminating the ends of the transmission line. The gap between the aluminum dish and the copper fins, creates a capacitor. The capacitance

reaches roughly 1 pfd, and is defined by the equation:

$$C = 2 \quad L / \ln (2h/r)$$

Where L = the width of the transmission line when it intersects the resistive card.

h = the separation between the copper fin and the dish

r = the width of the width of the transmission line

This causes a problem, because it creates a point of low impedance. This creates a impedance mismatch in the circuit, producing reflections back along the fins. As long as the transmission lines are resistively terminated and not directly attached to the dish this problem is unavoidable.

Conclusion

The design of this impulse radiating antenna is an on going process. To date the largest problem we have had in creating the antenna is creating a constant impedance throughout the system. Ideally the source should see that the antenna has a constant impedance throughout the coax cable, transmission lines and resistive termination. The example Time Domain Reflectromitery graph (diagram 4) shows the impedance of the system as seen from the source. The capacitance in the system will disrupt signal, however the design process will continue experimenting on ways to eliminate this and create a pulse that does not echo within the dish.

Diagram 4

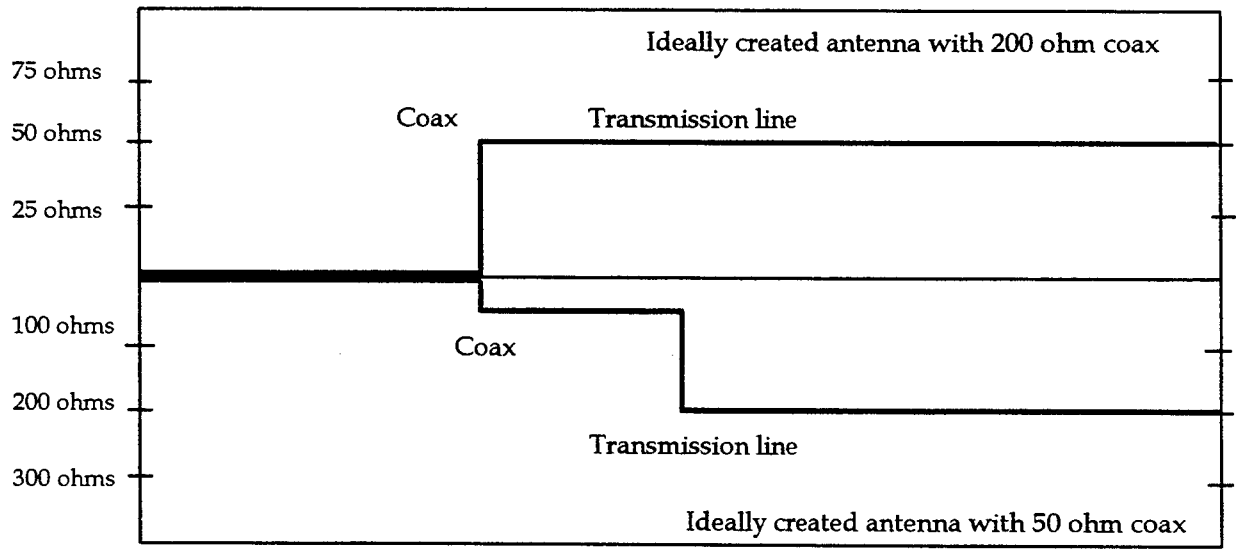

Raj C. Singaraju

Diagram 3

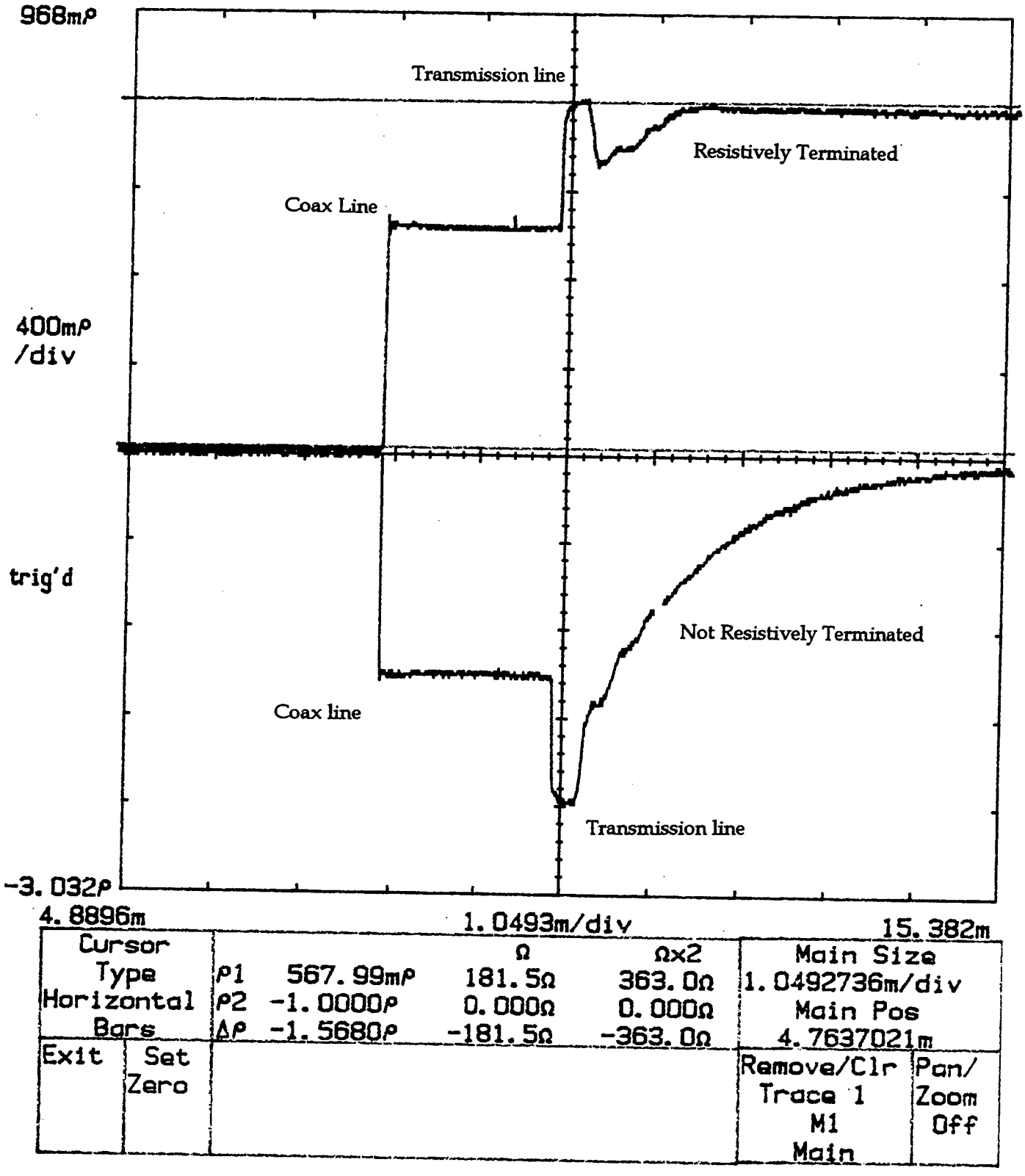

References

[1] Everett G. Farr, Off-Boresight for a lens IRA, Sensor and Simulation Note 370, October 1994

[2] Everett G. Farr and Carl E Baum, The Radiation Pattern for Reflector Impulse Radiating Antennas: Early Time Response, Sensor and Simulation Note 358, June 1993

[3] Everett G. Farr and Carl E Baum, Feed Point Lens for Half Reflector IRAs, Sensor and Simulation Note 385, November 1995

[4] Everett G. Farr and Carl E Baum, Compact Ultra-Short Pulse Fuzing Antenna Design and Measurements, Sensor and Simulation Note 380, June 1995

[5] Everett G. Farr and Carl E Baum, Development of a Reflector IRA and a Solid Dielectric Lens IRA, Part I: Design, Predictions, and Construction, Sensor and Simulation Note 396, April 1996

[6] D. V. Giri, H. Lackner, I. D. Smith, D. W. Morton, C. E. Baum, J. R. Marek, D. Scholfield and W. D. Prather, A reflector Antenna for Radiating Impulse-Like Waveforms, Sensor and Simulation Note 382, July 1995

A CELL STRUCTURED PLANE SYSTEM FOR MONTE CARLO PHOTON TRANSPORT

Gaurav Tuli

Waltham Senior High School
617 Lexington Street
Waltham, MA 02154

Final Report for:
High School Apprenticeship Program
Phillips Laboratory - Hanscom AFB

Sponsored by:
Air Force Office of Scientific Research
Bolling Air Force Base, DC

August, 1996

A CELL STRUCTURED PLANE SYSTEM FOR MONTE CARLO PHOTON TRANSPORT

Gaurav Tuli
Waltham Senior High School

Abstract

Tracing the probabilistic path of a photon requires a coordinate system that allows detailing of the position and motion of the particle. Several possibilities for such a system exist, however a cell structure offers a convenient and orderly approach for studying the interactions the photon may experience such as absorption and scattering. The process of building such a cell system is presented here. The source code has been written in Fortran 77 on a Silicon Graphics workstation to be used for the transfer code written originally by Dr. Michael Egan and Dr. Russell Shipman at Phillips Lab Geophysics Directorate, Hanscom AFB, Massachusetts.

A CELL STRUCTURED PLANE SYSTEM FOR MONTE CARLO PHOTON TRANSPORT

Gaurav Tuli

Introduction

The Monte Carlo method may be used to simulate photon-transport problems by applying specific probability laws to physical interactions. The advantage of using Monte Carlo are that scattering and absorption can be studied without creating large complicated relations.{5} Through random sampling of a large number of particle trajectories, a good approximation to the true solution of the problem can be reached. The simulation consists of a closed geometry with either an internal or external radiation source. The particle travels in a random direction for a random distance until an interaction occurs. Here probabilities determine what sort of interaction will take place. If scattering occurs, a new direction and distance are generated randomly and the cycle continues until the particle exits the system.{4}

Given information in such a simulation would be the average distance a photon can travel before a collision, the probability of being absorbed or scattered at a collision, and descriptive data on the material being traversed.{4} For every collision that results in scattering two pieces of data are needed, the distance to be traveled and a direction.

The probability of a photon traveling at least an optical depth τ is given in:

$$P = e^{-\tau} \qquad \text{where} \qquad \tau = \int_0^s B\,ds$$

and B is the volume scattering coefficient related to the material the photon is passing through and s is the distance. To calculate the new distance to be traveled one must solve for the limit of integration s.{4} Taking a random number R^* for the probability P the following can be performed:

$$R^* = \int_0^l e^{-t}\,dt \quad = \quad \left(-e^{-t}\right)\Big|_0^l \quad = \quad 1 - e^{-l}$$

$$R^* = 1 - e^{-l} \longrightarrow e^{-l} = 1 - R^* \longrightarrow l = -\ln(1 - R^*)$$

Therefore:

$$\int_0^s B\,ds = -\ln(1 - R^*)$$

Determining s in this equation will give the first piece of data needed for the particle's new trajectory. The second quantity needed is the new direction vector. Because the level of understanding in this aspect of transport is beyond my scope as a high school student, the reader should be referred to Particle Transport Simulation with the Monte Carlo Method {1} for a thorough discussion.

Methodology

The basis of studying interactions in any cell structure is the intersection of the particle trajectory with a plane surface. Methods to determine the distance to a single plane in space can be found in Monte Carlo Transport Of Photons And Electrons {2} and is similarly described in the following, as well as diagrammed in Figure 1:

Initial position vector	$X = xi + yj + zk$	
Initial direction unit vector	$U = ui + vj + wk$	$V \cdot N = 0$
Vector to intersection P2	$X1$	$V = X1 - C = X + tU - C$
Vector to P1 on plane surface	$C = cai + cbj + cck$	$(V + C - X) / U = t$
Unit vector normal to plane	$N = nai + nbj + nck$	$(V + C - X) \cdot N / (U \cdot N) = t$
Vector from P1 to P2	V	$(C - X) \cdot N / (U \cdot N) = t$
Distance to plane from X	t	

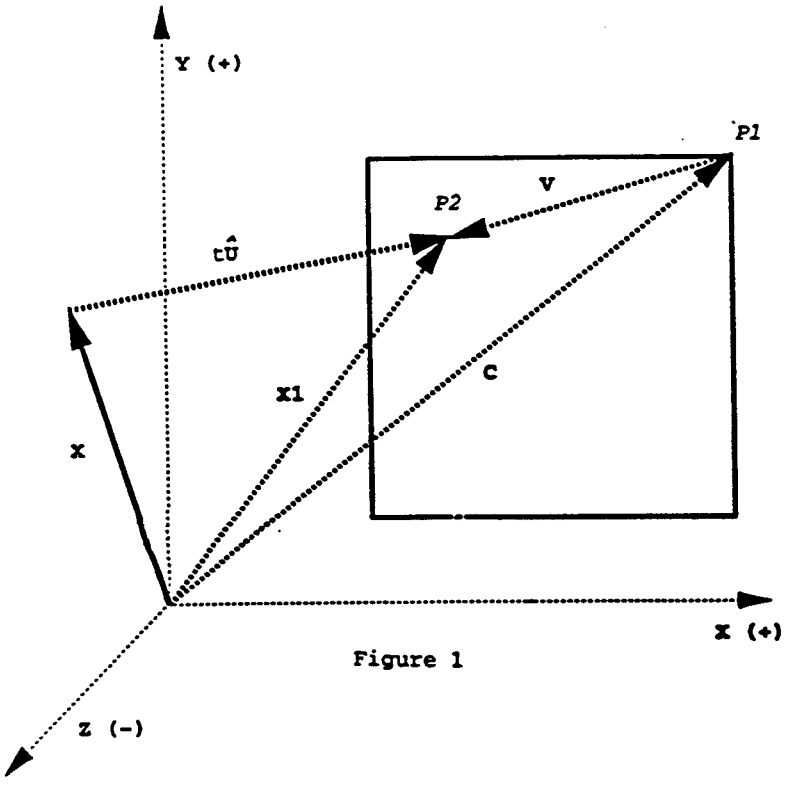

Figure 1

There are three distinct tests to eliminate a particular plane from being hit from an array of planes the particle is exposed to.

1. If (U.N) < 0 the particle trajectory is directed away from the plane surface because the angle between U and N is greater than 90 degrees.
2. If (U.N) = 0 the particle trajectory is parallel to plane surface because the angle between U and N is equal to 90 degrees.
3. If (X + tU) represents a point that does not fall within the boundaries of a definite plane, the trajectory has "overshot" the target.

A definite plane can be constructed by defining bounding planes. Repeating this process six times creates a cell and several times more builds the system. The arrays xcd, ycd and zcd contain coordinates of intersection points for planes perpendicular to the respective axes. By performing a simple algorithm on delta positioning of these planes, a coordinate field can be built. Therefore the statement:

delta_x(1) = 0.000 ... delta_x(2) = 1.000 ... delta_x(3) = 2.000

is translated into:

xcd(1) = 0.000 ... xcd(2) = 1.000 ... xcd(3) = 3.000

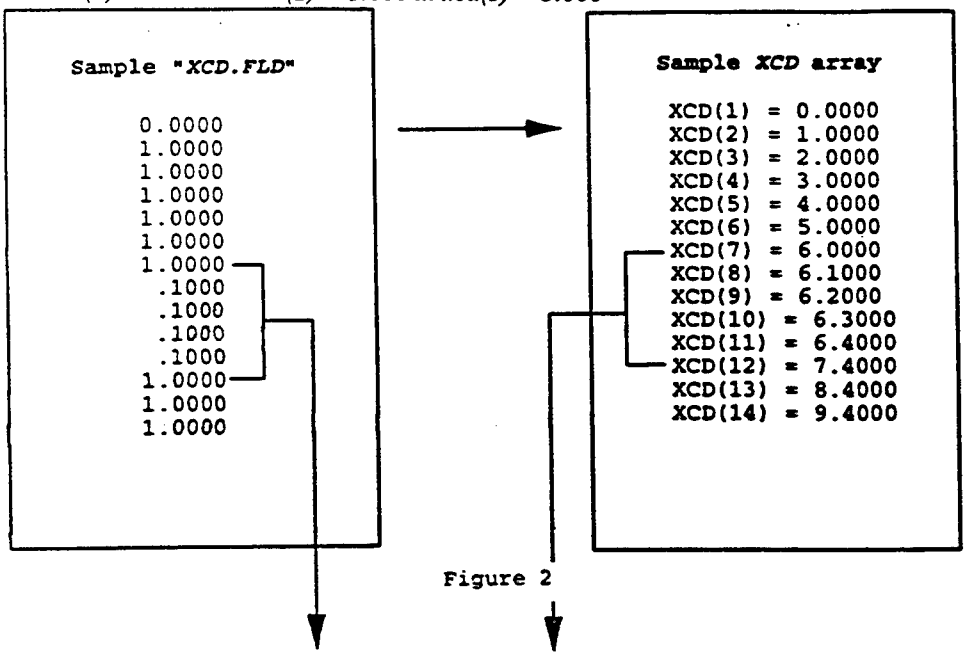

Figure 2

Area represents concentration of X cells

A list of delta positions for x planes are found in the data file, "xcd.fld." See figure 2 for a sample "xcd.fld." A cell index (ci) for xcd planes would represent a positioning between parallel planes numbered (ci) and (ci + 1), while its coordinate range is xcd(ci) and xcd(ci + 1). Cell indices exist for each direction and are increased or decreased according to which plane is passed through, however they remain greater than 0 and less than (mx - 1), where (mx) is the highest plane index in the respective direction. It would seem reasonable to call *_set_initial_ci* which can update all (ci) based on the current values of xpn, ypn, and zpn, however due to time constraints when in a large system, this is not a practical method.

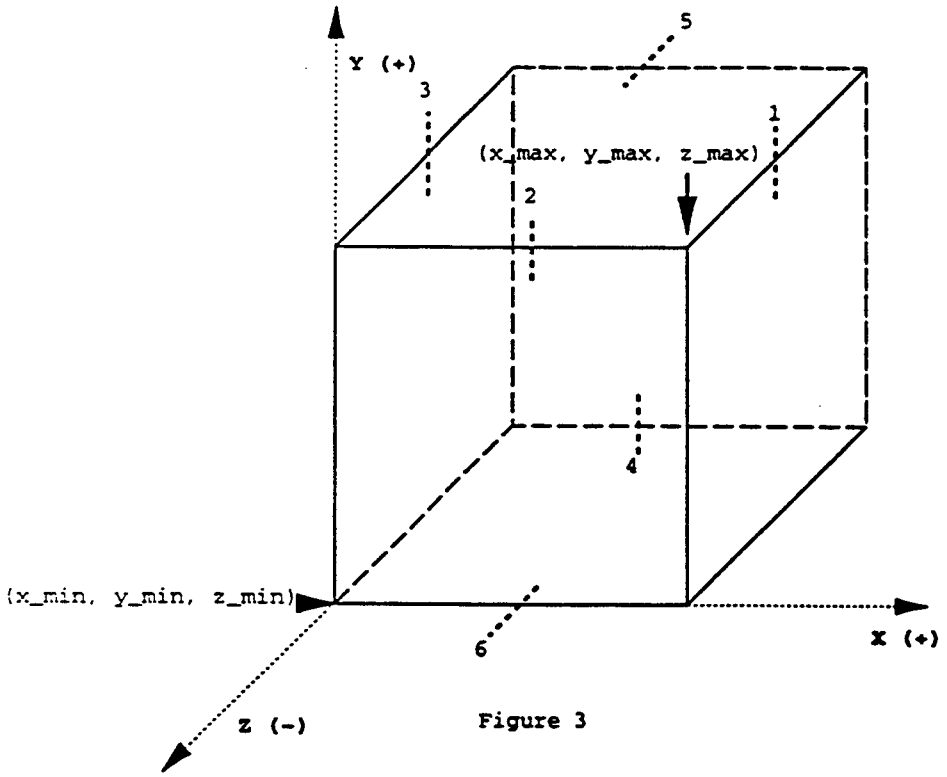

Figure 3

Constructing an individual cell is a matter of simply updating a cell array (cp) with planes defined by the cell indices. For a cell, (cp) would have dimensions six (for the six surrounding planes) by

nine (for each coordinate necessary to describe a plane). See figure 3. The six planes are identified accordingly by their coordinate normal vectors (data for which is found in "norm.fld" - See figure 4):

1. N = (1, 0, 0)	2. N = (0, -1, 0)
3. N = (-1, 0, 0)	4. N = (0, -1, 0)
5. N = (0, 0, 1)	6. N = (0, 0, -1)

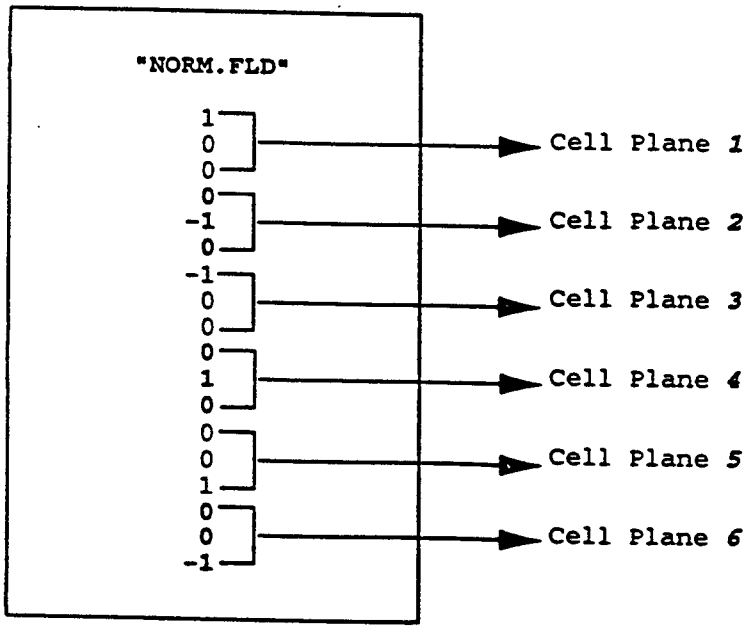

Figure 4

The nine coordinates represent:

1. x_max	2. y_max	3. z_max
4. x_min	5. y_min	6. z_min
7. na	8. nb	9. nc

With this approach, when a particle passes through the boundaries of a particular cell, the appropriate (ci) will change, and (cp) is updated with data for the current cell. Coordinates one through six are determined by the positioning of the planes associated with each of the three (ci). The simulation's main loop would run in a sequence of steps until the particle has exited the system. First Monte Carlo methods are used to find an initial random unit vector **U**, position vector **X**, and a transport distance d. Next the starting cell must be initialized. Taking the starting position, **X**, an algorithm to determine the cell indices in each direction is executed. Following this procedure, the particle begins its motion. The surrounding planes in cell (cp) are tested for the direction the particle is traveling. When (t) is found to the plane that would be hit, distances are compared as follows:

1. If (t + total distance traveled so far) > (d) the distance (t) is too great and the particle will not leave the current cell and stop.
2. If (t + total distance traveled so far) = (d) the particle will land on up to three planes (cell corner) and stop.
3. If (t + total distance traveled so far) < (d) the particle will pass through up to three planes and land in another cell and continue.

If the particle has stopped and has not yet exited the system, the loop is run again, with a new direction vector and distance to travel. However, if the particle has passed through a plane, the motion will continue until the total distance traveled is equal to (d) and then the entire process will be repeated, with new vectors and distance, until the particle has left the system. All interactions with other particles are controlled by the transfer code.

The outputs of the program into data file "output.txt" for each cycle are: starting position (coordinate and cell), particle transfer distance, unit vector **U**. For every step in motion the output includes: distance traveled in current cell, plane number passed through (1-6), new position (coordinate and cell).

Results

The cell coordinate system was successfully integrated into the transfer code. The previous coordinate system was defined by concentric spheres, which limited the different geometries that could be studied. However, a cell structure offers the possibilities of looking at more complex three-dimensional objects.

Problems that arose in incorporating the cell structure were as follows:

1. Cell indices in the transfer code needed to be adjusted from describing cells by which sphere they were in (one index) to describing cells by which 3D region they were in (three indices).
2. Cell spacing needed to be renormalized to match the [-1,1] coordinate region.
3. The coordinate system was shifted so that the point (0,0,0) was in fact the center of the entire system.
4. Accuracy in the computer's comparison operators were limited to 10^{-8}.

Several trial runs were conducted with the new cell system in the transfer code. Cubes were illuminated internally and externally and images of escaping radiation were created by programs written by Dr. Egan. An interesting note was the speed of each simulation. Even with high opacities, each simulation of 136,000 photons ran in minutes. Appendix 1 shows diagrams of two tests conducted where an onlooker is standing below the cell structure, which is being illuminated by a radiating source above it. The initial photon direction is (0,0,-1).

Figure A1 depicts the outcome of a low opacity, where much of the radiation is passing straight through the structure without interaction. In Figure A2, the optically thick case, where the opacity is 100 times that of the first simulation, considerably fewer photons exited at that surface because they underwent many collisions before leaving the system. In the optically thin simulation, three times as many photons reached that surface as compared to the thick trial, where most photons exited on the sides or were backscattered and left the system at the top.

Several improvements can be made to this program to improve its use in the transfer code. Although it is possible to create a virtual area of concentration, CELLS cannot create a true density because (as seen in Figure 5) the entire system is affected by the positioning of the planes that build the

concentration. A better program would be able to have a concentration located anywhere in the system, that has no influence on the plane positioning throughout the rest of the system. Another useful addition to CELLS would be the ability to position angled planes. With this feature, one could create complex objects (such as pyramids) with little trouble. Additionally there are methods to describe objects using sets of equations which would allow the program to find the nearest wall hit without much testing.

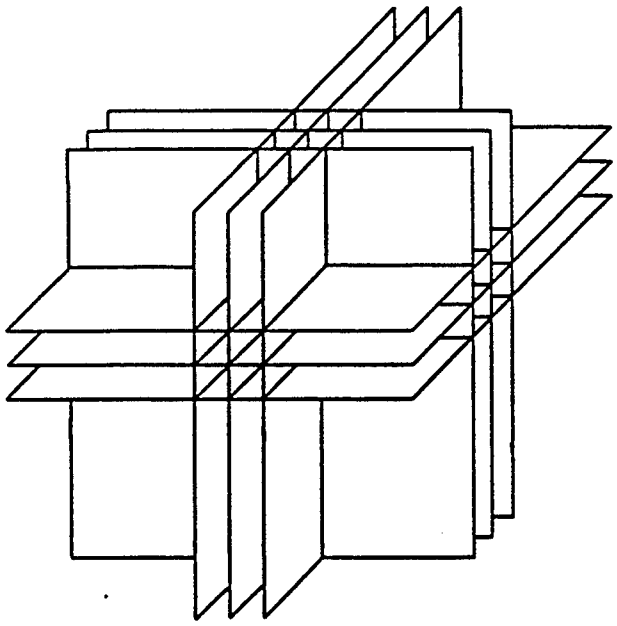

Figure 5

Conclusion

A cell coordinate system has been programmed for the photon transfer code written by Dr. Egan and Dr. Shipman. Although it is a small part of their more extensive and technical project, it may be a reliable addition as they involve more complicated geometries in the study. At this time however, it is not possible to draw any inferences from the outputs of the transfer code until more simulations can be conducted.

References

1. Carter, L. L. and Cashwell E. D. Particle-Transport Simulation with the Monte Carlo Method. USERDA Technical Information Center: Oak Ridge, TN, 1975.
2. Jenkins, Theodore M., et al., ed. Monte Carlo Transport of Electrons and Photons. New York: Plenum Press, 1988.
3. McCracken, Daniel D. "The Monte Carlo Method." Scientific American. Apr. 1955.
4. McKee Thomas B. and Stephen K. Cox. "Scattering of Visible Radiation by Finite Clouds." Journal of the Atmospheric Sciences. Oct. 1974.
5. Plass, Gilbert N. and George W. Katttawar. "Monte Carlo Calculations of Light Scattering from Clouds." Applied Optics. Mar. 1968.
6. Rybicki George B. and Alan P. Lightman. Radiative Processes in Astrophysics. New York: John Wiley and Sons, 1979.
7. Spanier, Jerome and Ely M. Gelbard. Monte Carlo Principles and Neutron Transport Problems. London: Addison-Wesley, 1969.

Appendix 1

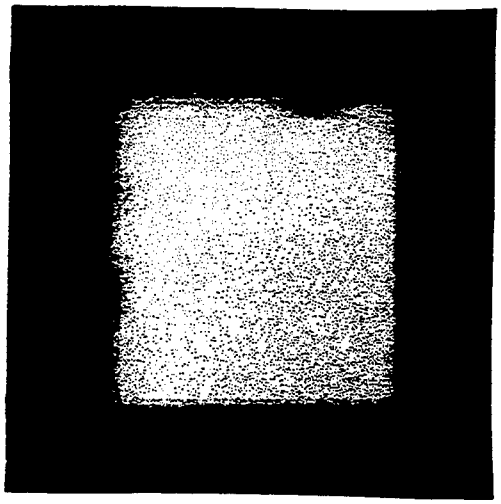

Figure A1

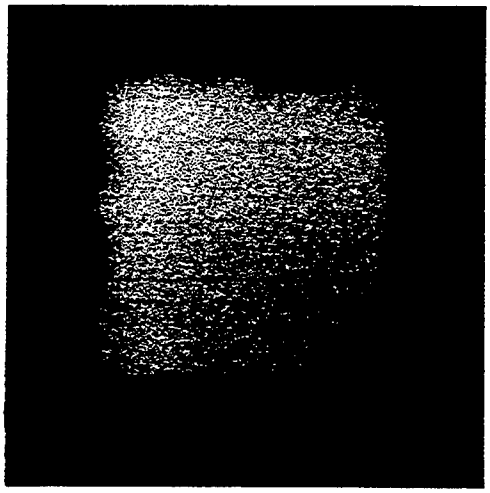

Figure A2

Appendix 2

The following is a description of all significant variables used in Program CELLS.

COMMON BLOCKS

vect:

xpn	current x position
ypn	current y position
zpn	current z position
ua	magnitude of direction vector **U** in **i**
ub	magnitude of direction vector **U** in **j**
uc	magnitude of direction vector **U** in **k**

cell:

ci(1) - cell index in x direction

ci(2) - cell index in y direction

ci(3) - cell index in z direction

max:

mx(1) - maximum number of x planes

mx(2) - maximum number of y planes

mx(3) - maximum number of z planes

cell_system:

xcd(...) - plane coordinates in x direction

ycd(...) - plane coordinates in y direction

zcd(...) - plane coordinates in z direction

plan:

cp - 6 X 9 array containing coordinate data of current cell's six planes

norm:

nm - 6 X 3 array containing coordinate data for normal unit vectors

LOCAL VARIABLES

d, ds, dt - forms of particle transfer distance

t, ta, tt - forms of distance to cell wall

p, k , j - plane identification numbers (1..6)

hit, hitpl - hit plane flag (1, 0)

Appendix 3

The following is a description of all subroutines and functions necessary (not including the transfer code itself) to execute the simulation with a cell structure in place.

1. Subroutine *main* initializes the cell field (*_init_system_field*, *_init_norm_field*) and the output file. From the starting position (which in an actual simulation would be created by the transfer code) the current cell indices are identified by calling (*_set_initial_ci*). An infinite loop is run (which breaks when the particle exits the system) which generates the random vectors and transfer distance and finally calls the motion to be run (*_execute_motion(d)*) for the distance.

2. Subroutine *_plane* tests a specific plane for the given particle trajectory and determines whether or not the plane will be hit by the particle. Taking the current position it returns the distance to the plane being tested and a flag for being hit (1:hit, 0:no hit).

3. Subroutine *_execute_motion* is the main loop. It accepts the distance to be traveled and transfers the particle through the interval while updating the output file with data on the particle's position. First, the starting cell is initialized by a call to (*_init_cur_cell*). Next, individual planes of that cell are tested against the trajectory using (*_plane*) until a hit is found. The cell indices are updated for all planes passed through and the new cell is initialized (*_init_cur_cell*). The program quits if the particle has exited the system.

4. Subroutine _init_random_vects would be replaced by the Monte Carlo calculations in an actual simulation. This simple routine, creates the particle trajectory with direction vector U and transfer distance (dt). In this simulation (dt) was held to less than 10 due to the size of the system.

5. Subroutine *_init_norm_field* reads normal vector data out of the file "norm.fld" into the array (nm).

6. Subroutine *_init_cur_cell* uses current cell indices to update plane data in (cp) and create the cell. Additionally it fills the array for normal vector data from (nm).

7. Subroutine *_init_system_field* builds the entire cell system from delta data in files, "xcd.fld", "ycd.fld", "zcd.fld" by creating coordinates into arrays xcd, ycd, zcd.

8. Subroutine *_set_initial_ci* determines the current cell indices from the given starting position.

9. Function *cmp* compares two numbers to the nearest 10^{-5}. It is used to test if a specific plane will be hit. When applied to the transfer code, the accuracy is to 10^{-8}.

```
      program cells
      call main
      end

c     ****************************************************************

      subroutine main

      common/vect/xpn,ypn,zpn,ua,ub,uc
      common/cell/ci(3)
      real d
      integer seedi,j

      j=1
1     format ('(',f7.3,',',f7.3,',',f7.3,')')

c     INITIALIZE SYSTEM AND NORMAL VECTORS
      call _init_system_field()
      call _init_norm_field()

c     INITIALIZE OUTPUT FILE

      open(1,file='output.txt',status='old')

c     OBTAIN STARTING POSITION AND SET CI

      write (1,*),'Starting position xpn,ypn,zpn'
      write (*,*),'Enter starting position xpn,ypn,zpn'
      read *,xpn,ypn,zpn
      write (1,1),xpn,ypn,zpn

      call _set_initial_ci()

      write (1,1),ci(1),ci(2),ci(3)

      write (*,*),'Enter seed'
      read *,seedi

c     PERFORM TRANSFER LOOP

      do while(j.ne.0)
      write (1,*)
      call _init_random_vects(d,seedi)
      write (1,*),'Particle transfer distance = '
      write (1,*),d
      write (1,*),'Unit vector U^ = '
      write (1,1),ua,ub,uc
      call _execute_motion(d)
      end do

      end

c     ****************************************************************

      subroutine _plane(p,hit,t)

      common/vect/xpn,ypn,zpn,ua,ub,uc
      common/plan/cp(6,9)
      common/norm/nm(6,3)
      real t

      integer p, hit

      hit=0
      t=0

c     DETERMINE U DOT N

      un=ua*nm(p,1)+ub*nm(p,2)+uc*nm(p,3)

c     RETURN IF PARTICLE RUNNING OPPOSITE DIRECTION

            if (un.le.0) then
            return
            end if

c     CALCULATE DISTANCE TO CELL PLANE p

      t=(nm(p,1)*(cp(p,1)-xpn)+nm(p,2)*(cp(p,2)-ypn)+nm(p,3)*(cp(p,3)-zpn))
        /un
      t=abs(t)

c     TEST IF PARTICLE WILL LAND ON DEFINITE PLANE
c     IF NEW X, Y, AND Z COORDINATES ON PLANE, THEN HIT = 1

      j=cmp((xpn+t*ua),cp(p,1))
      k=cmp((xpn+t*ua),cp(p,4))
            if ((j.eq.0.or.j.eq.2).and.(k.eq.0.or.k.eq.1)) then
      j=cmp((ypn+t*ub),cp(p,2))
      k=cmp((ypn+t*ub),cp(p,5))
            if ((j.eq.0.or.j.eq.2).and.(k.eq.0.or.k.eq.1)) then
      j=cmp((zpn+t*uc),cp(p,3))
      k=cmp((zpn+t*uc),cp(p,6))
            if ((j.eq.0.or.j.eq.2).and.(k.eq.0.or.k.eq.1)) then

            hit = 1

      end if
      end if
      end if

      return

      end

c     ****************************************************************

      subroutine _execute_motion(ds)

      common/vect/xpn,ypn,zpn,ua,ub,uc
      common/cell/ci(3)
      common/max/mx(3)
      common/cell_system/xcd(101),ycd(101),zcd(101)

      real ta,tt,ttot,ds
      integer k,hitpl,flag1,j

1     format ('(',f7.3,',',f7.3,',',f7.3,')')
2     format (' Particle passed through plane ',i1)
3     format (' Landed on plane ',i1,' at')
4     format (' Distance travelled in current cell is ',f7.3)
```

```
      j=0
      k=0
      ta=0
      hitpl=0
      flag1=0
      ttot=0
      cyc=0

c     INITIALIZE STARTING CELL

      call _init_cur_cell()

      write(1,*),'Starting in cell '
             write(1,1),ci(1),ci(2),ci(3)
             write(1,*)

c     BEGIN MAIN LOOP

      do while (flag1.eq.0)

c     DETERMINE WHICH PLANE (K) COULD BE HIT

        do while (hitpl.eq.0)
            k=k+1
            call _plane(k,hitpl,ta)
        end do

c     TTOT=TOTAL DISTANCE TRAVELLED SO FAR

            ttot=ttot+ta

c     CHECK IF PLANE IS TOO FAR AWAY TO REACH WITH CURRENT DS

            if (ttot.gt.ds) then
               ttot=ttot-ta
               write(1,4),ds-ttot
               if (cyc.eq.0) then
                      write(1,*),'Currently in cell '
                      write(1,1),ci(1),ci(2),ci(3)
               end if
               xpn=xpn+(ds-ttot)*ua
               ypn=ypn+(ds-ttot)*ub
               zpn=zpn+(ds-ttot)*uc

c     IF TOO FAR, REMAIN IN CURRENT CELL

               write(1,*),'New position is,'
               write(1,1),xpn,ypn,zpn
               flag1=1

c     EXIT LOOP

               go to 101
            end if

c     FIX ALL CELL INDICES FOR ALL PLANES PASSED THROUGH

      do while (j.le.5)
             j=j+1
             call _plane(j,hitpl,tt)
      if (hitpl.eq.1) then
          ta=tt
          if (j.eq.1) ci(1)=ci(1)+1
          if (j.eq.3) ci(1)=ci(1)-1
          if (j.eq.2) ci(2)=ci(2)-1
          if (j.eq.4) ci(2)=ci(2)+1
          if (j.eq.5) ci(3)=ci(3)+1
          if (j.eq.6) ci(3)=ci(3)-1
          write(1,2),j
      end if
      end do

c     RECALCULATE CURRENT POSITION - ON CELL WALL

          xpn=xpn+ta*ua
          ypn=ypn+ta*ub
          zpn=zpn+ta*uc

c     INITIALIZE CELL POSITION

      call _init_cur_cell()

c     EXIT LOOP IF TOTAL DISTANCE TRAVELLED EQUALS DS

          if (ttot.eq.ds) then
              write(1,3),k
              write(1,1),xpn,ypn,zpn
              write(1,4),ta
              write(1,*),'Currently in cell '
              write(1,1),ci(1),ci(2),ci(3)
              flag1=1
              go to 101
           end if

              write(1,4),ta
              write(1,*),'Particle passed through plane(s) at'
              write(1,1),xpn,ypn,zpn

c     TEST IF PARTICLE IS ON EDGE OF SYSTEM

      if ((xpn+.001*ua).lt.xcd(1).or.(ypn+.001*ub).lt.ycd(1).or.
      (zpn+.001*uc).lt.zcd(1).or.(xpn+.001*ua).gt.xcd(mx(1)).or.
      (ypn+.001*ub).gt.ycd(mx(2)).or.(zpn+.001*uc).gt.zcd(mx(3))) then
              write(1,*),'Particle has left system at '
              write(1,1),xpn,ypn,zpn
              stop
      end if

              write(1,*),'Currently in cell '
              write(1,1),ci(1),ci(2),ci(3)

              k=0
              hitpl=0
              ta=0
              j=0
              cyc=cyc+1

c     PARTICLE HAS NOT TRAVELLED FULL DISTANCE DS YET, GO BACK TO TOP
c     OF LOOP, AND CONTINUE
```

```
      end do

101   write(1,*),'Cycle complete...'

      return
      end

c     ***************************************************************

      subroutine _init_random_vects(dt,seed)

      common/vect/xpn,ypn,zpn,ua,ub,uc
      double precision rand
      integer seed
      real mag, i, dt

      call srand(seed)

c     FIND RANDOM VALUES FOR U

      ua=rand()
      ub=rand()
      uc=rand()

c     POSITIVE OR NEGATIVE

      i=rand()
      if (i.le..500) ua=-ua
      i=rand()
      if (i.le..500) ub=-ub
      i=rand()
      if (i.le..500) uc=-uc

c     MAKE U A UNIT VECTOR

      mag=sqrt(ua**2+ub**2+uc**2)
      ua=ua/mag
      ub=ub/mag
      uc=uc/mag

c     DETERMINE TRANSFER DISTANCE < 10

      dt=rand()*10

c     SET VALUE FOR NEW SEED

      seed=anint(rand()*1000)
      return
      end

c     ***************************************************************

      subroutine _init_norm_field()

      common/norm/nm(6,3)

      open (2,file='norm.fld')

c     READ DATA FOR NORMAL VECTORS

      do 14 l=1,6
         do 14 m=1,3
            read (2,*),nm(l,m)
14    continue

      end

c     ***************************************************************

      subroutine _init_cur_cell()

      common/cell/ci(3)
      common/plan/cp(6,9)
      common/norm/nm(6,3)
      common/cell_system/xcd(101),ycd(101),zcd(101)
      integer l,m

c     SET COORDINATES FOR ALL PLANES

      cp(1,1)=xcd(ci(1)+1)
      cp(1,2)=ycd(ci(2)+1)
      cp(1,3)=zcd(ci(3)+1)
      cp(1,4)=xcd(ci(1)+1)
      cp(1,5)=ycd(ci(2))
      cp(1,6)=zcd(ci(3))

      cp(3,1)=xcd(ci(1))
      cp(3,2)=ycd(ci(2)+1)
      cp(3,3)=zcd(ci(3)+1)
      cp(3,4)=xcd(ci(1))
      cp(3,5)=ycd(ci(2))
      cp(3,6)=zcd(ci(3))

      cp(2,1)=xcd(ci(1)+1)
      cp(2,2)=ycd(ci(2))
      cp(2,3)=zcd(ci(3)+1)
      cp(2,4)=xcd(ci(1))
      cp(2,5)=ycd(ci(2))
      cp(2,6)=zcd(ci(3))

      cp(4,1)=xcd(ci(1)+1)
      cp(4,2)=ycd(ci(2)+1)
      cp(4,3)=zcd(ci(3)+1)
      cp(4,4)=xcd(ci(1))
      cp(4,5)=ycd(ci(2)+1)
      cp(4,6)=zcd(ci(3))

      cp(5,1)=xcd(ci(1)+1)
      cp(5,2)=ycd(ci(2)+1)
      cp(5,3)=zcd(ci(3)+1)
      cp(5,4)=xcd(ci(1))
      cp(5,5)=ycd(ci(2))
      cp(5,6)=zcd(ci(3)+1)

      cp(6,1)=xcd(ci(1)+1)
      cp(6,2)=ycd(ci(2)+1)
      cp(6,3)=zcd(ci(3))
      cp(6,4)=xcd(ci(1))
      cp(6,5)=ycd(ci(2))
      cp(6,6)=zcd(ci(3))
```

```
c       FILL CP FOR NORMAL VECTORS AS WELL

        do 13 l=1,6
                do 13 m=7,9
                cp(l,m)=nm(l,m-6)
13      continue

        return
        end

c       ****************************************************************

        subroutine _init_system_field()

        common/max/mx(3)
        common/cell_system/xcd(101),ycd(101),zcd(101)
        real sum

        write (*,*),'Enter numbers of x,y,z planes'
        read (*,*),mx(1),mx(2),mx(3)

c       BUILD X COORDINATES IN XCD FROM DELTA_X IN FILE

        sum=0
        open (3,file='xcd.fld')
        do 15 j=1,mx(1)
                read(3,*),x
                sum=sum+x
                xcd(j)=sum
15      continue
        close (3)

c       BUILD Y COORDINATES IN YCD FROM DELTA_Y IN FILE

        sum=0
        open (4,file='ycd.fld')
        do 16 j=1,mx(2)
                read(4,*),y
                sum=sum+y
                ycd(j)=sum
16      continue
        close (4)

c       BUILD Z COORDINATES IN ZCD FROM DELTA_Z IN FILE

        sum=0
        open (53,file='zcd.fld')
        do 17 j=1,mx(3)
                read(53,*),z
                sum=sum+z
                zcd(j)=sum
17      continue
        close (53)

        return
        end

c       ****************************************************************
```

```
        subroutine _set_initial_ci()

        common/vect/xpn,ypn,zpn,ua,ub,uc
        common/cell/ci(3)
        common/max/mx(3)
        common/cell_system/xcd(101),ycd(101),zcd(101)
        integer a


c       FIND WHICH CELL XPN, YPN, ZPN FALL IN FOR XCD, YCD, ZCD FIELDS

        do 21 a=1,(mx(1)-1)
         if (xpn.ge.xcd(a).and.xpn.lt.xcd(a+1)) ci(1)=a
21      continue
        do 22 a=1,(mx(2)-1)
         if (ypn.ge.ycd(a).and.ypn.lt.ycd(a+1)) ci(2)=a
22      continue
        do 23 a=1,(mx(3)-1)
         if (zpn.ge.zcd(a).and.zpn.lt.zcd(a+1)) ci(3)=a
23      continue

        return
        end

c       ****************************************************************

        function cmp(a,b)

        real a,b

c       IF A=B ... RETURN 0
c       IF A>B ... RETURN 1
c       IF A<B ... RETURN 2

        if (abs(a-b).lt..00001) then
                cmp=0
                go to 150
        end if

        if ((a-b).gt.0) then
                cmp=1
                go to 150
        end if

        if ((a-b).lt.0) then
                cmp=2
                go to 150
        end if
150     return
        end
```